Wnt/β-catenin pathway functions by inactivation of Tcf7l1 protein

By

Chun-I Wu

B.S., National Yang-Ming University, Taiwan, 2000

M.S., National Yang-Ming University, Taiwan, 2002

Thesis

Submitted as partial fulfillment of the requirements for the degree of Doctor of Philosophy in Biochemistry and Molecular Genetics in the Graduate College of the University of Illinois at Chicago, 2014

Chicago, Illinois, USA

Defense Committee:

Bradley Merrill, Chair and Advisor

Elizaveta Benevolenskaya

Maxim Frolov

Lester Lau

Jennifer Schmidt, Biological Sciences

This thesis is dedicated to my wife, Yu-Ling Hu, and to my son, Jin-Heng Wu.

ACKNOWLEDGMENTS

I would like to thank all the people that have helped me along the way to make this thesis possible.

In particular, I would like to thank my thesis advisor, Dr. Bradley Merrill. Without his help, support, and continuous challenges along the way, none of my accomplishments is possible. He taught me everything I know about science - from asking a question, designing an experiment, troubleshooting, putting figures together, putting a manuscript together, preparing a presentation, to writing a thesis. In particular, he spent hundreds of hours listening to me practice my presentations. I am very grateful for his help and patience with me.

I would also like to thank my thesis committee members: Dr. Lester Lau, Dr. Jennifer Schmidt, Dr. Maxim Frolov, and Dr. Elizaveta Benevolenskaya. Thank you all very much for your guidance. Also, thank you for your support in writing recommendation letters for me.

Next, I would like to thank the current and past members of the Merrill lab: Jackson, Laura, Fei, Yuka, Brian, and Jenny. You all have been great friends and I have learned a lot from each one of you.

Finally, I would like to thank my family. My parents have been very supportive about every choice I have made. I would like to thank my wife, Yu-Ling Hu. She has gone through the ups and downs with me throughout my graduate life. Her unconditional support has made this thesis possible.

TABLE OF CONTENTS

CHAPTER **PAGE**

TABLE OF CONTENTS (continued)

CHAPTER **PAGE**

TABLE OF CONTENTS (continued)

CHAPTER **PAGE**

LIST OF FIGURES

FIGURE **PAGE**

LIST OF FIGURES (continued)

FIGURE **PAGE**

LIST OF ABBREVIATIONS

AER……...apical ectodermal ridge

APC……...adenomatous polyposis coli

AVE……...anterior visceral endoderm

CaMKII……...calcium/calmodulin-dependent protein kinase II

ChIP……...chromatin immunoprecipitation

CK1……...casein kinase 1

CRD……...context-dependent regulatory domain

E……embryonic day

ESCs……....embryonic stem cells

EXE……...extraembryonic ectoderm

Fgf……..fibroblast growth factor

Fz……...Frizzled

GSK3……glycogen synthase kinase 3

HMG……...high-mobility group

IP……immunoprecipitation

JNK……c-Jun N-terminal kinases

KI……knock-in

KO……...knockout

Lrp5/6……low density lipoprotein receptor-related protein 5/6

MCJ……mucocutaneous junction

NFAT……..nuclear factor of activated T cell

LIST OF ABBREVIATIONS (continued)

NLK…….Nemo-like kinase

NLS…….nuclear localization signals

P……..postnatal day

PC……...palebral conjunctiva

PE……...palebral epidermis

PKC……protein kinase C

PP1…….protein phosphatase 1

PP2Cα……protein phosphatase 2Cα

PS…….……...primitive streak

qPCR…….....quantitative real-time PCR

ROCK……Rho-associated protein kinase

Ser…….....serine

Shh……..sonic hedgehog

Tcf/Lef…….....T-cell factor/lymphoid enhancer factor

Thr…….....threonine

WRE……...Wnt responsive element

WRG……Wnt/β-catenin responsive target genes

WT……...wild-type

ZPA……..zone of polarizing activity

SUMMARY

The canonical Wnt/β-catenin signaling pathway is classically thought to function through formation of Tcf/Lef-β-catenin complexes for activation of target gene transcription. In this model, β-catenin binding acts as a switch, turning Tcf/Lefs from transcriptional repressors to transcriptional activators. My thesis work shows that mouse Tcf7l1 (formerly named Tcf3) plays a distinct and novel role in the Wnt/β-catenin pathway. Instead of switching Tcf7l1 into a transactivator, β-catenin binding to Tcf7l1 results in its removal from chromatin and subsequent degradation in a proteasome-dependent manner. Experiments using mouse embryonic stem cells (ESCs) show that recombinant Wnt3a, GSK3-inhibition, or increasing β-catenin levels are all sufficient to reduce Tcf7l1 protein independent of mRNA levels. This effect does not occur in Tcf7l1ΔN/ΔN ESCs, which lack nine Tcf7l1 residues necessary for β-catenin binding. Interestingly, Tcf7l1ΔN/ΔN mice exhibit severe morphogenetic defects, including exencephaly, poor vascular integrity, open eyelids at birth and oligodactyly. However, Tcf7l1-/ΔN mice develop into viable and ostensibly normal adult mice, suggesting that reducing the amount of Tcf7l1 replaces the requirement for Tcf7l1-β-catenin interaction. Thus, Wnt/β-catenin signaling regulates Tcf7l1 activity through a fundamentally different mechanism as compared to other Tcf/Lefs, independent of Tcf/Lef-β-catenin transactivator activity. These findings impact understanding of the mechanisms whereby Wnt/β-catenin mediates its effects, especially in the self-renewal capabilities of Tcf7l1-expressing stem cells and tumor cells.

Chapter I

Introduction

1.Wnt signaling

Wnt ligands function in canonical and non-canonical pathways, which share the common features of using the seven-pass transmembrane Frizzled (Fz) receptor, its coreceptor, single-pass transmembrane low density lipoprotein receptor-related protein 5/6 (Lrp5/6), and Dishevelled proteins to transduce signaling. Various Dishevelled proteins are thought to uniquely interpret Wnt activation by recruiting different downstream effectors (1). Of these pathways, canonical Wnt/β-catenin signaling is the best characterized, while less is understood about Wnt-signaling that induces a biological response independent of β-catenin.

Of the non-canonical Wnt pathways, the Wnt/planar cell polarity pathway controls developmental process that affects cell polarity within an epithelial plane, including neural tube closure, eyelid closure, and cochlear hair cell orientation in inner ear (1). This pathway requires activation of small GTPases, Rho and Rac, to induce cytoskeletal rearrangement. Rho activates Rho-associated protein kinase (ROCK) to regulate cytoskeleton, while Rac activates c-Jun N-terminal kinase (JNK) to induce actin polymerization (2,3). ROCK and JNK reorganize the cytoskeleton to coordinate cell polarity and control cell migration (2,3).

The Wnt/calcium pathway plays an important role in the development of dorsoventral polarity, somite patterning, and formation of various organs (4-6). This pathway involves the release of calcium from the endoplasmic reticulum through heterotrimeric G-protein activation of phospholipase C (5,7). Subsequent

calcium fluxes can activate several mediator proteins including calcium/calmodulin-dependent protein kinase II (CaMKII), protein kinase C (PKC), and the protein phosphatase, calcineurin (8,9). Both CaMKII and PKC go on to activate NF-kB and CREB transcription factors, while calcineurin activates nuclear factor of activated T cell (NFAT) transcription factor (10).

1.1 The function of canonical Wnt/β-catenin signaling

Canonical Wnt/β-catenin signaling controls many biological activities throughout embryonic development and tissue homeostasis. Through mouse loss-of-function genetic experiments, Wnt/β-catenin signaling has been shown to be required at multiple stages of mouse development, including gastrulation and limb development (11-13). Furthermore, aberrant Wnt/β-catenin signaling has been implicated in many cancers, providing an axis for discovery of potential therapeutic targets (14).

1.2 Wnt signaling during development

1.2.1 Gastrulation

Gastrulation occurs early in development when the epiblast, a single layer of cells derived from the inner cell mass, divides and differentiates into three primary germ layers consisting of ectoderm, mesoderm and definitive endoderm. The

epiblast is symmetrical and maintained in a pluripotent state while surrounded by visceral endoderm. Gastrulation begins with formation of the primitive streak (PS), a transient structure that defines the posterior of the embryo (11).

PS formation is triggered by a break in epiblast symmetry. Visceral endoderm at the distal tip of the embryo migrates to the anterior to form the anterior visceral endoderm (AVE). The AVE acts as a signaling center, expressing ligands like Cer1, Lefty1, and DKK which antagonize Nodal and Wnt signaling. A second signaling center in the extraembryonic ectoderm (EXE) is formed adjacent to the proximal epiblast. EXE-secreted ligands, such as Nodal, Wnt3, and BMP4, promote PS formation. Thus, ligands secreted by the AVE and EXE establish opposing morphogen gradients, which break epiblast symmetry and initiate PS formation (12).

During PS formation, epiblast cells ingress through the primitive streak to give rise to the mesoderm and definitive endoderm via epithelial-to-mesenchymal transition. Epiblast cells, which do not enter through the primitive streak, go on to form ectoderm. Thus, three primary germ layers establish a basic body plan, eventually developing into all tissues types of the organism (12).

1.2.2 Wnt, Nodal, and BMP signaling during gastrulation

Mouse genetic experiments have shown that several signaling pathways are required for gastrulation. β-catenin-null, Wnt3-/-, and Lrp5-/-Lrp6-/- mutants have

defects in primitive streak formation, resulting in a gastrulation block (15-17). Genetic ablation of Nodal, its cofactor, Cripto, or BMP receptor 1 also block PS formation (18-20). In congruence, double knockout of Nodal antagonists, Cer1 and Lefty1, result in PS expansion or formation of multiple PS (21). Thus, Wnt/β-catenin, Nodal, and BMP signaling pathways are each required for PS formation.

1.2.3 Limb bud formation

The early limb bud first protrudes from the lateral embryo body wall, and is comprised of mesenchyme and overlying ectoderm. As the limb bud develops, specialized signaling centers are formed which are required for outgrowth and patterning of the vertebrate limb. The anatomy of the limb can be divided into three axes: proximal-distal (from shoulder to finger tip), anterior-posterior (from thumb to little finger), and dorsal-ventral (from back of hand to palm) (22).

The apical ectodermal ridge (AER) is an ectodermal structure that runs along the distal tip of the limb bud. Microsurgical removal of the AER from the developing chick limb bud results in loss of limb structure, demonstrating a requirement of the AER for limb development (23). Fibroblast growth factor (Fgf) expressed in the AER is the major protein required for limb bud outgrowth (24-26).

The posterior region of the limb mesenchyme is called the zone of polarizing activity (ZPA). Sonic hedgehog (Shh) expression in the ZPA is required to

determine the anterior-posterior axis of the limb bud. Heterotopic transplantation of the ZPA to the anterior of the developing chick limb bud produces a limb with double number of digits and posterior digits on both sides. This demonstrates the ability of the ZPA to specify posterior identity in the limb bud (27).

Coordination between these signaling centers determines the size and shape of the limb bud. Genetic experiments in mice and manipulation of chick limb buds indicate that Fgf8 in the AER induces Shh expression in the ZPA (24,28). Shh promotes the expression of Fgf4 in the AER by inducing the BMP antagonist, Gremlin (29,30). Therefore, signals from the AER and ZPA co-potentiate a positive feedback loop of Shh and Fgfs.

1.2.4 Wnt signaling during limb development

Members of the Wnt family and their downstream effectors are differentially expressed either within the ectoderm and/or mesenchyme of the limb bud, suggesting that they may play a number of different roles during limb development (13). For instance, Wnt3 is expressed ubiquitously in limb bud ectoderm. Conditional knockout of Wnt3 in limb bud ectoderm disrupts AER formation and results in severe limb deformation (31). Wnt5a is expressed in both ventral limb ectoderm and mesenchyme. Gene inactivation of Wnt5a in mice results in a shortening of the limb, reflecting an overall retardation in development (32). Wnt7a is expressed in the dorsal ectoderm of the limb bud, and loss of

Wnt7a results in mice lacking both dorsal structures and posterior digits. In addition, Shh expression is decreased in Wnt7a$^{-/-}$ limbs in a manner that corresponds with loss of posterior digits (33). The role of β-catenin in the ectoderm and mesoderm of limb bud has also been investigated via conditional knockout mice. Loss of β-catenin in limb ectoderm causes defects in AER formation (31). Furthermore, loss of mesenchymal β-catenin activity results in limb truncations due to defects in AER maintenance, while overactivation of β-catenin in limb mesenchyme causes premature AER regression (34).

1.3 Wnt/β-catenin signaling molecular pathway

Activity of the Wnt/β-catenin pathway is controlled through regulation of β-catenin protein stability (35). In the absence of Wnt ligand, β-catenin is constitutively targeted for ubiqutination and proteasome-mediated degradation by phosphorylation at serine (Ser) and threonine (Thr) residues near its amino terminus (36,37). Mutagenesis experiments have shown that substitution of Ser33, Ser37, Thr41, and Ser45 with alanine in β-catenin inhibit its ubiquitination and resulted in its stabilization (36). Phosphorylation of β-catenin occurs within a polyprotein destruction complex that includes adenomatous polyposis coli (APC), scaffolding protein Axin, Dishevelled, and the kinases, casein kinase 1α (CK1α) and glycogen synthase kinase 3 (GSK3) (37-39). Using a panel of antibodies that specifically recognizes different β-catenin phosphorylation sites on Ser and Thr residues, CK1α was identified and found to first phosphorylate β-catenin at Ser45,

which is required for subsequent GSK3 phosphorylation of β-catenin at Ser33, Ser37, and Thr41 (37). β-TrCP E3 ubiqutin ligase binds to phosphorylated β-catenin, targeting it for ubiquitylation and proteasome-mediated degradation (36,40). Thus, without Wnt ligands, free, cytoplasmic β-catenin is kept at a low level. When Wnt ligands bind to the Fz-Lrp5/6 receptor complex, a signaling cascade is initiated which inhibits the β-catenin destruction complex. Free β-catenin accumulates in the cytoplasm and translocates into the nucleus to stimulate the expression of Wnt/β-catenin target genes.

β-catenin is a multifunctional protein. Besides its functions in transcription factor regulation in the nucleus, β-catenin also serves as an essential cell adhesion molecule to maintain adherens junctions. Interestingly, β-catenin contains no intrinsic DNA binding ability, relying instead on interactions with DNA-binding proteins to regulate target genes (41-43). Luciferase reporter assays have shown that β-catenin protein can stimulate transcription of target genes when it binds to a Tcf/Lef (41,42). Deletion mutagenesis experiments have localized the primary transactivation activity of β-catenin to its carboxy-terminal portion (43).

Tcf/Lefs are DNA-binding transcription factors which depend on interaction with co-activators or co-repressors to exert their effect on target gene expression. In the absence of Wnt/β-catenin signaling, Tcf/Lefs interact with co-repressor proteins, Groucho and CtBP, to repress target genes (44-46). *In vitro* analysis of protein-protein interactions using purified proteins show that β-catenin binding to

Tcf/Lefs directly disrupts Tcf/Lef-Groucho complexes to form Tcf/Lef-β-catenin complexes (47). Tcf/Lef-β-catenin complexes subsequently recruit transcriptional co-activators like BCL9, Pygopus, Brg-1, and CBP to activate Wnt target genes (48-52). Thus, Wnt activation stimulates a β-catenin-mediated switch of Tcf/Lefs from transcriptional repressors to transcriptional activators of Wnt target genes.

1.4 Evolving models of β-catenin destruction complex inhibition

Since the discovery of β-catenin's role as a nuclear transcriptional activator (41,42), several models have been proposed to explain how Wnt ligand binding results in β-catenin stabilization. The research elucidating these models have focused on the molecular dynamics associated with disassembly of the destruction complex and inhibition of β-catenin phosphorylation. The details of models have changed over time, which has led to a good understanding of several cytoplasmic events which occur downstream of Wnt ligand binding.

1.4.1 Membrane sequestration of Axin

To understand how the Wnt coreceptor, LRP5/6, transduces Wnt/β-catenin signaling, yeast two-hybrid systems were used to identify factors that interact with LRP5/6's intracellular domain. In this manner, Axin was identified (53). In addition, the amount of Axin bound to plasma membranes was found to synergistically increase with combined LRP5/6 overexpression and *in vitro* treatment of 3T3 cells with Wnt-3a conditioned medium (53). After stimulation with Wnt-3a, GSK3 and

CK1γ induce several phoshorylations of the cytoplasmic domain of LRP5/6, creating docking sites for Axin (54,55). Mutagenesis and *in vitro* kinase assay experiments show that GSK3 phosphorylates serines in five PPPSPXS Axin-binding motifs (55), while CK1γ phosphorylates two adjacent Ser/Thr clusters (54). Thus, it is possible that Wnt stimulation results in membrane sequestration of Axin by LRP5/6, resulting in the disruption of the β-catenin destruction complex and accumulation of free β-catenin.

1.4.2 Axin degradation

Wnt/β-catenin signaling leads to a decrease in Axin striping pattern expression in Drosophila embryos, suggesting Wnt/β-catenin negatively regulates Axin levels *in vivo* (56). In addition to Wnt-activated phosphorylation of the LRP5/6 cytoplasmic domain to sequester Axin away from the β-catenin destruction complex, Poly-ADP-ribosylating enzymes tankyrase 1 and tankyrase 2 also interact with Axin and stimulate its degradation via the ubiquitin-proteasome pathway (57).

1.4.3 Protein phosphatase dephosphorylation of Axin

In addition to β-catenin and LRP5/6, Axin and APC are also substrates for CKI and GSK3. Phosphorylation of Axin and APC enhances their binding affinity for GSK3 and β-catenin, shifting equilibrium to favor β-catenin destruction complex formation. While the role of CKI and GSK3 phosphorylation activity has

been implicated in regulating Wnt signaling, the role of phosphatases is less clear. Protein phosphatase 1 (PP1) was identified in an RNAi screen targeting catalytic subunits of protein phosphatases as an activator of Wnt/β-catenin signaling (58). In addition, protein phosphatase 2Cα (PP2Cα) was identified in a yeast two-hybrid screen for factors that interact with Dishevelled protein (59). Immunoprecipitation, *in vitro* phosphastase, and electrophoretic mobility assays showed that PP1 and PP2Cα can bind to and dephosphorylate Axin (58,59). Thus, Axin dephosphorylation by PP1 and PP2Cα leads to less β-catenin destruction complexes.

1.4.4 Inhibition of GSK3 kinase activity

Overexpression of LRP6's intracellular domain is sufficient to inhibit GSK3-mediated phosphorylation of β-catenin independent of Axin degradation (60). In addition, introduction of phosphorylated PPPSPXS motif peptides results in inhibition of GSK3 phosphorylation of β-catenin *in vitro* (61). Furthermore, *in vitro* recombinant protein experiments show that phosphorylated PPPSPXS motifs inhibit GSK3 phosphorylaton of β-catenin at Ser33/Ser37/Thr41, but not CK1 phosphorylation of β-catenin at Ser45 (62). These experiments suggest a dual role of LRP5/6-mediated stimulation of Axin degradation and inhibition of GSK3 activity upon Wnt activation.

1.4.5 Current model: Wnt signaling blocks β-catenin ubiquitination

Unlike previous studies of the β-catenin destruction complex, which utilized overexpression or *in vitro* analysis, Hans Clevers' group analyzed the endogenous complex via immunoprecipitation of Axin (63). Their work showed that β-catenin is phosphorylated, ubiquitinated and degraded by proteasome within the intact complex. They have proposed that Wnt signaling blocks β-catenin ubiquitination by dissociating β-TrCP E3 ligase from the destruction complex, resulting in saturation of the Axin complex with phospho-β-catenin (63). This allows newly synthesized β-catenin to accumulate in the cytosol and translocate into the nucleus. Furthermore, Clevers' group was unable to find evidence that supports models of destruction complex disassembly or Wnt-mediated inhibition of phospho-β-catenin. Thus, the current model shows that Wnt activates β-catenin through inhibition of β-catenin ubiquitination in the destruction complex.

2. Tcf/Lef transcription factors

T-cell factor/lymphoid enhancer factor (Tcf/Lef) transcription factors are the downstream effectors of the Wnt/β-catenin signaling pathway. In mouse, there are four Tcf/Lefs, originally named Tcf1, Tcf3, Tcf4 and Lef1. Recently, the nomenclature of mouse Tcf/Lefs was updated to match human Tcf/Lefs. Thus, they were renamed Tcf7 (Tcf1), Tcf7l1 (Tcf3), Tcf7l2 (Tcf4) and Lef1.

2.1 Shared characteristics of Tcf/Lefs

As downstream regulators of the canonical Wnt/β-catenin pathway, the four mammalian Tcf/Lef factors share several important characteristics. All Tcf/Lefs have a highly conserved β-catenin binding domain near the amino terminus, which is required for their modulation of Wnt target genes in response to Wnt-stabilized β-catenin (41,42,64,65). All Tcf/Lefs also possess nearly identical high-mobility group (HMG) domains which bind DNA in a sequence-specific manner, as well as highly similar nuclear localization signals (NLS) recognized directly by importin α subunits for nuclear import (66). In addition, all Tcf/Lefs bind to the same consensus sequence ($^{A}/_{T}{}^{A}/_{T}$CAAAG) and can regulate transcription of target genes (67-69). The nearly identical DNA-binding and β-catenin-binding domains of Tcf/Lef factors support the idea that they similarly regulate a common set of target genes.

2.2 Diverse characteristics of individual Tcf/Lefs

In addition to highly conserved domains, Tcf/Lefs also have less conserved regions which suggest that there may be unique functions specific to each Tcf/Lef. Between the β-catenin-binding and DNA-binding domains, each Tcf/Lef contains a context-dependent regulatory domain (CRD). The CRD is the least conserved domain with sequence similarity as low as 15~20%. However, all Tcf/Lefs have

been shown to recruit Groucho/TLE for transcriptional repression via their CRD (70).

The carboxyl terminal is another region that varies significantly between Tcf/Lefs. Tcf7 and Tcf7l2 each have an E tail domain, which interacts with transcriptional p300 in a non-sequence specific manner. Interestingly, Tcf7 and Tcf7l2 can activate *Lef1* and *Cdx1* promoters, while Tcf7l1 and Lef1, without E tail domains, cannot activate *Lef1* and *Cdx1* promoters (71). This suggests that presence or absence of an E tail domain influences how each Tcf/Lef interacts with various DNA regulatory regions.

At the end of the carboxyl terminal, Tcf7l1 and Tcf7l2 contain two CtBP-binding motifs. CtBP is a non-DNA-binding protein that recognizes the PLSLXXK motif in Tcf7l1 and Tcf7l2. CtBP was first identified to function as a Tcf/Lef corepressor during Xenopus development (46). Luciferase reporter assays showed that CtBP-binding motifs in the carboxy-terminal of Tcf/Lefs are important for the repressor activity of Tcf/Lefs. However, in mouse skin and embryonic stem cells, CtBP-binding motifs are not required for Tcf7l1-mediated repression (72,73).

2.3 Unique function of individual Tcf/Lefs during development

Tcf/Lefs are expressed in a tissue- and temporally-specific manner throughout development. Genetic ablation of individual Tcf/Lefs in mice has suggested unique roles of each Tcf/Lef throughout embryogenesis and in adult

tissue function. For example, Lef1-knockout mice have defects in the formation of multiple tissues, such as teeth, mammary glands, and hair follicles (74). Loss of Lef1 results in postnatal lethality, indicating that Lef1 is essential for several tissue formations.

Tcf7 knockout mice develop normally but deteriorate progressively in thymocyte proliferation and differentiation after birth (75,76). Thus, Tcf7 is essential for thymocyte expansion but is not absolutely required for the formation of other developing tissues it is expressed in.

Tcf7l2 knockout mice die shortly after birth. Tcf7l2 knockout mice show a decrease in villi number and amount of epithelial cells in the intervillus regions of the small intestine (77). Thus, Tcf7l2 is required for small intestine epithelial cell development.

2.4 Tcf7l1 function as a repressor during development

Tcf7l1 function has been genetically examined in zebrafish, *Xenopus*, and mouse (78-80). In these organisms, Tcf7l1 appears to function as a transcriptional repressor during development. The *headless* mutant in zebrafish was confirmed to have a mutation, which produces a truncated form of the Tcf7l1 protein which cannot bind DNA (79). Genetic complementation of *headless* mutation with different forms of Tcf7l1 demonstrates that interaction with β-catenin is not required to rescue the mutant phenotype. *Xenopus* embryos depleted of XTcf3 showed ectopic expression of dorsal genes in the ventral embryo, indicating that

XTcf3 is required to repress dorsal genes ventrally (78). Genetic ablation of Tcf7l1 in mouse alters gastrulation to produce embryos with ectopic and partially duplicated axes (80). This phenotype is similar to APC-hypomorphic (81), Axin-knockout (82) and Wnt8c-transgenic mice (83), suggesting that loss of Tcf7l1 is similar to over-activation of Wnt/β-catenin signaling during gastrulation.

2.5 Shared function of Tcf/Lefs

Each Tcf/Lef has unique essential functions in addition to redundant roles during development. Double-knockout mice show how different Tcf/Lefs can compensate for each other. Tcf7 and Lef1 have much overlap in expression patterns during early mouse development. Interestingly, knockout of Lef1 or Tcf7 individually results in no obvious defects during these stages. However, when Lef1 and Tcf7 are both ablated, the resulting mouse embryos display defects in paraxial mesoderm development, leading to ectopic formation of neural tubes (84). This phenotype resembles that of Wnt3a-deficient mice (85). In addition, Lef1 and Tcf7 double knockout embryos exhibit defects in limb development and placenta formation, which mimic defects observed in Wnt7a- and Wnt2-knockout mice, respectively (33,84,86). The observation that Lef1 and Tcf7 double knockout mice possess severe defects in stages unaffected in Lef1 and Tcf7 single knockouts suggests that there are functional redundancies of Lef1 and Tcf7 during mouse development.

In adult mouse skin, Tcf7l1 and Tcf7l2 are both expressed in slow-cycling hair follicle stem cells (87). When Tcf7l1 or Tcf7l2 is individually knocked out in mouse, there is no overt phenotype. However, Tcf7l1 and Tcf7l2 skin-specific conditional double knockout mice show defects in hair follicle down-growth and have much thinner epidermis compared to wild-type mice (87). These results indicate functional redundancy between Tcf7l1 and Tcf7l2 in hair follicle stem cell homeostasis.

3. Wnt/β-catenin asymmetry pathway in *C. elegans*

In *C. elegans*, the Wnt/β-catenin asymmetry pathway is widely used to specify cell fates during most asymmetry cell divisions. For example, at the four-cell embryo stage, the EMS blastomere asymmetrically receives a Wnt/β-catenin asymmetry signal from the neighboring P2 blastomere (88). This triggers the EMS cell to undergo asymmetric cell division, resulting in an anterior MS (mesoderm) daughter cell and a posterior E (endoderm) daughter cell. The MS cell will then go on to receive low Wnt activation, resulting in development of mesoderm, while the E cell will receive robust Wnt ligand binding, subsequently forming endoderm. The endoderm determining gene, *end-1,* is activated by Wnt activation of the posterior E cell, while it is repressed in the anterior MS cell.

The Wnt/β-catenin asymmetry pathway results in asymmetric expression of POP-1, the single Tcf/Lef homolog in *C. elegans*, and SYS-1, one of four β-catenin homologs in *C. elegans*. Pop-1 was first thought to function only as a

transcriptional repressor. However, analysis of Pop-1 mutant embryos at the four-cell embryo stage show higher expression of *end-1,* an endoderm-determining gene, in the MS cell but lower expression of *end-1* in the E cell, as compared to wildtype embryos (89). This indicates a role for Pop-1 not only in repression of E-specific lineage genes in the MS cell, but also in their activation in the E cell.

The dual functions of β-catenin in cell adhesion and canonical Wnt signaling occur through four β-catenin homologs in *C. elegans* (90). HMP-2 functions specifically as a structural protein in adherens junctions, BAR-1 acts as a coactivator in canonical Wnt/β-catenin signaling, while WRM-1 and SYS-1 are involved in Wnt/β-catenin asymmetry pathway**.** Immunoprecipitation and deletion assays demonstrate that WRM-1 binds to POP-1 at its carboxy-terminal domain instead of its β-catenin-binding domain at the amino terminal (91). In addition, immunoprecipitation assays show WRM-1 forms a stable complex with LIT-1, a Nemo-like kinase (NLK) homolog in *C. elegans* (92). In addition, *in vitro* phosphorylation assays show that coexpression of LIT-1 with WRM-1 results in POP-1 phosphorylation. Phosphorylated POP-1 is subsequently exported to the cytoplasm, decreasing the level of nuclear Pop-1 (93). Nuclear Pop-1 levels are low and can bind SYS-1 to act as a coactivator in Wnt-activated asymmetrical cell division (94). Thus, Pop-1 must be reduced to activate Wnt target genes (89). In conclusion, the posterior E cell receiving Wnt/β-catenin asymmetry signaling has lower levels of Pop-1 and higher levels of Sys-1. Conversely, the anterior MS cell

without Wnt/β-catenin asymmetry signaling has higher levels of Pop-1 and lower levels of Sys-1. The current model of the Wnt/β-catenin asymmetry pathway indicates that high levels of Pop-1 functions as a transcriptional repressor, while low levels of Pop-1 acts as a transcriptional activator when is bound to SYS-1 coactivator (88).

Chapter II

Function of Wnt/β-catenin in counteracting Tcf7l1 repression through the Tcf7l1-β-catenin interaction

With the exception of minor additions and formatting changes, the content of this chapter has been adapted from the content of the following manuscript:

Wu CI, Hoffman JA, Shy BR, Ford EM, Fuchs E, Nguyen H, Merrill BJ. *Function of Wnt/β-catenin in counteracting Tcf7l1 repression through the Tcf7l1-β-catenin interaction.* **Development**. 2012 Jun;139(12):2118-29

1. Abstract

The canonical Wnt/β-catenin signaling pathway classically functions through the activation of target genes by Tcf/Lef-β-catenin complexes. In contrast to β-catenin-dependent functions described for Tcf7, Tcf7l2 and Lef1, the known embryonic functions for Tcf7l1 in mice, frogs and fish are consistent with β-catenin-independent repressor activity. In this chapter, I genetically define Tcf7l1-β-catenin functions in mice by generating a *Tcf7l1*ΔN knock-in mutation that specifically ablates Tcf7l1-β-catenin. Mouse embryos homozygous for the knock-in mutation (*Tcf7l1*ΔN/ΔN) progress through gastrulation without apparent defects, thus genetically proving that Tcf7l1 function during gastrulation is independent of β-catenin interaction. *Tcf7l1*ΔN/ΔN mice were not viable, and several post-gastrulation defects revealed the first *in vivo* functions of Tcf7l1-β-catenin interaction affecting limb development, vascular integrity, neural tube closure and eyelid closure. Interestingly, the etiology of defects indicated an indirect role for Tcf7l1-β-catenin in the activation of target genes. Tcf7l1 directly represses transcription of *Lef1*, which is stimulated by Wnt/β-catenin activity. These genetic data indicate that Tcf7l1-β-catenin is not necessary to activate target genes directly. Instead, my findings support the existence of a regulatory circuit whereby Wnt/β-catenin counteracts Tcf7l1 repression of *Lef1*, which subsequently activates target gene expression via Lef1-β-catenin complexes. I propose that the Tcf/Lef circuit model provides a mechanism downstream of

β-catenin stability for controlling the strength of Wnt signaling activity during embryonic development.

2. Introduction

The canonical Wnt signaling pathway is required for morphogenesis of many organs, and its activity is necessary in adults through the regulation of stem cell properties. Overactivation of Wnt/β-catenin signaling causes cancer (95), which demonstrates a need to regulate the pathway through adulthood. Activity of the pathway is controlled through the regulation of β-catenin protein stability (35). In the absence of a Wnt ligand, β-catenin is targeted for ubiquitin- and proteasome-mediated degradation by phosphorylation at serine and threonine residues near the N-terminus (36,37). Phosphorylation of β-catenin occurs within a polyprotein complex that includes adenomatous polyposis coli (APC), Axin, and the kinases casein kinase 1 and glycogen synthase kinase 3 (GSK3) (37-39). Wnt ligands bind to Frizzled-Lrp5/6 receptor complexes and initiate a downstream cascade that inhibits GSK3 phosphorylation of β-catenin. This effect stabilizes β-catenin and stimulates its interaction with DNA-binding transcriptional regulators, of which Tcf/Lef proteins are the best characterized (41,42). When bound to Tcf/Lef proteins, β-catenin can function as a transcriptional co-activator by recruiting several nuclear factors to chromatin, such as BCL9, Pygopus, Brg-1 and CBP (48-52).

Mammals have four Tcf/Lef factors: Tcf7 (Tcf1), Tcf7l1 (Tcf3), Tcf7l2 (Tcf4) and Lef1. They possess nearly identical DNA binding domains that allow them to bind the same consensus sequence ($^{A}/_{T}{}^{A}/_{T}$CAAAG) and regulate the transcription of target genes (67-69). All Tcf/Lefs also possess conserved β-catenin interaction

domains near the N-terminus, which are necessary for Tcf/Lef proteins to stimulate target gene transcription in response to Wnt-stabilized β-catenin (41,42,64,65). Fulllength Tcf/Lef proteins also have β-catenin-independent activities as transcriptional repressors. Although all Tcf/Lef proteins have been reported to interact with co-repressor proteins such as Groucho (70), the extent to which the embryonic function of Tcf/Lefs depends on β-catenin-independent activities appears to be different for each Tcf/Lef protein (96). Lef1 sits at one end of the spectrum, as knockout and transgenic mouse models predominantly show Wnt/β-catenin dependent functions for Lef1 (74,97).

At the other end of the spectrum, Tcf7l1 appears to function primarily as a transcriptional repressor. Transgenic mice showed that full-length wild-type Tcf7l1 and β-catenin interaction-defective ΔNTcf7l1 cause essentially identical phenotypes when ectopically expressed in the epidermis (72). Importantly, transgenic mice engineered to overexpress repressor-defective mutant forms of Tcf7l1 did not exhibit an abnormal phenotype (72). Subsequently, through the use of inducible Tcf7l1 expression in the skin, the Tcf7l1 overexpression phenotype was shown to be caused by a reversion of adult cells to an embryonic like state, and analysis of downstream transcriptional effects showed that Tcf7l1 did not require Wnt/β-catenin (98). Genetic ablation of *Tcf7l1* affected gastrulation to produce embryos that display ectopic and partially duplicated axes, which ostensibly phenocopies several embryos engineered for overactivation of Wnt/β-catenin signaling during gastrulation (81-83,99). In frogs and fish,

loss-of-function experiments showed that Tcf7l1 acts as a transcriptional repressor in its first necessary function in embryos (78,79,100).

Despite the lack of direct evidence of a physiological requirement for Tcf7l1-β-catenin interaction *in vivo*, all *Tcf7l1* homologs encode a conserved β-catenin-binding domain. Analysis of Tcf7l1 overexpression has focused on effects of Tcf7l1 in cells that do not endogenously activate Tcf/Lef-β-catenin target genes (72,98). Thus, a potential role for the Tcf7l1-β-catenin interaction *in vivo* seemed plausible; however, the predominant repressor activity of Tcf7l1 obscured elucidation of any *in vivo* processes that require the Tcf7l1-β-catenin interaction.

I set out to determine genetically whether the Tcf7l1-β-catenin interaction is necessary for mouse embryogenesis or viability. I generated a *Tcf7l1*ΔN knock-in mutation and examined *Tcf7l1*ΔN/ΔN mice, which specifically lack the Tcf7l1-β-catenin interaction. I show that *Tcf7l1*ΔN/ΔN embryos progress through gastrulation without the defects associated with *Tcf7l1*-/- embryos, demonstrating that the first requirement for Tcf7l1 in the mouse is independent of Tcf7l1-β-catenin interaction. After gastrulation, *Tcf7l1*ΔN/ΔN embryos exhibited a diverse array of phenotypes. Interestingly, Tcf7l1-β-catenin is needed for Tcf/Lef-β-catenin activation of target genes; however, the mechanism of target gene activation is indirect and involves Wnt-β-catenin inhibiting Tcf7l1 repression of *Lef1*, followed by Lef1-β-catenin activation of transcription in the eyelid.

The findings presented here indicate a novel Tcf/Lef circuit through which Tcf7l1-expressing cells respond to Wnt/β-catenin signaling. Given the expression

of Tcf7l1 in stem cells (73,101,102) and poorly differentiated tumors (103), this work impacts not only developmental contexts but has the potential to be important for the manipulation of stem cells and treatment of aggressive cancers.

3. Results

3.1 Tcf7l1ΔN KI mutation demonstrates the requirement for Tcf7l1 during gastrulation is independent of β-catenin interaction

Knockout mouse experiments have shown that Wnt3 and β-catenin are required for induction of the primitive streak and specification of mesoderm (15,17). Subsequently, Wnt3a and the combined effects of Tcf7 and Lef1 specify paraxial mesoderm in a process characterized by activation of Tcf/Lef target genes (84,104,105). Overactivation of Wnt/β-catenin signaling stimulated ectopic mesoderm and partial duplication of the anteroposterior axis (81-83,99). Ablation of the *Tcf7l1* gene product caused a remarkably similar phenotype to overactivation of Wnt/β-catenin signaling, with partial axis duplication and ectopic mesoderm, but *Tcf7l1*-/- mutants also displayed reduced paraxial and lateral mesoderm (80). Thus, it was not clear whether the requirement for Tcf7l1 during gastrulation reflected a combination of Tcf7l1 repressor and Tcf7l1-β-catenin activities.

To determine the function of Tcf7l1-β-catenin interaction *in vivo*, we engineered a *Tcf7l1*ΔN mutation that replaced ten Tcf7l1 residues necessary for β-catenin binding with a single alanine (Figure 1A) (106). When wild-type (WT) Tcf7l1 was transiently expressed in Cos-7 cells, binding to endogenous β-catenin was detected by immunofluorescence (Figure 1B) and immunoprecipitation (Figure 1C) assays. By contrast, Tcf7l1ΔN was unable to relocalize endogenous β-catenin (Figure 1B), was deficient in co-immunoprecipitation of β-catenin

Figure 1. Tcf7l1-β-catenin interaction is required after gastrulation for survival.

(**A**) Three-dimensional structure of the Tcf7l1-β-catenin interaction. Amino acid sequence of Tcf7l1 proteins from Xenopus and Mouse are aligned atop the structure. Red denotes the Tcf7l1 residues constituting the core β-catenin-interaction domain in the structure from Graham et al (106).

(**B**) Immunofluorescent staining detects nuclear co-localization of endogenous β-catenin (green; all panels) in Cos-7 cells and transiently transfected Tcf7l1 (red, top panels only). Expression of the Tcf7l1ΔN mutant protein (+Tcf7l1ΔN, right panels) failed to cause nuclear β-catenin localization.

(**C**) Co-immunoprecipitation (IP) using a Tcf7l1-specific antibody and total cell lysate (TCL) from Cos-7 cells transiently transfected with the Tcf7l1 expression plasmid for wild-type (Tcf7l1), a mutant lacking the first 71 residues (Tcf7l1ΔN71), or the Tcf7l1ΔN knock-in mutation.

(**D**) Whole mount *in situ* hybridization with a labeled Brachyury cRNA probe and Tcf7l1+/+ (WT), Tcf7l1ΔN/ΔN (KI) or Tcf7l1-/- (KO) embryos. Expression patterns and morphology of KI embryos were unremarkable relative to WT embryos, and KI embryos did not display defects observed in KO embryos.

(**E**) Recovery of embryos with indicated genotypes obtained from time pregnancies of Tcf7l1+/ΔN x Tcf7l1+/ΔN matings.

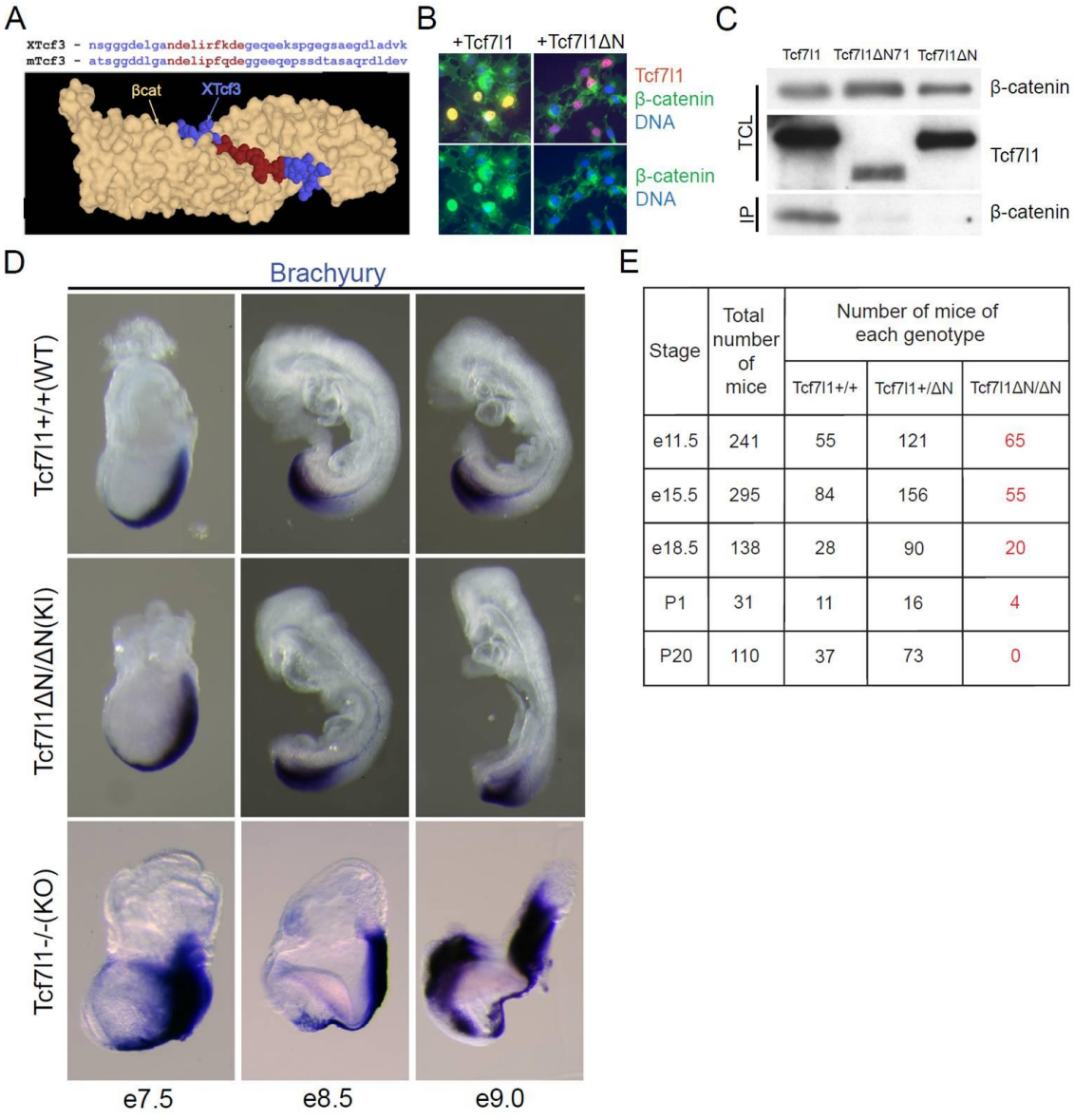

E

Stage	Total number of mice	Number of mice of each genotype		
		Tcf7l1+/+	Tcf7l1+/ΔN	Tcf7l1ΔN/ΔN
e11.5	241	55	121	65
e15.5	295	84	156	55
e18.5	138	28	90	20
P1	31	11	16	4
P20	110	37	73	0

(Figure 1C), and blocked β-catenin activation of the TOPFlash luciferase reporter (Figure 2A). The *Tcf7l1*ΔN mutation and a more extensive *Tcf7l1*ΔN71 mutation caused similar defects (Figure 1C). Previously, homologous recombination in ESCs incorporated the *Tcf7l1*ΔN mutation into the genome (80,107), and *Tcf7l1*+/ΔN ESCs were used to generate new *Tcf7l1*+/ΔN lines of mice. The *Tcf7l1*ΔN allele generated a stable *Tcf7l1*ΔN mRNA (Figure 2B) and Tcf7l1ΔN protein (Figure 2C) in mice. *Tcf7l1*+/ΔN mice did not display any detectable abnormalities during development or as adult mice. Thus, the *Tcf7l1*ΔN knock-in mutation provided an excellent means of determining the role of Tcf7l1-β-catenin interaction *in vivo*.

*Tcf7l1*ΔN/ΔN embryos, hereafter referred to as knock-in (KI) embryos, were first examined between E7.5 and E9.0. All embryos exhibited a normal morphology (Figure 1D), and genotyping revealed the expected Mendelian ratios of *Tcf7l1*+/+, *Tcf7l1*+/ΔN and *Tcf7l1*ΔN/ΔN embryos (not shown). Whole-mount *in situ* hybridization using cRNA probes to detect brachyury (Figure 1D) and *Foxa2* (not shown) mRNAs revealed normal patterns of expression in KI mutants through E9.0 (Figure 1D). By contrast, *Tcf7l1*-/- mutants displayed characteristic ectopic and expanded brachyury expression when stained alongside KI and control embryos (Figure 1D). Normal viability of KI embryos was observed through E11.5 (Figure 1E), which is well past the point of lethality in *Tcf7l1*-/- embryos (80). This result demonstrates genetically that the first requirement for Tcf7l1 in mouse is

Figure 2. Gene product from the Tcf7l1ΔN KI allele.

(**A**) Tcf/Lef-β-catenin Luciferase reporter assay showing effects of expressing combinations of β-catenin, Tcf7l1, Lef1, and Tcf7l1ΔN gene products by transient transfection in Cos-7 cells. Relative SuperTOPFlash activity is shown compared to Renilla Luciferase control for each transfection. Values represent the mean of biological triplicates +/- standard deviation.

(**B**) Reverse Transcriptase-PCR analysis of *TCF7L1* 5' region of $TCF7L1^{+/+}$ and $TCF7L1^{+/\Delta N}$ heart, lung, and liver cDNA samples. The KI mutation introduces an EagI site in PCR amplified region. EagI digested RT-PCR amplicons shows EagI-containing cDNA only in $TCF7L1^{+/\Delta N}$ samples.

(**C**) PCR genotyping of a litter of e8.5 embryos from mating two Tcf7l1+/ΔN mice (top). Western blot shows expression of WT and Tcf7l1ΔN proteins in $TCF7L1^{+/\Delta N}$ ESCs (bottom). Increased mobility of Tcf7l1ΔN protein reflects correct incorporation of ΔN mutation.

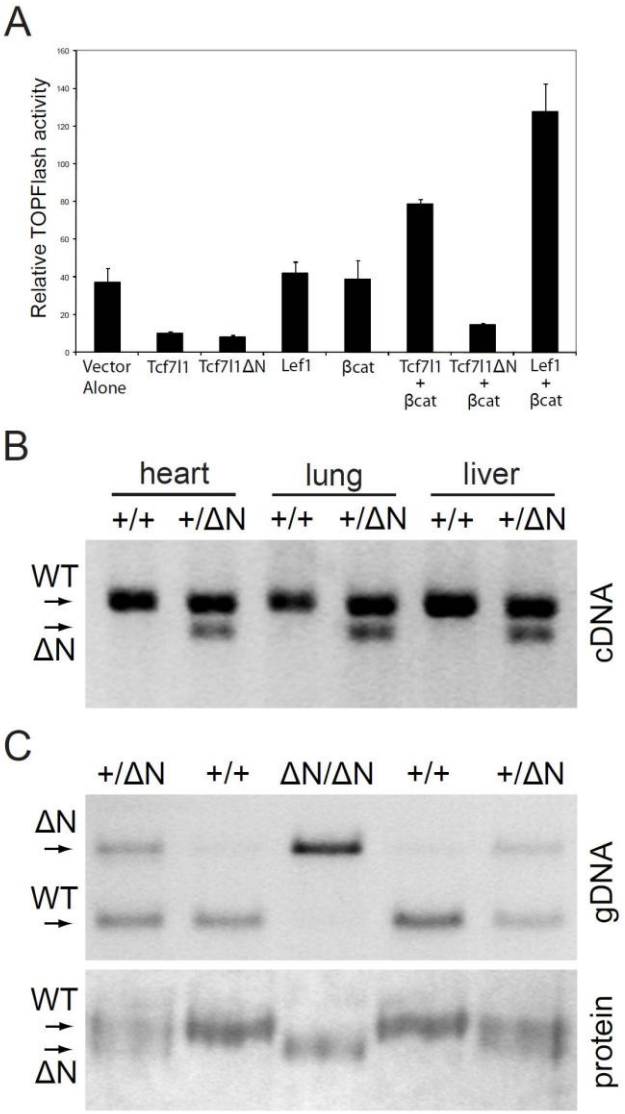
A
Relative TOPFlash activity
160
140
120
100
80
60
40
20
0
Vector Alone
Tcf7l1
Tcf7l1ΔN
Lef1
βcat
Tcf7l1 + βcat
Tcf7l1ΔN + βcat
Lef1 + βcat
B
heart
lung
liver
+/+
+/ΔN
+/+
+/ΔN
+/+
+/ΔN
WT
ΔN
cDNA
C
+/ΔN
+/+
ΔN/ΔN
+/+
+/ΔN
ΔN
WT
gDNA
WT
ΔN
protein

independent of Tcf7l1-β-catenin activity, indicating that Tcf7l1 is needed to function exclusively as a repressor during gastrulation.

3.2 Tcf7l1-β-catenin interaction is necessary for viability

To determine whether Tcf7l1-β-catenin interaction is necessary for any stage of development in mice, I examined the frequency and morphology of KI embryos after gastrulation. A drop in the frequency of KI embryos was first observed at E15.5 and was maintained at E18.5 and postnatal day (P) 1 (Figure 1E). No viable KI mice survived past P1, demonstrating that the Tcf7l1-β-catenin interaction is necessary for viability.

Mutant KI embryos displayed a variety of phenotypes with variable penetrance (proportion of mutants affected) and expressivity (extent of phenotypic defect). Neural tube defects in the form of exencephaly were observed in KI embryos (Figure 3A); the low frequency (less than 5% of embryos were affected) indicated that exencephaly was not the primary cause of KI lethality (Figure 3B). Edema occurred at high frequency between E12.5 and E15.5 (76% of KI embryos), and was not detected at later stages (Figure 3A,B). Vascular integrity defects and hemorrhages were externally visible in 50% of embryos between E15.5 and E18.5 (Figure 3A,B). The vascular integrity defects after E15.5 developed multiple presentations as telangiectasia (Figure 3A) or rupture of major blood vessels including the internal carotid artery (Figure 3C-F'). Since the frequency of KI inviability (100%) was greater than that of externally visible

Figure 3. Diverse requirements for Tcf7l1-β-catenin interaction during mouse embryogenesis.

(**A**) Representative images showing externally visible abnormal phenotypes of e15.5 to e18.5 KI embryos.

(**B**) Penetrance of abnormal phenotypes observed in KI mutants.

(**C,C'**) Images of intact WT (C) and KI (C') e18.5 embryos. Arrow in (C') points to externally visible hemorrhage.

(**D,D'**) Higher magnification view of the neck region of same embryos shown in (C,C'). Arrow in (D') points to externally visible hemorrhage.

(**E-F'**) H&E stained tissue sections from the neck region of the embryos shown in (C-D'). Boxed region contains the internal carotid artery (arrow) and is shown at higher magnification in (F,F'). Chevrons in (E') point to abnormal accumulation of blood in the KI embryo at the site of the externally visible embryo.

(**G,H**) H&E strained tissue sections from a submandibular salivary gland (G) and liver (H) of separate KI e18.5 embryos show abnormal red blood cell accumulation.

A

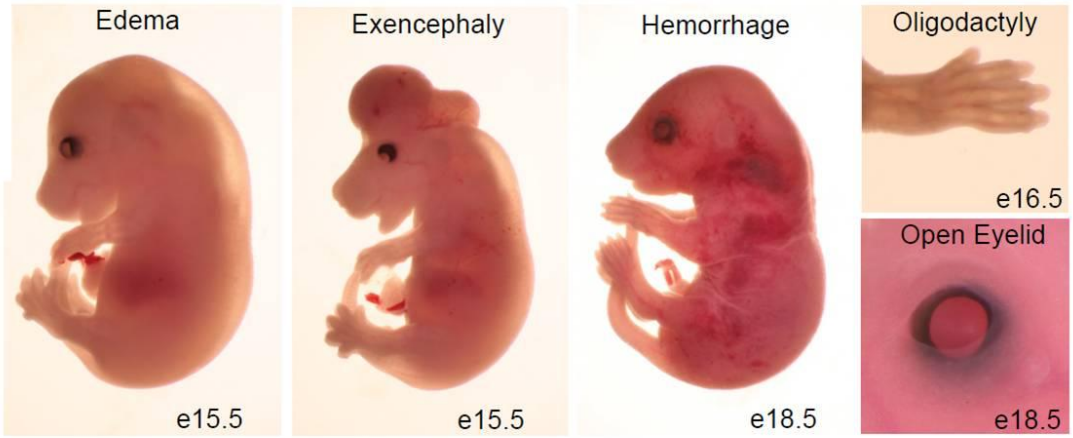

B

Genotype	Tcf7l1ΔN/ΔN				
	Edema	Exencephaly	Hemorrhage	Open Eyelid	Oligodactyly
e12.5	NA	NA	NA	NA	10/16(63%)
e15.5	42/55(76%)	1/55(2%)	NA	NA	34/55(62%)
e18.5	0/20(0%)	1/20(5%)	10/20(50%)	11/20(55%)	13/20(65%)
P1	0/4(0%)	0/4(0%)	0/4(0%)	2/4(50%)	2/4(50%)

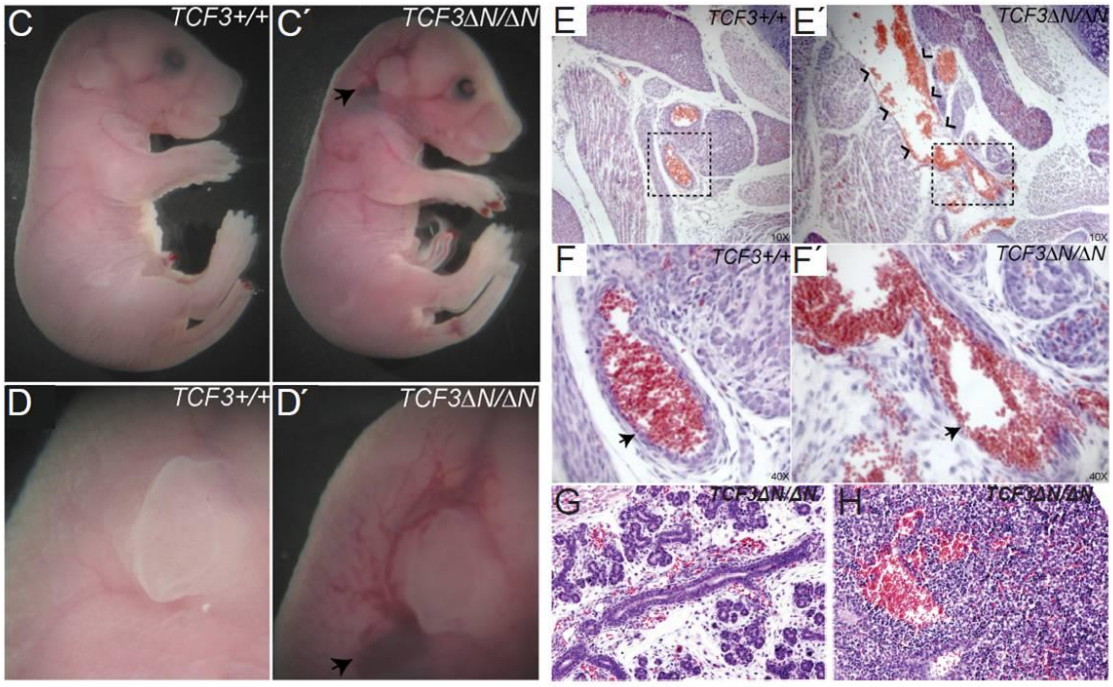

vascular integrity defects, I subjected E18.5 KI embryos lacking externally visible signs of defects to a comprehensive histopathological examination. Upon internal examination, each KI embryo displayed vascular integrity defects in organs such as the submandibular salivary gland (Figure 3G) and liver (Figure 3H). Based on the frequency and severity of the vascular integrity defects in KI embryos, I suggest that they are the primary cause of lethality in the mutants.

3.3 Tcf7l1-β-catenin interaction in early limb buds is necessary to specify posterior digits

In contrast to the variable expressivity of vascular integrity defects, two phenotypes exhibited consistent expressivity and high penetrance in KI embryos, simplifying elucidation of the etiology of the morphogenetic defects. First, distal limb morphogenesis was defective in 62% of KI embryos, which displayed oligodactyly characterized by the absence of the most posterior digit (digit #5) (Figure 3A,B; Figure 4A,A'). Four KI mutants also lacked digit #4 (not shown), and defects always manifested only in the forelimbs. Alizarin Red staining of mineralized tissue revealed the complete absence of digit #5 and the mineralization of bone tissue in other digits in KI limbs (Figure 4B,B').

To determine the etiology of the oligodactyly, I sought to identify the earliest defect affecting morphogenesis of KI limbs. *Tcf7l1* mRNA is expressed in the mesenchyme of the WT limb bud prior to E10.5 (Figure 4C) and becomes restricted to digit condensates by E11.5 (Figure 4C'). By E11.5, *Tbx2* expression

Figure 4. Tcf7l1-β-catenin interaction is required for post-axial digit formation.

(**A-B'**) Gross morphology of autopod limb segment in WT (A,B) and affected KI (A'B') limbs at e16.5 (A,A') and P1 (B,B'). Limbs were stained with Alizarin red (B,B') and numbers correspond anterior (#1) to posterior (#5) digits.

(**C,C'**) *In situ* hybridization of limb buds from e10.5 (C) and e11.5 (C') wild-type embryos using a labeled cRNA probe for Tcf7l1.

(**D-E'**) Whole mount *in situ* hybridization using a cRNA probe specific for Tbx2 mRNA and e11.5 (D,D') and e12.5 (E,E') embryos. The posterior edge of Tbx2 expression (arrows) in WT (D,E) limb buds was absent in KI (D',E') limb buds.

(**F,F'**) Tcf-β-catenin activity was detected with the BAT-Gal transgene in WT (F) and KI (F') limb buds at e10.0 (31ss). Arrows point to the high BAT-Gal activity in the posterior mesenchyme region of in WT limb buds (F) that is absent from KI limb buds (F').

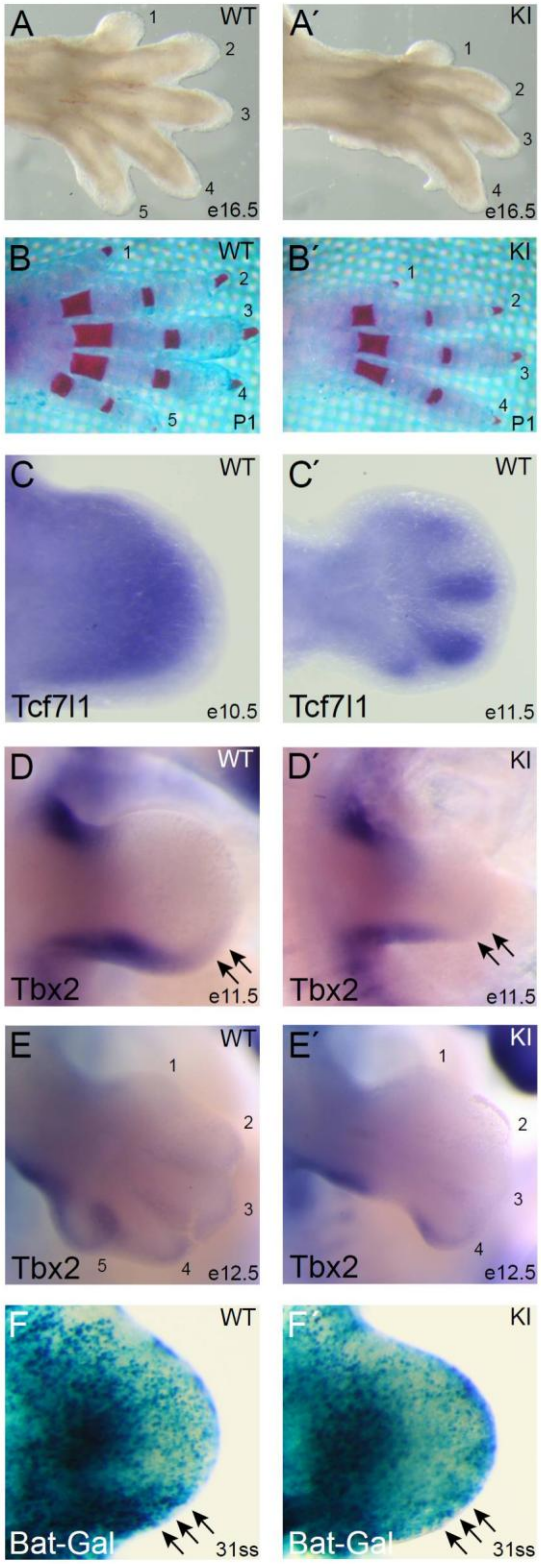
A
WT
1
2
3
4
5
e16.5
A´
KI
1
2
3
4
e16.5
B
WT
1
2
3
4
5
P1
B´
KI
1
2
3
4
P1
C
WT
Tcf7l1
e10.5
C´
WT
Tcf7l1
e11.5
D
WT
Tbx2
e11.5
D´
KI
Tbx2
e11.5
E
WT
1
2
3
Tbx2
5
4
e12.5
E´
KI
1
2
3
4
Tbx2
e12.5
F
WT
Bat-Gal
31ss
F´
KI
Bat-Gal
31ss

was reduced specifically at the distal posterior of the KI limb bud compared with control limb buds (arrows, Figure 4D,D'), indicating that the defect occurred prior to E11.5. By E12.5, loss of the posterior limb bud became apparent, the visualization of which being aided by the pattern of *Tbx2* expression, which outlines the forming digit #5 (Figure 4E,E').

The BAT-Gal transgene, in which Tcf/Lef binding sites drive the expression of *lacZ*, was used here to determine the pattern of Tcf/Lef-β-catenin-dependent transactivation in the limb bud (108). BAT-Gal was active in several compartments of the forming limb bud, including the apical ectodermal ridge (AER), the proximal mesenchyme and the posterior mesenchyme (Figure 4F). When BAT-Gal was examined in KI embryos, it was slightly diminished throughout the limb, but showed a substantial loss of activity specifically in the posterior mesenchyme at E10.0 (arrows, Figure 4F'). Furthermore, phospho-histone H3 and cleaved caspase 3 staining did not reveal a significant difference in proliferation or cell death, respectively, between WT and KI limb buds (Figure 5A-B'). These suggest that the loss of fifth digit is not caused by a decrease number of posterior mesenchymal cells in the limb bud but caused by alteration of signaling pathways during limb development. Immunofluorescent staining for each Tcf/Lef factor in WT E10.0 limb buds showed Tcf7l1 throughout the mesenchyme, Lef1 and Tcf7 in anterior and posterior mesenchyme, and Tcf7l2 in central mesenchyme (Figure 5C,D,E,F). In KI limb buds, there was a small but reproducible decrease in Lef1 and Tcf7 expression in the central and

Figure 5. Proliferation, apoptosis and Tcf/Lef expression during limb morphogenesis.

(**A,A'**) Immunofluorescence staining for phospho-histone H3 (green) and nuclei (red) in e10.0 limb buds from WT (A) and KI (A') embryos. A representative near the dorsoventral center is shown.

(**B,B'**) Immunofluorescence staining for cleaved caspase 3 (green) and nuclei (red) in e10.0 limb buds from WT (B) and KI (B') embryos. A representative near the dorsoventral center is shown.

(**C-F'**) Immunofluorescence staining for Tcf7l1 (C,C'), Lef1 (D,D'), Tcf7 (E,E') and Tcf7l2 (F,F') in e10.0 limb buds from WT (C,D,E,F) and KI (C',D',E',F') embryos. Solid lines indicate Lef1 and Tcf7 decrease expression in KI (D',E') embryos and dashed lines indicate regions where Lef1 and Tcf7 expression is similar to WT (D,E).

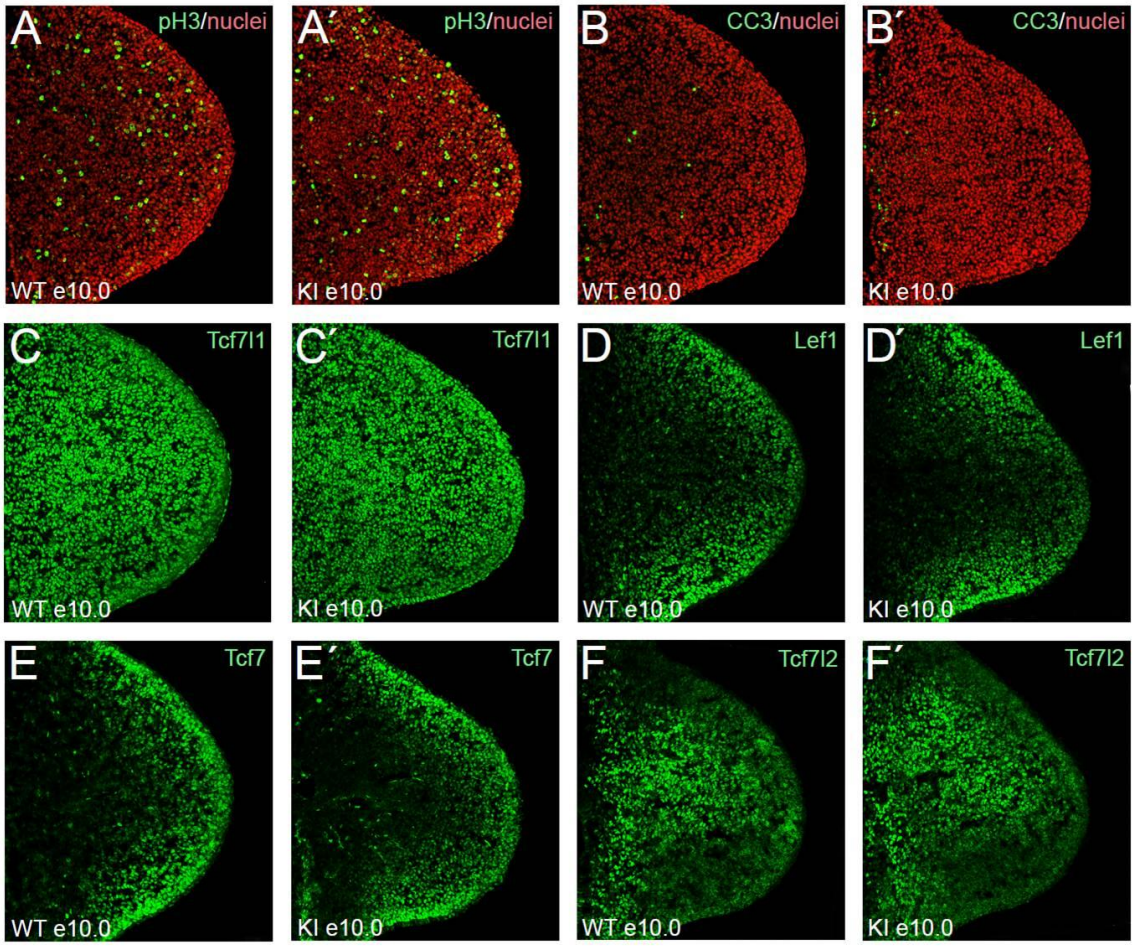
A
pH3/nuclei
WT e10.0
A´
pH3/nuclei
KI e10.0
B
CC3/nuclei
WT e10.0
B´
CC3/nuclei
KI e10.0
C
Tcf7l1
WT e10.0
C´
Tcf7l1
KI e10.0
D
Lef1
WT e10.0
D´
Lef1
KI e10.0
E
Tcf7
WT e10.0
E´
Tcf7
KI e10.0
F
Tcf7l2
WT e10.0
F´
Tcf7l2
KI e10.0

distal mesenchyme, and Lef1 was reduced in the distal posterior mesenchyme (Figure 5C',D',E',F'). These observations indicate that the Tcf7l1-β-catenin interaction has a direct effect on the posterior mesenchyme of the limb bud during early stages of morphogenesis.

The posterior mesenchyme of the limb bud is the location of an important organizer called the zone of polarizing activity (ZPA). The ZPA is necessary for posterior digit identity through Shh signaling and for maintenance of the AER (30,109,110). In addition to Shh, reciprocal signaling between the AER and ZPA involves the activity of other signaling pathways, including Fgf, Bmp and Wnt. Among the important interactions, Fgf and Wnt induce and maintain the expression of Shh (30,33,109), whereas Bmp inhibits Shh signaling (111,112). Wnt7a has been shown to maintain Shh expression, but this effect was suggested to be independent of Tcf/Lef-β-catenin because it was not inhibited by ΔNLef1 expression in chicken (111).

I tested the role of Tcf7l1-β-catenin interaction in regulating the relationship between the signaling pathways during early limb morphogenesis. *Shh* expression was induced normally in KI limb buds at E9.5 compared with WT limb buds (Figure 6A,A'), but it did not increase after E10.0 in KI limb buds in contrast to WT limb buds (Figure 6B-D'). The reduced *Shh* expression in KI limb buds reduced the activity of the pathway as detected by expression of the Shh target gene patched 1 (Figure 6E-F'). Reduction of *Shh* occurred prior to reduction of *Fgf8* (Figure 6G-H'), indicating that reduced Shh activity led to a reduction of Fgf8

Figure 6. Maintenance of Shh expression in the ZPA requires Tcf7l1-β-catenin interaction.

(**A-B'**) Whole mount *in situ* hybridization using cRNA probe specific for Shh mRNA and e9.5 (A,A') and e10.0 (B,B') embryos. Higher magnification views of the limbs are shown in Figure 4 C-D'.

(**C-N'**) Whole mount *in situ* hybridization of WT (C,D,E,F,G,H,I,J,K,L,M,N) and KI (C',D',E',F',G',H',I',J',K',L',M',N') limb buds using labeled cRNA probes for Shh (C-D'), Patched1 (E-F'), Fgf8 (G-H'), Gremlin1 (I-J'), Msx1 (K-L') and Msx2 (M-N') genes. Two stages of development observed in e10 embryos are shown and correspond to 30-31 somite stage (ss) (C,C',E,E',G,G',I,I',K,K',M,M') and 33-34ss (D,D',F,F',H,H',J,J',L,L',N,N').

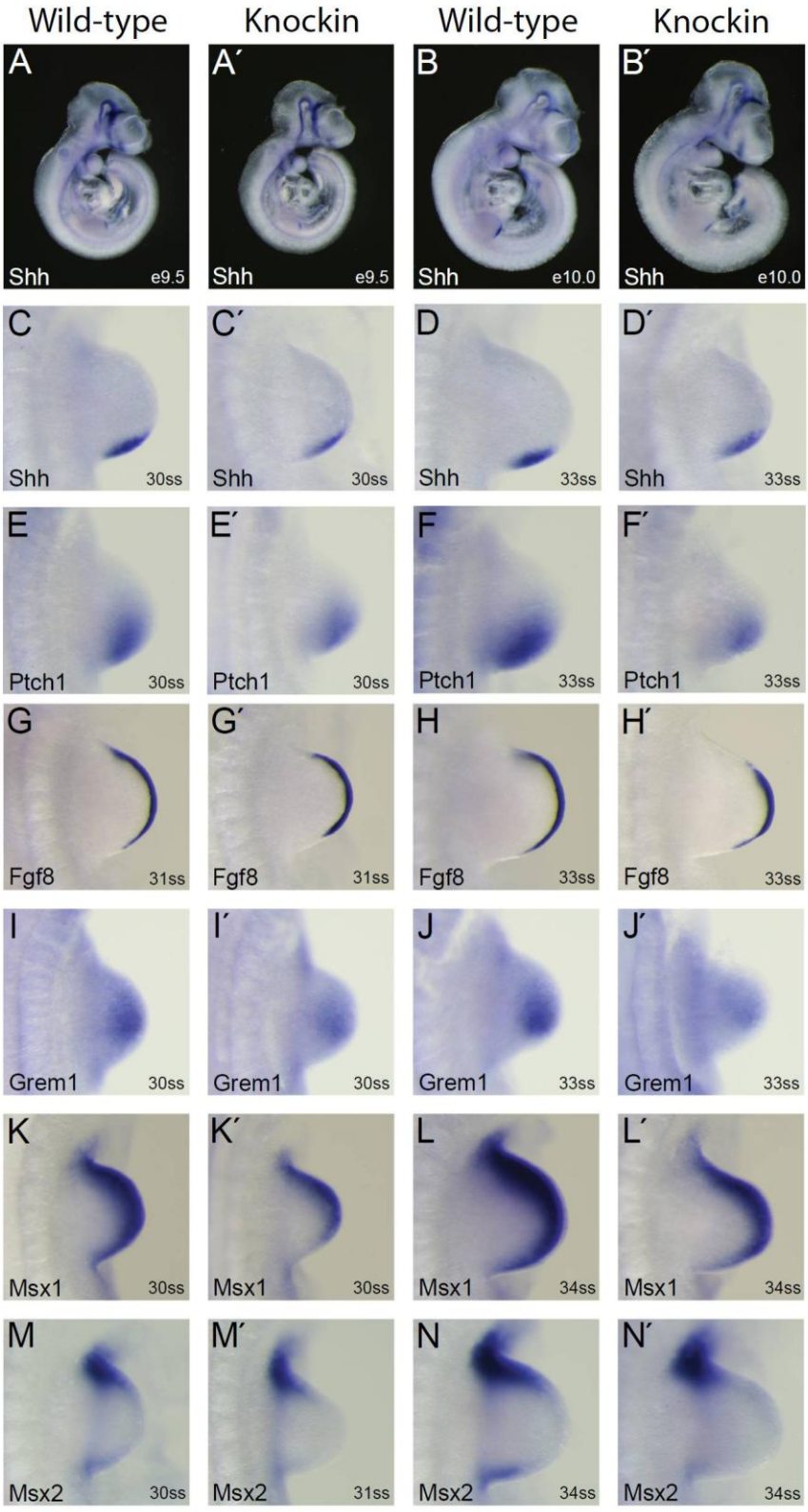
Wild-type
Knockin
Wild-type
Knockin
A
A´
B
B´
Shh e9.5
Shh e9.5
Shh e10.0
Shh e10.0
C
C´
D
D´
Shh 30ss
Shh 30ss
Shh 33ss
Shh 33ss
E
E´
F
F´
Ptch1 30ss
Ptch1 30ss
Ptch1 33ss
Ptch1 33ss
G
G´
H
H´
Fgf8 31ss
Fgf8 31ss
Fgf8 33ss
Fgf8 33ss
I
I´
J
J´
Grem1 30ss
Grem1 30ss
Grem1 33ss
Grem1 33ss
K
K´
L
L´
Msx1 30ss
Msx1 30ss
Msx1 34ss
Msx1 34ss
M
M´
N
N´
Msx2 30ss
Msx2 31ss
Msx2 34ss
Msx2 34ss

in the AER (Figure 6H'). Expression of gremlin 1, a Bmp antagonist important for maintenance of Shh in the ZPA (29), was decreased in KI compared with WT limb buds (Figure 6I-J'). To test whether *Shh* reduction in KI limb buds could be due to increased Bmp signaling, I examined expression of the Bmp target genes *Msx1* and *Msx2* (Figure 6K-N'). The decreased levels of *Msx1* and *Msx2* in KI limb buds indicated that decreased *Shh* was not caused by increased Bmp activity. Therefore, I suggest that the Tcf7l1-β-catenin interaction is necessary for the Wnt/β-catenin mediated maintenance of high levels of Shh in the ZPA. The partially decreased activity in the ZPA leads to secondary effects reducing signaling throughout the limb bud.

3.4 Tcf7l1-β-catenin interaction in the mucocutaneous junction is necessary for eyelid closure

A second highly penetrant and consistent morphogenetic defect was incomplete eyelid closure, which occurred in 54% of KI mutants (Figure 3A,B). Mice are normally born with fused eyelids, which stay closed until P12-14 (113). Closure occurs between E15 and E16, stages when periderm cells at the tips of eyelids migrate towards the center of the eye (Figure 7A) (113). The eyelid primordia follow the periderm projections until the upper and lower eyelids meet and fuse to form a conjunctival sac necessary for corneal development (Figure 7B) (113). Closure requires actin polymerization and activation of Fgf10, Shh, Tgfα and Mekk1/JNK kinases (Figure 8A,B,C,D) (114-117) and does not occur when

Figure 7. Discrete requirement for Tcf7l1-β-catenin interaction in the eyelid.
(**A-B'**) Hematoxylin and eosin (H&E) staining of the eye and eyelids in WT (A,B) and KI (A',B') embryos at e15.5 (A,A') and e16.5 (B,B').
(**C,C'**) Tissue sections of e14.5 eyelids from BAT-Gal transgenic mice were stained with X-gal. The mucocutaneous junction (MCJ) stains positively for BAT-Gal activity (dotted line) in WT (C) and is reduced in size in KI (C') eyelids. Solid lines at the basement membrane denote palebral epidermis (PE) and palebral conjunctiva (PC) regions (C).
(**D,D'**) Immunofluorescence staining for β-galactosidase (red) and Ki67 (green) in e14.5 eyelids from BAT-Gal+ WT (D) and KI (D') embryos. The BAT-Gal activity (bar) is in Ki67-negative cells and its size is reduced in KI eyelids.
(**E-F'''**) Immunofluorescence staining for Lef1 (E,F; red), Tcf7l1 (E',F'; green), and β-galactosidase (E'',F''; blue) in e14.5 eyelids from BAT-Gal transgenic WT (E-E''') and KI (F-F''') embryos. Arrows point to Lef1 positive nuclei with low levels of Tcf7l1. Arrowheads point to Tcf7l1 and Lef1 double positive nuclei, which were observed in WT (E-E''') but not KI (F-F'''). The dotted demarcates the BAT-Gal positive region of the MCJ.

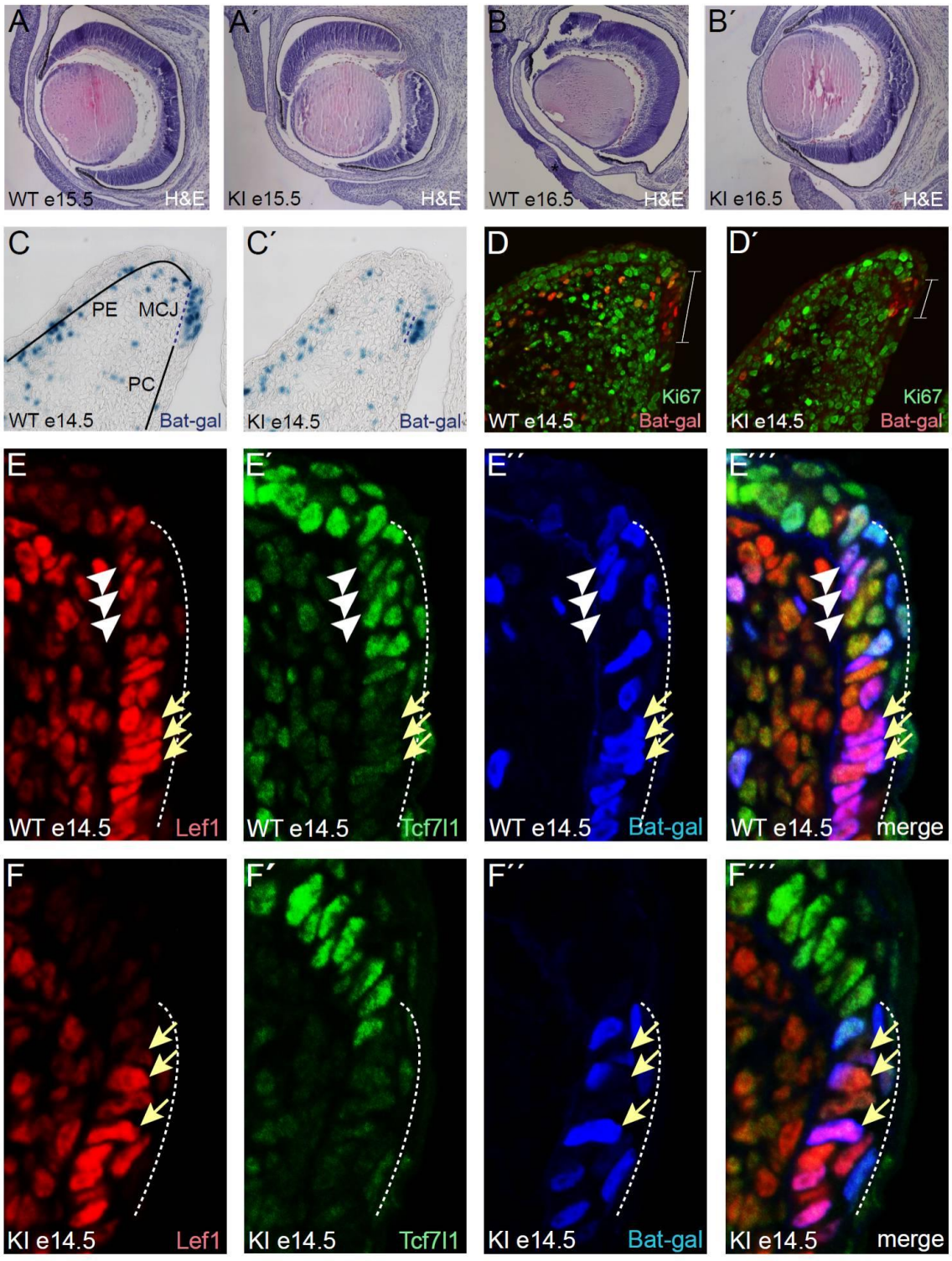
A
WT e15.5
H&E
A´
KI e15.5
H&E
B
WT e16.5
H&E
B´
KI e16.5
H&E
C
PE
MCJ
PC
WT e14.5
Bat-gal
C´
KI e14.5
Bat-gal
D
Ki67
WT e14.5
Bat-gal
D´
Ki67
KI e14.5
Bat-gal
E
WT e14.5
Lef1
E´
WT e14.5
Tcf7l1
E´´
WT e14.5
Bat-gal
E´´´
WT e14.5
merge
F
KI e14.5
Lef1
F´
KI e14.5
Tcf7l1
F´´
KI e14.5
Bat-gal
F´´´
KI e14.5
merge

Figure 8. Signaling in the KI eyelid.

(**A-C'**) Immunofluorescent staining of eyelids from WT (A,B,C) and KI (A',B',C') e14.5 embryos. Antibodies detected phosphorylated-ERK (A,A'), phosphorylated-JNK (B,B'), and phosphorylated-c-Jun (C,C').

(**D,D'**) FITC-phalloidin (green) staining of filamentous actin is abundant in the periderm tip of the eyelid in WT (D), but not KI (D'), eyelids at e15.5.

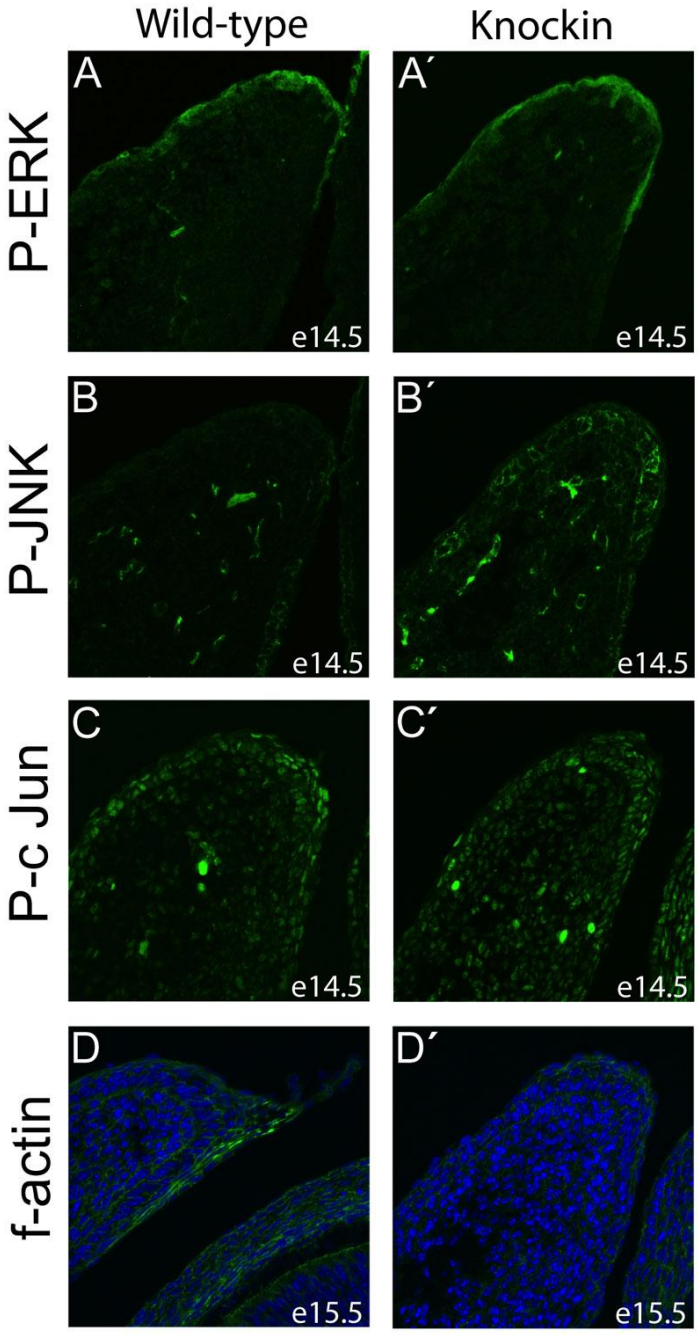
Wild-type
Knockin
P-ERK
P-JNK
P-c Jun
f-actin
A
A´
B
B´
C
C´
D
D´
e14.5
e14.5
e14.5
e14.5
e14.5
e14.5
e15.5
e15.5

Tcf7l1 is overexpressed in the skin epidermis (72). In KI eyelids, the projection of migrating periderm cells was severely diminished at E15.5 (Figure 7A') and remained incomplete at E16.5 (Figure 7B'). Signaling detected by phospho-ERK, phospho-JNK and phospho-c-Jun antibody staining did not appear to be defective in KI eyelids prior to closure (Figure 8 A',B',C',D'). By contrast, whereas filamentous actin was increased in the migrating cells in the WT, it was not increased in the KI periderm cells (Figure 8D,D'), indicating that KI defects occurred during or prior to periderm cell migration.

To identify the cells requiring Tcf7l1-β-catenin interaction, the activity of Tcf-β-catenin reporter transgenes was examined. In WT eyelids, BAT-Gal and TOPGal activity was present in a band of cells at the forming mucocutaneous junction (MCJ) (Figure 7C; Figure 9A,B,C,D). The MCJ is positioned at the transition between two epithelia: the palpebral conjunctiva on the eyelid surface facing the eye and the palpebral epidermis on the eyelid surface at the exterior of the embryo (118,119). Intriguingly, based on their slow cycling, cells from the MCJ have been suggested to be the stem cells for conjunctival epithelia in primates and rabbits (120,121). The slow cycling of the mouse MCJ cells was made apparent by the lack of immunofluorescent staining for the Ki67 cell proliferation marker in the MCJ patch compared with the highly proliferative cells throughout the growing eyelid (Figure 7D). Double immunofluorescent staining for β-galactosidase showed that the Ki67-negative MCJ cells were also the BAT-Gal-positive cells in the eyelid epithelium (Figure 7D). Immunofluorescent

Figure 9. TOPGal activity in WT and KI eyelids.

(**A-B'**) Whole mount X-gal staining of TOPGal-positive WT (A,B) and KI (A'B') embryos at e14.5 (A,A') and e15.5 (B,B'). U - upper eyelid; L - lower eyelid.

(**C-D'**) X-gal staining of coronal sections through the eye and eyelid of WT (C,D) and KI (C',D') embryos at e14.5 (C,C') and e15.5 (D,D').

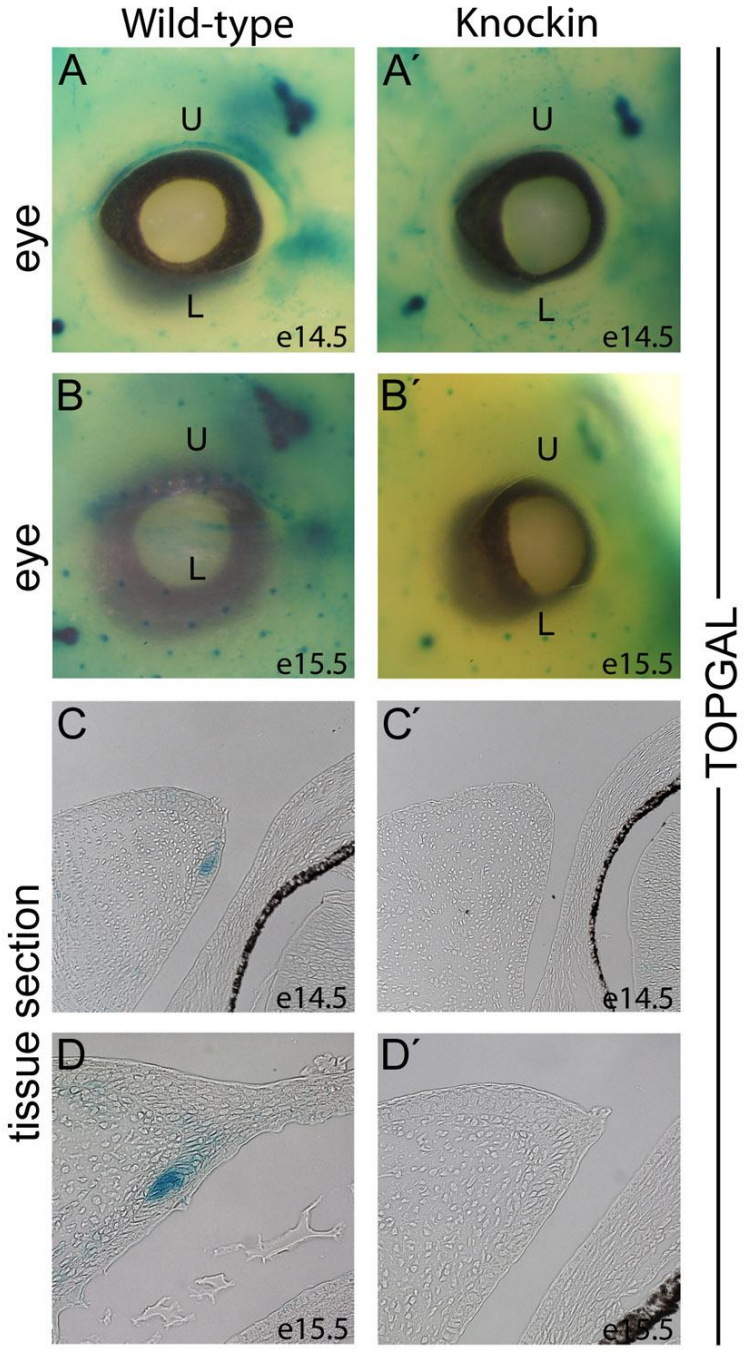
Wild-type
Knockin
A
A´
U
L
e14.5
B
B´
e15.5
C
C´
D
D´
eye
eye
tissue section
TOPGAL

staining at E12.5 and E13.5 indicated that the onset of slow cycling coincided with BAT-Gal activation (Figure 10C,D).

In KI eyelids, BAT-Gal activity was detectable in both the mesenchyme and MCJ region; however, the domain of activity in the KI MCJ region was less than half that in the WT (Figure 7C'). Compared with BAT-Gal, TOPGal displayed weaker activity in WT MCJ, and TOPGal activity was effectively undetectable in KI eyelids at E14.5 and E15.5 (Figure 9). The reduction of Tcf-β-catenin reporter activity in the KI perfectly coincided with the reduced size of the slow-cycling (Ki67- negative) band of cells at the MCJ region (Figure 7D'). Considering the three-dimensional structure of the band of MCJ cells lining the edge of the eyelid, I suggest that the reduction observed on the KI eyelid is substantial and represents the source of initial defects leading to the open eyelid at birth phenotype observed in KI mice.

The observation that BAT-Gal activity was reduced, but not completely absent, in KI eyelids indicated a potentially interesting effect of Tcf7l1-β-catenin on target gene activation. Since Tcf7l1ΔN cannot directly activate Tcf-β-catenin reporters, BAT-Gal activity in KI eyelids indicated the presence of another Tcf/Lef protein. Immunofluorescent staining for each Tcf/Lef factor showed Lef1 in eyelid epithelium from E12.5 to E14.5 (Figure 7E; Figure 10A,B); Tcf7 was only present in underlying mesenchyme and Tcf7l2 was not detected (Figure 10E,F). Interestingly, Lef1 (Figure 7E) and Tcf7l1 (Figure 7E') proteins were expressed in opposing gradients over the typically 10- to 15- cell-wide zone of BAT-Gal activity

Figure 10. Tcf/Lef and BAT-Gal expression during eyelid morphogenesis.
(**A-B’’’**) Immunofluorescent staining of coronal section through the eyelid primordia of a BAT-Gal-positive WT embryo at e12.5 (A-A’’’) and e13.5 (B-B’’’). Antibodies specific for Lef1 (red; A,B), Tcf7l1 (green; A’,B’), and β-galactosidase (blue; A’’,B’’) were used simultaneously on each tissue section.
(**C,D**) Immunofluorescent staining of coronal section through the eyelid primordia of a BAT-Gal-positive WT embryo at e12.5 (C) and e13.5 (D). Antibodies specific for β-galactosidase (red) and Ki67 (green) were used simultaneously on each tissue section.
(**E**) Immunofluorescent staining of coronal section through an e14.5 eyelid with an antibody specific for Tcf7.
(**F**) Immunofluorescent staining of coronal section through an e14.5 eyelid with an antibody specific for Tcf7l2.

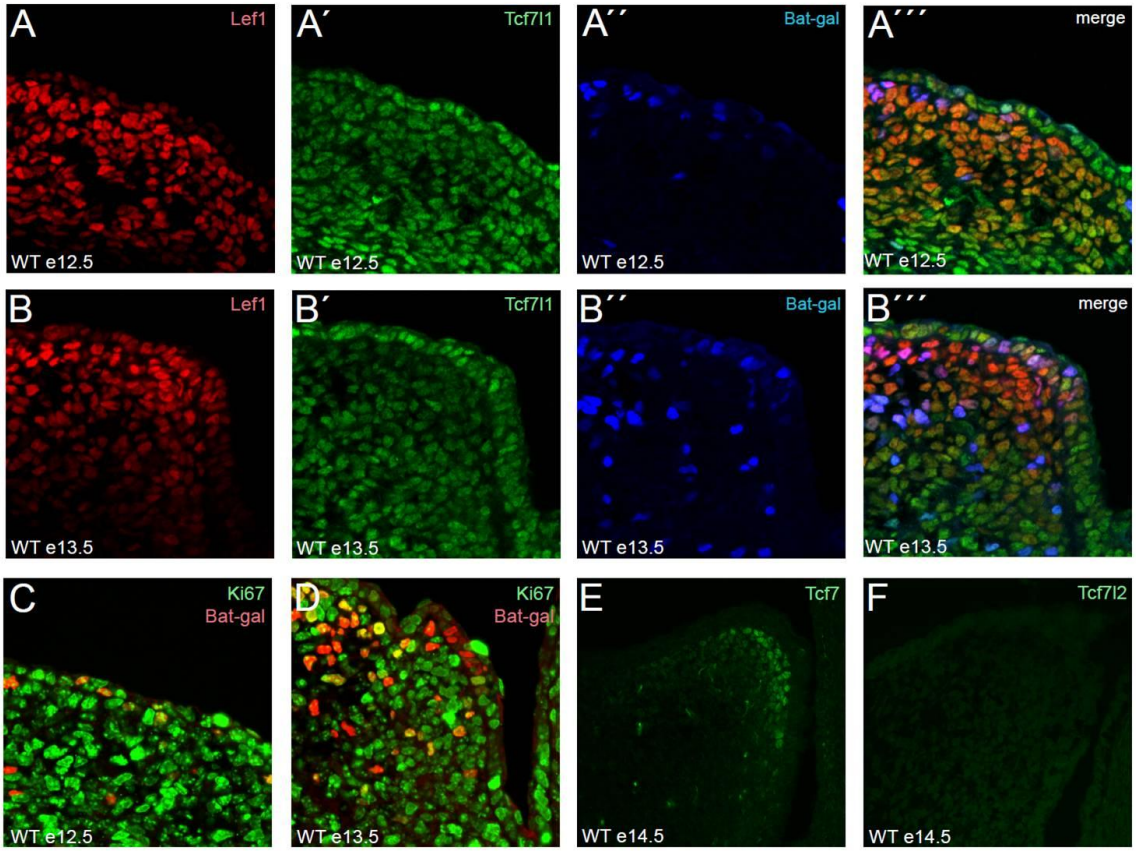
A
Lef1
WT e12.5
A´
Tcf7l1
WT e12.5
A´´
Bat-gal
WT e12.5
A´´´
merge
WT e12.5
B
Lef1
WT e13.5
B´
Tcf7l1
WT e13.5
B´´
Bat-gal
WT e13.5
B´´´
merge
WT e13.5
C
Ki67
Bat-gal
WT e12.5
D
Ki67
Bat-gal
WT e13.5
E
Tcf7
WT e14.5
F
Tcf7l2
WT e14.5

(Figure 7E'') at the WT MCJ region (dotted line, Figure 7E-E'''). Tcf7l1 was most highly expressed at the epidermal side (Figure 7E') and Lef1 was most highly expressed at the conjunctival side of the MCJ (Figure 7E). BAT-Gal was active in both Tcf7l1-high (arrowheads, Figure 7E-E''') and Tcf7l1-low (arrows, Figure 7E-E''') cells, but only in cells with high levels of Lef1 (Figure 7E-E'''). Instead of the overlapping, opposing gradients of Tcf7l1 and Lef1 seen in WT, KI eyelids displayed an abrupt transition from Tcf7l1-high/Lef1-low (Figure 7F') to Tcf7l1-low/Lef1-high expression (arrows, Figure 7F). BAT-Gal was active only in Tcf7l1-low/Lef1-high cells (arrows, Figure 7F-F'''). Thus, in KI eyelids, the domain of BAT-Gal activity was reduced in size, and this restriction directly corresponded with a restriction of Lef1 expression. I interpret the observation that BAT-Gal was active only in Lef1-expressing cells to suggest that Lef1-β-catenin, and not Tcf7l1-β-catenin, is necessary for the activation of downstream target genes.

3.5 Wnt/β-catenin stimulates Lef1 levels by inhibiting Tcf7l1 repression

Since Lef1 expression is lost in Tcf7l1-positive cells in the KI, I examined the possibility that β-catenin inhibits Tcf7l1 repression of *Lef1* transcription. ESCs were used to test this possible relationship because they had been previously found to express high levels of Tcf7l1 and other Tcf/Lef proteins (73,122). Treating ESCs with recombinant Wnt3a for 24 hours increased *Lef1* mRNA levels 2.5-fold (Figure 11A), demonstrating that they were a good system with which to examine Wnt regulation of Lef1 expression. Chromatin immunoprecipitation

Figure 11. Wnt3a stimulates gene expression through regulation of Tcf7l1 and Lef1 levels in ESCs.

(**A**) Quantitative real-time PCR (qPCR) analysis of cDNA made after treating WT ESCs with 50ng/ml Wnt3a for 12hrs. Values represent fold-changes to the mRNA levels of Tcf7l1 and Lef1 factor relative to starting levels.

(**B,C**) Quantitative ChIP-qPCR analysis of Tcf7l1 binding to target genes *Axin2* and *Cdx1* in ESCs chromatin from WT (B) or KI (C) ESCs treated with control or Wnt3a-conditioned media for 24 hours. Values represent the mean of five biological replicates ± s.d. Neg: negative control sites not bound by Tcf7l1.

(**D**) SuperTOPFlash luciferase reporter assay in ESCs. Tcf7l1 KO ESCs were transiently transfected with expression plasmids for ΔNβ-catenin, Lef1, and/or Tcf7l1. SuperTOPFlash activity is shown compared to Renilla luciferase control for each transfection. Values represent the mean of biological triplicates ± s.d.

(**E**) Schematic showing the human Lef1 promoter constructs used for transfections. Numbers refer to base pairs from the Lef1 translation start site. Numbers in parentheses refer to the equivalent sites in the mouse Lef1 gene.

(**F**) Quantitative ChIP-qPCR analysis of Tcf7l1 binding to different regions of the mouse Lef1 promoter. Chromatin from KO ESCs (gray bars) was used as a negative control. Values represent mean of three biological replicates ± s.d.

(**G**) Quantitative ChIP-qPCR analysis of β-catenin binding to different regions of the mouse *Lef1* promoter. WT ESCs were treated with 50 ng/ml Wnt3a for 24 hours. Values represent the mean of three biological replicates ± s.d.

(**H,I**) Lef1 promoter luciferase reporter plasmids were transiently transfected into ESCs with a Tcf7l1-expression plasmid or its empty vector control. Cells were treated with Wnt3a conditioned media or control conditioned media for 24 hours.

(**J,K**) *Lef1* promoter luciferase reporter constructs were cotransfected with three concentrations of Tcf7l1 expression constructs and treated for 24 hours with three concentrations of Wnt3a-conditioned media.

(**L**) Model illustrating the role of balancing Tcf7l1 and Lef1 levels in mediating Wnt/β-catenin signaling. Genes are boxed; proteins are in ovals. Wnt/β-catenin-responsive target genes (WRG) are repressed (red line) by Tcf7l1 and activated (green line) by Lef1–β-catenin. Wnt inhibits Tcf7l1 repression of WRG and *Lef1* gene expression in a β-catenin-dependent manner.

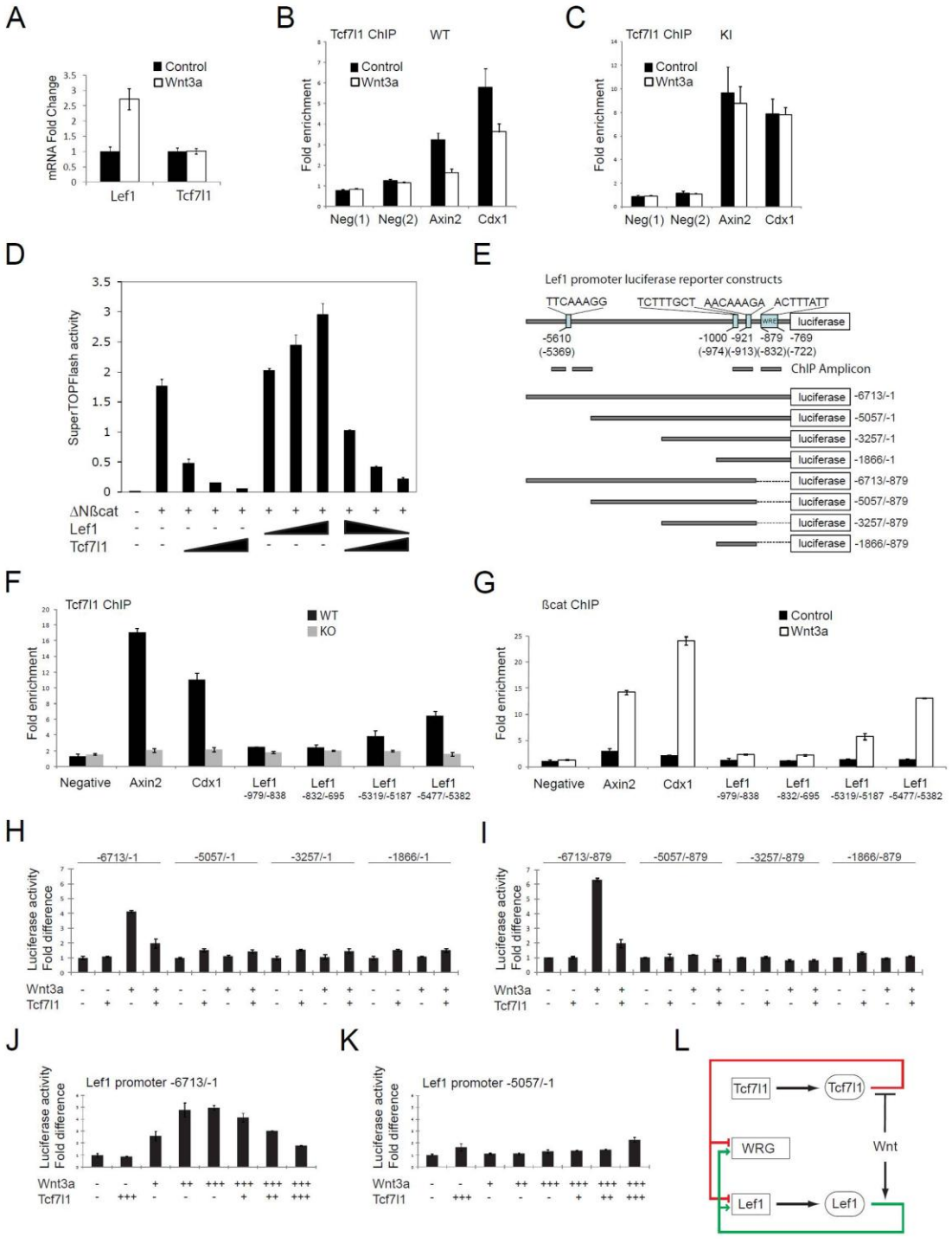
A
mRNA Fold Change
Control
Wnt3a
Lef1
Tcf7l1
B
Tcf7l1 ChIP WT
Fold enrichment
Neg(1) Neg(2) Axin2 Cdx1
C
Tcf7l1 ChIP KI
D
SuperTOPFlash activity
ΔNßcat
Lef1
Tcf7l1
E
Lef1 promoter luciferase reporter constructs
TTCAAAGG
TCTTTGCT AACAAAGA ACTTTATT
luciferase
-5610
(-5369)
-1000 -921 -879 -769
(-974)(-913)(-832)(-722)
ChIP Amplicon
-6713/-1
-5057/-1
-3257/-1
-1866/-1
-6713/-879
-5057/-879
-3257/-879
-1866/-879
F
Tcf7l1 ChIP
WT
KO
Negative Axin2 Cdx1 Lef1 -979/-838 Lef1 -832/-695 Lef1 -5319/-5187 Lef1 -5477/-5382
G
ßcat ChIP
H
Luciferase activity Fold difference
I
J
Lef1 promoter -6713/-1
K
Lef1 promoter -5057/-1
L
Tcf7l1
WRG
Wnt
Lef1

followed by quantitative PCR showed that Wnt3a decreased the occupancy of Tcf7l1 on endogenous target genes in a Tcf7l1-β-catenin-dependent manner (Figure 11B,C). As described previously, Tcf7l1 functioned as a transcriptional repressor in ESCs, whereas Lef1 functioned as a β-catenin-dependent activator of target gene transcription (Figure 11D) (107).

To determine whether Tcf7l1 directly represses *Lef1* transcription, the Lef1 upstream regulatory region was examined. Several potential Tcf/Lef binding sites were noted based on the consensus sequence ($^{A}/_{T}{}^{A}/_{T}$CAAAG), including a previously identified Wnt responsive element (WRE) (Figure 11E) (69). Tcf7l1 occupied positive control sites (*Axin2*, *Cdx1*) (123,124) and the -5.3 kb *Lef1* site, but not the previously described WRE in ESCs (Figure 11F).

A DNA fragment consisting of -6713 to -1 bp of human *LEF1* was inserted upstream of a luciferase reporter gene to generate a Lef1 reporter plasmid active in ESCs (Figure 11H) (125). To test the effects of Wnt and Tcf7l1, the Lef1 reporter was transfected into *Tcf7l1*-/- ESCs with and without Wnt3a stimulation and with and without cotransfection with a Tcf7l1 expression plasmid. Wnt3a stimulated Lef1 reporter activity, whereas Tcf7l1 repressed activity (Figure 11H,I). Comparing Lef1 reporter activity in WT and *Tcf7l1* knockout (KO) ESCs indicated that endogenous Tcf7l1 protein acted only as a repressor and that Tcf7l1 did not contribute to Wnt3a activation of the Lef1 reporter (Figure 12). Wnt3a stimulated β-catenin occupancy at the -5.3 kb site (Figure 11G). Removing the Tcf7l1 binding site at -5.3 kb prevented Wnt3a-mediated activation and Tcf7l1-mediated

Figure 12. Endogenous Tcf7l1 represses a Lef1 reporter.

(**A**) −6713/−1 Lef1 reporter plasmid was transiently transfected into WT and KO ESCs. Cells were co-transfected with myc-Tcf7l1 expression plasmid or its empty vector control and treated with Wnt3a-conditioned media or control conditioned media for 24 hours prior to processing for luciferase activity. Values represent mean of biological triplicates ± s.d.

(**B**) Same experiment as A except the −6713/−879 Lef1 reporter plasmid was used.

A

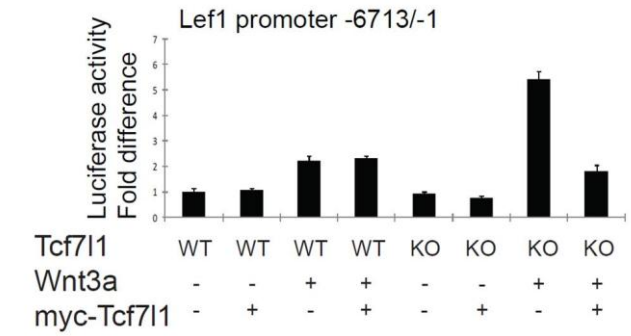
Lef1 promoter -6713/-1
Luciferase activity
Fold difference
0
1
2
3
4
5
6
7
Tcf7l1 WT WT WT WT KO KO KO KO
Wnt3a - - + + - - + +
myc-Tcf7l1 - + - + - + - +

B

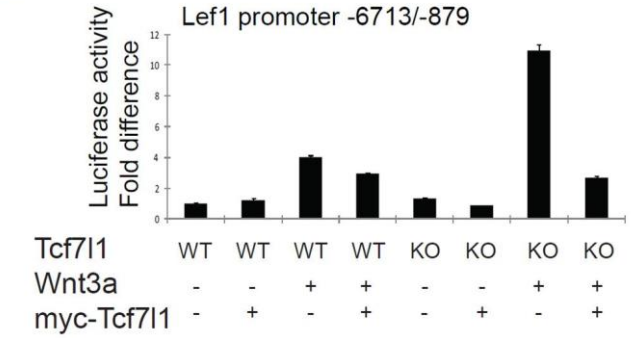
Lef1 promoter -6713/-879
Luciferase activity
Fold difference
0
2
4
6
8
10
12
Tcf7l1 WT WT WT WT KO KO KO KO
Wnt3a - - + + - - + +
myc-Tcf7l1 - + - + - + - +

repression of the Lef1 reporter (Figure 11H,I). Further truncation of the Lef1 reporter did not restore significant responsiveness to Wnt3a or Tcf7l1 (Figure 11H,I). Tcf7l1 repression and Wnt3a activation of the Lef1 reporter displayed a competitive concentration dependence (Figure 11J,K).

Taken together, these data indicate that Tcf7l1 represses Lef1 and that endogenous Tcf7 and Lef1 mediate Wnt3a stimulation of *Lef1* transcription. They support the existence of the circuit illustrated in Figure 11L.

3.6 Transgenic overexpression of Tcf7l1 represses endogenous Tcf/Lef-β-catenin activity

I hypothesized that Tcf7l1-β-catenin is not required to activate target genes but instead must alleviate Tcf7l1 repression of genes, particularly *Lef1* (Figure 11L). Results from previous Tcf7l1 overexpression experiments in mouse skin ostensibly support this hypothesis (98); however, it must be noted that the transgenic mouse experiments focused on cells lacking endogenous Tcf/Lef-β-catenin transcriptional activity (72,98). Thus, it was not known whether Tcf7l1 would repress or activate transcription when it was transgenically expressed in a cell type that both endogenously expresses Tcf7l1 and endogenously activates Tcf/Lef-β-catenin targets. Owing to the Tcf7l1 expression and BAT-Gal activity in the MCJ region, it provided a perfect context in which to test whether Tcf7l1-β-catenin activates target genes *in vivo*.

Tcf7l1 was overexpressed in the MCJ using a bi-transgenic doxycycline-inducible system (98). The expression of Tcf7l1 occurred in a mosaic pattern (Figure 13A), which was useful for distinguishing cell-autonomous from non-cell autonomous effects. In cells with overexpressed Tcf7l1, BAT-Gal activity was not detected (Figure 13A'), indicating that full-length Tcf7l1 functioned as a transcriptional repressor and not an activator in these cells. Moreover, Tcf7l1 overexpression in the MCJ repressed Lef1 expression (Figure 13A''). Both the repression of BAT-Gal and Lef1 occurred in a cell-autonomous manner, as neighboring cells that did not overexpress Tcf7l1 displayed Lef1 expression and BATGal activity. The mosaic expression of Tcf7l1 and the mosaic repression of Lef1 in the transgenic mice were sufficient to recapitulate the eyelid closure defect observed in KI mice (Figure 13C,C'). Given that the MCJ cells activate BAT-Gal in cells without Tcf7l1 overexpression, these data indicate that Tcf7l1 only represses target genes. Instead, β-catenin interaction with Tcf7l1 derepresses *Lef1* expression, leading to the formation of Lef1-β-catenin activator complexes (Figure 11L).

Figure 13. Full length Tcf7l1 represses Lef1 and BAT-Gal in the MCJ.

(**A-B’’’**) Immunofluorescent staining of e14.5 eyelids from Tcf7l1-overexpressing double-transgenic (A-A’’’) and control single-transgenic (B-B’’’) embryos. Transgenic Tcf7l1 (A; green) was expressed in a mosaic pattern in double transgenic embryos. BAT-Gal activity (A’; blue) and Lef1 expression (B’’; red) was low in Tcf7l1-overexpressing cells (arrowheads). In neighboring cells that did not overexpress Tcf7l1 (arrows), BAT-Gal activity and Lef1 expression was similar to levels in control embryo (B’,B’’).

(**C,C’**) Image of the eye region for a control single transgenic embryo (C) and a Tcf7l1-overexpressing bitransgenic littermate (C’) at e16.5.

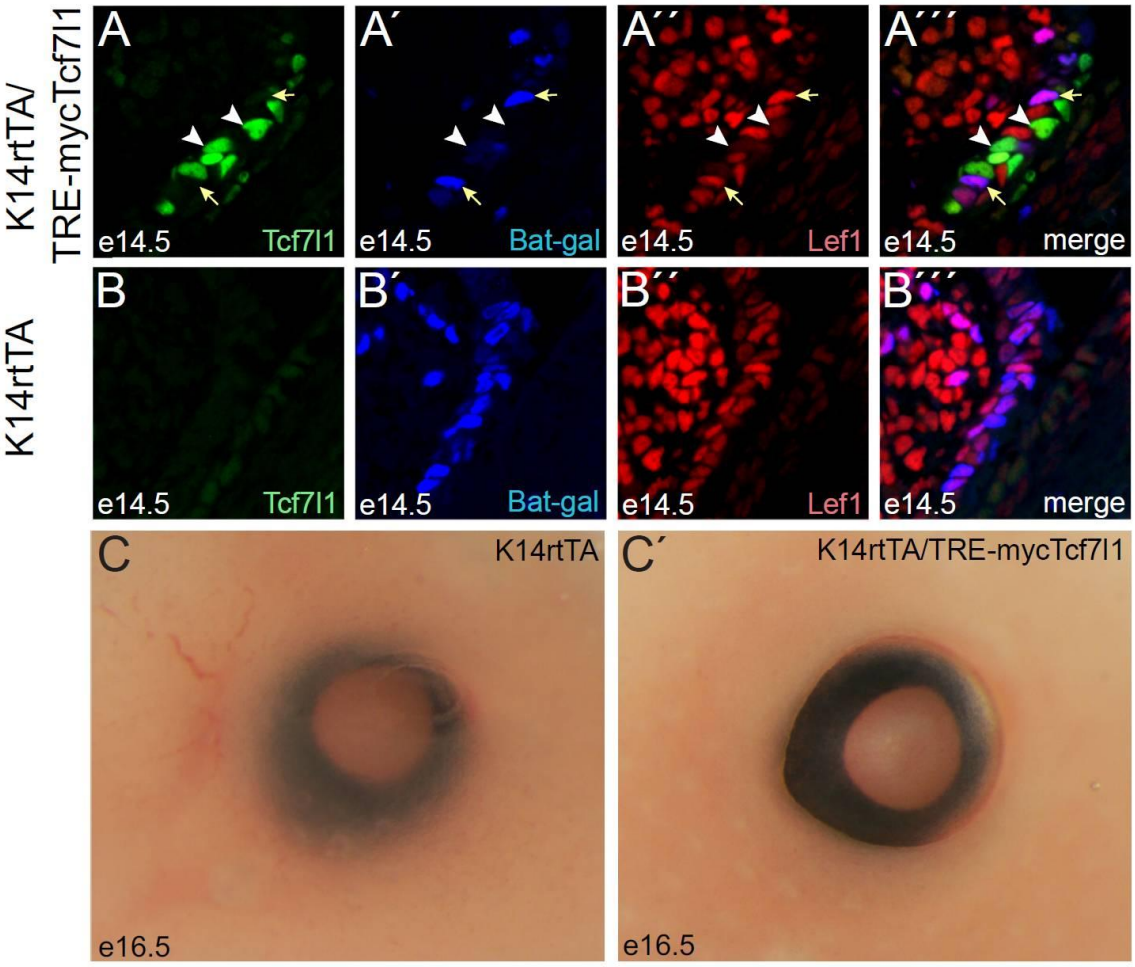
K14rtTA/
TRE-mycTcf7l1
K14rtTA
A
A´
A´´
A´´´
B
B´
B´´
B´´´
e14.5
Tcf7l1
Bat-gal
Lef1
merge
C
C´
K14rtTA
K14rtTA/TRE-mycTcf7l1
e16.5

4. Discussion

The core components of the canonical Wnt/β-catenin signaling pathway have been evolutionarily conserved from cnidaria to chordates, and the pathway classically functions by β-catenin binding to Tcf/Lef proteins and converting them to transcriptional activators (41,42,65). Although Tcf7l1-β-catenin interaction has been well characterized (106,126), fitting Tcf7l1 into this model has been somewhat problematic. This is primarily because Tcf7l1 appeared to act as a transcriptional repressor in loss-of-function experiments in diverse organisms (78-80,100). In addition, overexpression experiments in mice showed that Tcf7l1 affected cell fates *in vivo* independently of β-catenin interaction (72,98). We investigated this paradox by performing a powerful and direct test of genetically ablating β-catenin binding from Tcf7l1 with a *Tcf7l1*ΔN knock-in mutation. The morphogenetic defects in KI embryos and lethality of KI mice provide formal genetic proof that Tcf7l1-β-catenin interaction is necessary for embryogenesis and viability. To my knowledge, the limb morphogenesis, vascular integrity and eyelid closure defects in the KI mice identify the first locations where Tcf7l1 functions in animals have been genetically proven to require β-catenin interaction.

The phenotype of oligodactyly observed in KI embryos suggests that Tcf7l1-β-catenin interaction controls the level of Wnt target gene expression in the posterior mesenchyme of the limb bud. Wnt3, Wnt5a and Wnt7a have been implicated in limb bud development (31-33). Furthermore, β-catenin in the ectoderm and mesoderm of limb bud has been investigated via conditional

knockout in mice (31,34). In addition, Lef1 and Tcf7 double knockout embryos exhibit severe limb defects (84). However, in each of these cases, distal limb elements did not form, a more severe limb development phenotype as compared to KI mutants. Interestingly, varying severity of oligodactyly was previously observed with an allelic series of LRP6 and Lef1 alleles. LRP6+/-Lef1-/- produces an average of four digits in forelimb, while LRP6-/-Lef1+/+ resulted in two or three digits in forelimb. LRP6-/-Lef1+/- gave the most severe phenotype with one or two forelimb digits (127). These experiments suggest that Tcf7l1-β-catenin interaction may contribute to fine-tuning of canonical Wnt signaling during limb development.

It remains unclear whether Wnt7a specifies posterior digits through canonical or noncanonical Wnt signaling. The expression of Wnt7a in the dorsal ectoderm specifies dorsal pattern by inducing Lmx1b expression in the dorsal mesenchyme. In Wnt7a knockout mice, Lmx1b expression was lost in the distal mesenchyme (128). In chicken, a dominant active form of β-catenin cannot activate Lmx1b expression, suggesting that Wnt7a acts through a noncanonical pathway (111). However, in mice, a conditional knockout of β-catenin in the limb mesenchyme results in a reduced Lmx1b expression (34), suggesting Wnt7a acts through canonical signaling in mice. However, there is currently no direct evidence that proves Wnt7a acts through β-catenin in mice. The similar defects in posterior digit patterning in Wnt7a knockout and KI mutant mice suggest that they may act in the same pathway. More mouse genetic experiments are required to determine if Wnt7a acts through Tcf7l1-β-catenin interaction in patterning posterior digits.

Upon examination of these defects in the KI embryos, it became clear that although Tcf7l1-β-catenin interaction was necessary, the function of Tcf7l1 did not fit well into the classical model that suggests transcriptional activator activity for Tcf7l1-β-catenin. One potential explanation for the poor ability of Tcf7l1 to activate target genes involves a requirement for an unknown cell-specific co-factor that other Tcf/Lef-β-catenin complexes do not require. This possibility is indirectly supported by the differentiation that occurs upon overexpression of Tcf7l1 in ESCs but not upon overexpression of ΔNLef1, ΔNTcf7 or ΔNTcf7l2, indicating that Tcf7l1 possesses a unique biochemical property not shared by other Tcf/Lefs (107,122). This would explain why most cells activate Tcf/Lef reporters when co-expressing Lef1 and β-catenin, but very few cell types activate Tcf/Lef reporters when co-expressing Tcf7l1 and β-catenin (41,72).

To test whether a putative Tcf7l1-β-catenin activator activity was required for normal development, I focused on the eyelid MCJ region. I reasoned that the MCJ provided an ideal *in vivo* test because Tcf7l1-expressing MCJ cells displayed strong BAT-Gal and TOPGal activity in WT but not KI embryos. As such, MCJ cells should express the complement of factors essential for Tcf7l1-β-catenin-mediated transactivation. When full-length Tcf7l1 with a functional β-catenin-binding domain was overexpressed in MCJ cells, it sharply repressed BAT-Gal activity instead of activating it. I interpret this result to suggest that Tcf7l1 does not directly activate target genes.

As an alternative to the conventional roles ascribed to mammalian Tcf/Lef factors in the canonical Wnt/β-catenin pathway, I present a model in which Tcf7l1-β-catenin interaction has an important function that is independent of transactivator activity. Wnt3a-stimulated reduction of Tcf7l1 occupancy on target genes supports this model by providing a mechanism of inhibiting repression. The Tcf/Lef circuit model suggests that Tcf7l1 represses an overlapping set of Wnt-responsive genes that Lef1-β-catenin activates (Figure 11L). The DNA-binding HMG domains of Tcf7l1 and Lef1 are nearly identical and bind the same consensus sequence, supporting their potential to regulate the same genes (67-69). Moreover, the model includes a switch from Tcf7l1 repressor to Lef1-β-catenin activator through Wnt/β-catenin release of Tcf7l1- mediated repression of *Lef1* expression. My data indicate that Wnt3a stimulates *Lef1* expression directly through Tcf/Lef binding sites upstream of its transcription start site.

Several observations support a broad usage of the Tcf/Lef circuit model in embryos. Interestingly, the *Lef1* WRE (at -5.3 kb) that I identified in ESCs is the third WRE shown to regulate Lef1 expression in cells. Previously, a *Lef1* WRE (at -0.9 kb) was shown to be responsive to Wnt/β-catenin signaling in Jurkat T lymphocytes (129), and another *Lef1* WRE (at -0.8 kb) was shown to be responsive in HEK293 cells (130). Like *Lef1*, *Tcf7* gene expression is stimulated directly by Wnt/β-catenin activity (131); Tcf7 acts similarly to Lef1 as a transactivator in Tcf7l1-expressing cells (107). In colorectal cancer,

Tcf/Lef-β-catenin appears to stimulate the expression of endogenous ΔNTcf7 and full-length Lef1 isoforms, which provide feedback on Tcf/Lef-β-catenin activity (129,131,132). In limb buds, the expression of Tcf7 and Lef1 was affected in KI mutants (Figure 5). In ESCs, endogenous Tcf7 effectively opposed Tcf7l1 repressor activity in Wnt3a-treated ESCs in terms of self-renewal and target gene expression (107). Although Tcf7 is not included in the model shown in Figure 11L, it is likely to function similarly to Lef1 in most contexts. Thus, I note that previous work supports a high level of regulation of Tcf/Lef gene product expression by multiple WREs, and I suggest that the Tcf7l1-Lef1 relationship elucidated here provides a model for additional Tcf/Lef circuits robustly integrated into a single network.

It is also notable that the morphogenetic defects in KI mice bore significant similarity to those of other mutations that cause a decrease, but not complete loss, of Wnt/β-catenin signaling activity. In particular, the constellation of defects in KI mice and their variable penetrance are reminiscent of some effects caused by *Lrp5* and *Lrp6* mutations. By acting redundantly as co-receptors for Wnt ligands, either Lrp5 or Lrp6 is necessary for activation of Wnt/β-catenin signaling, and their effects are sensitive to gene dosage (133). Since Lrp5 and Lrp6 are each ubiquitously expressed, some allelic combinations of *Lrp5* and *Lrp6* null mutations cause widespread, but partial, reduction of Wnt/β-catenin activity in embryos (16,134). Interestingly, a relatively weak combination of alleles, *Lrp5*+/+ *Lrp6*+/-, causes tail kinks that I also observed, but did not count, in KI mutants (134). A

slightly stronger combination, *Lrp5*+/- *Lrp6*+/-, causes an oligodactyly phenotype essentially identical to that observed in KI mutants (16). Finally, *Lrp6*+/- and *Lrp6*-/- embryos each display exencephaly similar to that in KI embryos (134,135). Only the combinations of *Lrp5/6* alleles that cause partial reduction of Wnt/β-catenin activity resemble KI phenotypes, and more substantial loss of Wnt/β-catenin activity causes more severe defects that were not observed in KI embryos. I suggest that this similarity supports a role for Tcf7l1-β-catenin in attenuating the output of signaling through the Tcf/Lef circuit, as opposed to a role as a direct activator of target gene expression.

Chapter III

Regulation of Tcf7l1 DNA Binding and Protein Stability as Principal Mechanisms of Wnt/β-Catenin Signaling

With the exception of minor additions and formatting changes, the content of this chapter has been adapted from the content of the following manuscript:

Shy BR*, **Wu CI***, Khramtsova GF, Zhang JY, Olopade OI, Goss KH, Merrill BJ. *Regulation of Tcf7l1 DNA Binding and Protein Stability as Principal Mechanisms of Wnt/β-Catenin Signaling*. **Cell Reports**. 2013 Jul 11;4(1):1-9.
*These authors contributed equally to this work as co-first authors.

1. Abstract

Wnt/β-catenin signal transduction requires direct binding of β-catenin to Tcf/Lef proteins, an event that is classically associated with stimulating transcription by recruiting coactivators. This molecular cascade plays critical roles throughout embryonic development and normal postnatal life by affecting stem cell characteristics and tumor formation. Here, I show that this pathway utilizes a fundamentally different mechanism to regulate Tcf7l1 (formerly named Tcf3) activity. β-catenin inactivates Tcf7l1 without a switch to a coactivator complex by removing it from DNA, which leads to Tcf7l1 protein degradation. Mouse genetic experiments demonstrate that Tcf7l1 inactivation is the only required effect of the Tcf7l1-β-catenininteraction. Given the expression of Tcf7l1 in pluripotent embryonic and adult stem cells, as well as in poorly differentiated breast cancer, these findings provide mechanistic insights into the regulation of pluripotency and the role of Wnt/β-cateninin breast cancer.

2. Introduction

Canonical Wnt/β-catenin signaling impacts a wide range of biological activities, including stem cell self-renewal, organ morphogenesis, and tumor formation (136,137). Regulation of the pathway centers on the stability of β-catenin, which is targeted for proteasome-mediated degradation by a complex containing adenomatous polyposis coli (APC), Axin structural proteins, and glycogen synthase kinase 3 (GSK3) (138). Phosphorylation of β-catenin by GSK3 stimulates degradation dependent upon APC, Axin, and the β-TrCP E3 ligase (36,139,140). Wnt signaling inhibits degradation of β-cateninby blocking its ubiquitination (63). Pharmacological GSK3 inhibitors similarly inhibit β-catenin degradation by blocking β-catenin phosphorylation.

An important downstream mechanism of the Wnt/β-catenin pathway occurs as β-catenin binds to the amino terminal of Tcf/Lef proteins, thereby displacing corepressor proteins bound to the Tcf/Lef (44,45,47). Tcf-β-catenin binding subsequently recruits transactivator proteins to the genomic sites that were previously occupied by corepressors (41,42,65). This accepted model of canonical Wnt/β-catenin signaling is consistent with observed effects of Tcf/Lef proteins in many contexts (141); however, it is not consistent with recent observations for mammalian Tcf7l1 (formerly Tcf3). In cells where Lef1 and Tcf7 (formerly Tcf1) act as β-catenin-dependent transactivators, only transcriptional repressor activity for Tcf7l1 was detected (72,142). Here, I show that β-catenin binding to Tcf7l1 does not form a transactivation complex, but instead initiates a

fundamentally distinct mechanism. β-catenin binding inactivates Tcf7l1 by reducing its chromatin occupancy and secondarily stimulates its protein degradation. Mouse genetic experiments demonstrate that this inactivation is the only necessary function of the Tcf7l1-β-catenin interaction. These molecular and genetic findings provide insights into the role of Wnt/β-catenin signaling in cells where Tcf7l1 expression is prominent, including embryonic stem cells (ESCs) and poorly differentiated breast cancer.

3. Results

3.1 β-catenin reduces Tcf7l1 protein levels by stimulating protein degradation

Molecular support for a conversion into transactivators by β-catenin includes the ability of a β-catenin-Tcf7 fusion protein to activate target genes without Wnt pathway stimulation (143). If Tcf7l1 were switched to a transactivator by β-catenin, one would expect a β-catenin-Tcf7l1 fusion protein to similarly activate target genes. In ESCs, the β-catenin-Tcf7l1 fusion was unable to activate TOPFlash and LRH-1 reporters, and instead repressed Wnt3a-stimulation of reporter genes (Figure 14A). Rather than converting Tcf7l1 to a transactivator, Wnt/β-catenin stimulation notably decreased Tcf7l1 protein in ESCs treated with recombinant Wnt3a or the GSK3 inhibitor, Chiron99021 (CHIR; Figure 14B). These results indicate a significant difference in the downstream effects of Tcf7-β-catenin and Tcf7l1-β-catenin interaction.

To elucidate the transactivation-independent effects of β-catenin on Tcf7l1, we investigated how Tcf7l1 protein levels were reduced. Wnt3a- and CHIR-treated ESCs displayed increased Lef1 and Tcf7 messenger RNA (mRNA) levels that correlated with increased protein levels (Figure 14B), consistent with Lef1 and Tcf7 being Wnt/β-catenin target genes (130-132,144). In contrast, decreased Tcf7l1 protein was not paralleled by a significant change in mRNA levels (Figure 14B), indicating that β-catenin regulation of Tcf7l1 does not occur transcriptionally. Because Dgcr8 is a required component of the microprocessor

Figure 14. Wnt/β-catenin stimulates Tcf7l1 protein degradation.

(**A**) Transient transfection of Tcf7l1-/- ESCs with β-catenin-Tcf fusion plasmids and SuperTOPFlash (top) or LRH1 promoter (bottom) luciferase reporter plasmids. Values represent mean +/- standard deviation for triplicate transfections.

(**B**) Western blot (top) and Quantitative RT-PCR (bottom) analyses of ESCs treated with 50ng/ml recombinant Wnt3a (left) or 3μM CH (right) for the indicated time.

(**C-E**) Western blot analysis of ESCs treated with 3μM CH for 24 hrs in DGCR8 mutant cells (C), for 6 hrs together with MG-132 (5μM) in Tcf7l1 +/+ and Tcf7l1Δn/ΔN mutant cells (D), and for 12 hrs together with leptomycin B (E)

(**F**) Distribution of relative levels of nuclear Tcf7l1 immunoreactivity in Tcf7l1+/+ (top) and Tcf7l1ΔN/ΔN (bottom) cells expressing either GFP (red bars) or ΔNβ-catenin (blue bars). A total of 200 nuclei were counted for each condition. Data are representative of three separate experiments.

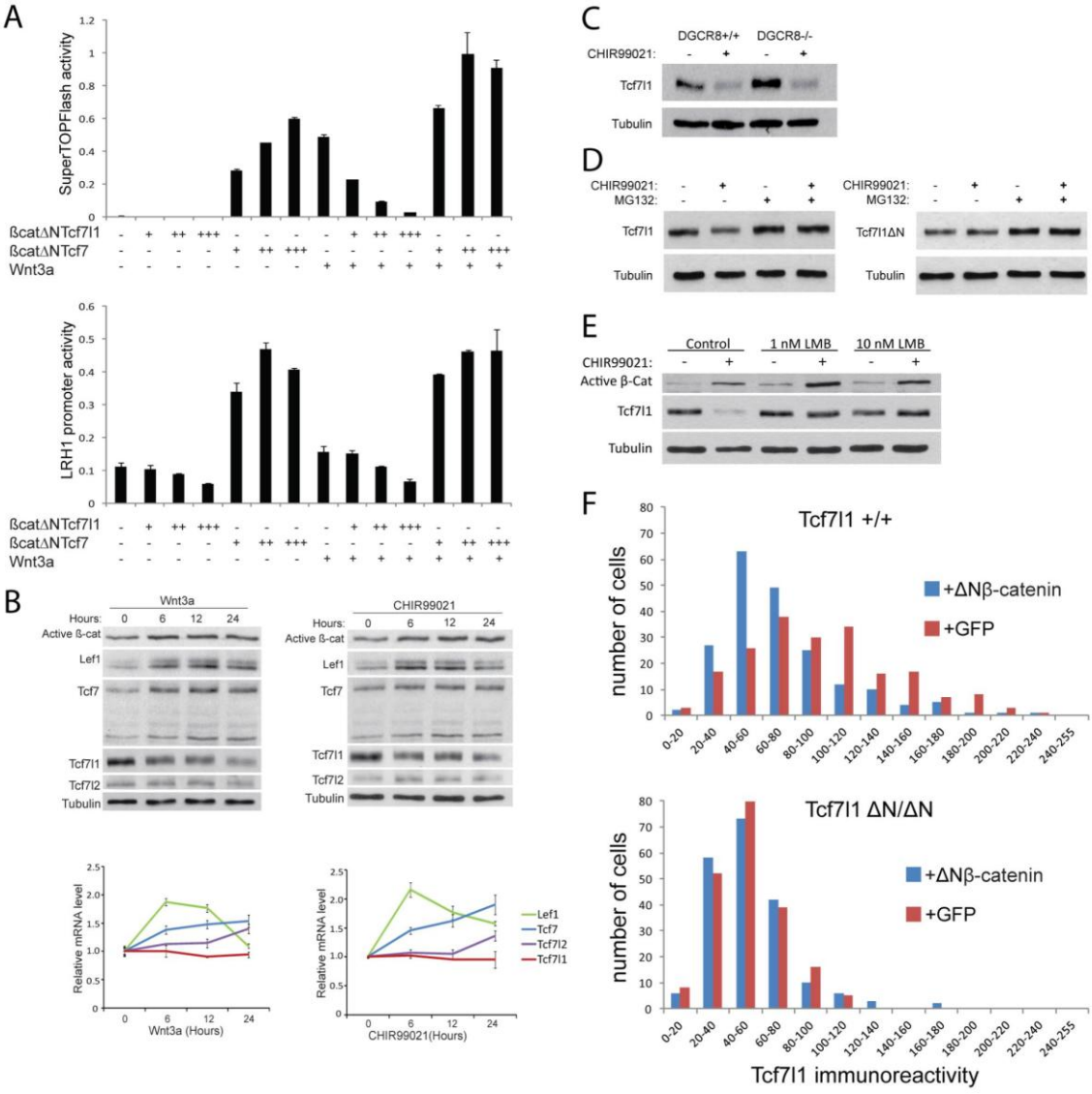
A
SuperTOPFlash activity
ßcatΔNTcf7l1
ßcatΔNTcf7
Wnt3a
LRH1 promoter activity
B
Wnt3a
CHIR99021
Hours:
Active ß-cat
Lef1
Tcf7
Tcf7l1
Tcf7l2
Tubulin
Relative mRNA level
Wnt3a (Hours)
CHIR99021(Hours)
C
DGCR8+/+
DGCR8-/-
CHIR99021:
D
MG132:
Tcf7l1ΔN
E
Control
1 nM LMB
10 nM LMB
Active β-Cat
F
Tcf7l1 +/+
Tcf7l1 ΔN/ΔN
number of cells
+ΔNβ-catenin
+GFP
Tcf7l1 immunoreactivity

complex, which is necessary for biogenesis of microRNAs (145), the CHIR-stimulated reduction of Tcf7l1 in Dgcr8-/- ESCs showed that reduction of Tcf7l1 protein was also not microRNA mediated (Figure 14C). Treatments with the proteasome inhibitors MG-132 and MG-115 effectively blocked the CHIR-stimulated reduction of Tcf7l1 protein (Figures 14D and 15A), demonstrating that reduction of Tcf7l1 required protein degradation. Finally, reduction of Tcf7l1 was blocked by leptomycin B, indicating that it required Exportin1-mediated nuclear transport (Figure 14E).

To determine the role of β-catenin binding to Tcf7l1, I used Tcf7l1ΔN/ΔN knock-in ESCs. In contrast to wild-type Tcf7l1, Tcf7l1ΔN was not degraded in response to CHIR or Wnt3a (Figures 14D and 15B), indicating that the Tcf7l1-β-catenin interaction was necessary for degradation. To determine whether the interaction was sufficient for degradation, I expressed ΔNβ-catenin in ESCs and measured the Tcf7l1 levels by quantitative immunofluorescence. ΔNβ-catenin expression was sufficient to reduce nuclear Tcf7l1 levels in Tcf7l1+/+ but not in Tcf7l1ΔN/ΔN cells (Figures 14F and 15C). Interestingly, several recent studies showed that a mutant form of β-catenin (β-cateninΔC) supported self-renewal of mouse ESCs and complemented defects caused by ablation of β-catenin despite the lack of the C-terminal transactivation domain in the β-cateninΔC mutant (122,146,147). Therefore, it is notable that expression of ΔNβ-cateninΔC was also sufficient to reduce nuclear Tcf7l1 protein levels in ESCs (Figure 15D). Given the substantial effects of altering Tcf7l1 levels in ESCs,

Figure 15. ΔNΔCβ-catenin is sufficient to reduce nuclear Tcf7l1 protein levels in ESCs.

(**A**) Western blot analysis of Tcf7l1 protein levels in ESCs treated for 6 hours +/- 3μM CHIR and/or 5 μM MG115.

(**B**) Western blot analysis and quantitation of Tcf7l1 protein levels in Tcf7l1ΔN/ΔN ESCs treated for 12 hours +/- 50 ng/mL recombinant Wnt3a.

(**C**) Transient transfection of GFP or ΔNβ-catenin expression plasmids was performed in Tcf7l1+/+ (top) and Tcf7l1ΔN/ΔN (bottom) ESCs. Immunofluorescent detection of Tcf7l1 protein (cyan), GFP (green) or β-catenin (magenta), and DNA (blue) was measured in nuclei of transfected cells. Images were processed for quantitative immunofluorescence to generate data for graphs (Figure 14F).

(**D**) Quantitative immunofluorescence for Tcf7l1 protein in ESCs transiently transfected with ΔNβ-catenin (blue), ΔNΔCβ-catenin (green), or GFP only (red) expression plasmids. Bars indicate number of cells (of a total of 200 counted) display the indicated relative intensity of Tcf7l1 immunoreactivity.

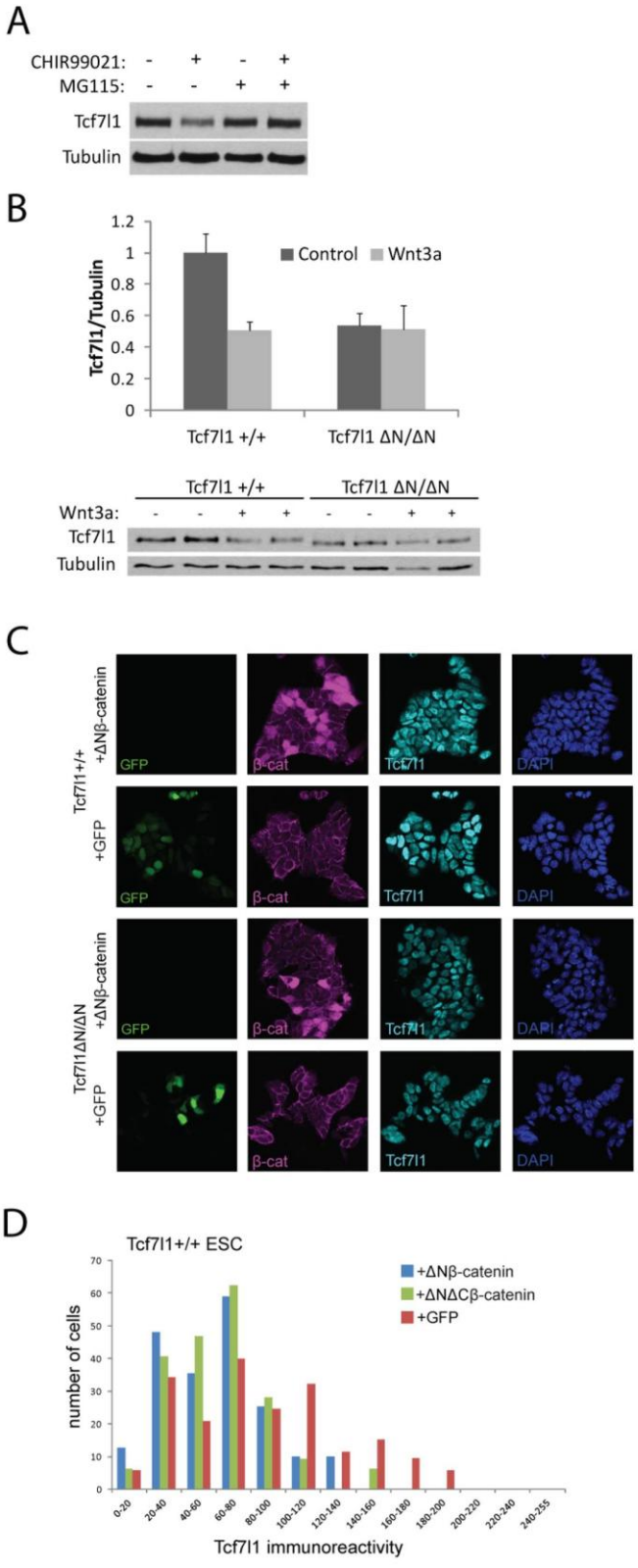
A
CHIR99021: - + - +
MG115: - - + +
Tcf7l1
Tubulin
B
Tcf7l1/Tubulin
Control
Wnt3a
Tcf7l1 +/+
Tcf7l1 ΔN/ΔN
Wnt3a:
C
Tcf7l1+/+ +ΔNβ-catenin
+GFP
Tcf7l1ΔN/ΔN +ΔNβ-catenin
GFP
β-cat
Tcf7l1
DAPI
D
Tcf7l1+/+ ESC
+ΔNβ-catenin
+ΔNΔCβ-catenin
+GFP
number of cells
Tcf7l1 immunoreactivity

the reduction of Tcf7l1 protein provides a mechanism for the poorly understood pro-self-renewal effects of β-cateninΔC in ESCs.

3.2 Reduction of Tcf7l1 is sufficient to replace the Tcf7l1-β-catenin interaction

If a principal mechanism of Wnt/β-catenin signaling functions through inactivation of Tcf7l1, and not conversion to a Tcf7l1-β-catenin transactivator complex, reducing the level of Tcf7l1 should be sufficient to replace the Tcf7l1-β-catenin interaction. I first tested this hypothesis in ESCs, where reducing the amount of Tcf7l1ΔN by small interfering RNA (siRNA) stimulated the reporter gene response to Wnt3a (Figures 16A and 16B). To examine the broader effects of reducing Tcf7l1 in mice, I reduced the level of Tcf7l1 by breeding for hemizygous mice (i.e., Tcf7l1+/- or Tcf7l1-/ΔN; Figure 16C). It is important to note that Tcf7l1-/- mice die shortly after gastrulation (80). Tcf7l1ΔN/ΔN embryos progress normally through gastrulation, but later develop a constellation of morphogenetic defects that result in death for all Tcf7l1ΔN/ΔN mice at or before birth (142,148). Mating Tcf7l1+/- with Tcf7l1+/ΔN mice produced the Mendelian-expected ratio of Tcf7l1-/ΔN offspring, despite the genetic absence of a Tcf7l1 protein capable of interacting with β-catenin (Figures 17A and 16D). Moreover, Tcf7l1-/ΔN mice did not display any of the morphogenetic defects observed in Tcf7l1ΔN/ΔN mice, including poor vascular integrity, edema, oligodactyly, and opened eyelids (Figures 17C-17D'', 16E, and 16F). Indeed,

Figure 16. Reduction of Tcf7l1ΔN rescues Wnt activation.

(**A**) Transient transfection of Tcf7l1+/+ (WT) or Tcf7l1ΔN/ΔN (KI) ESCs with SuperTOPFlash Luciferase reporter and various concentrations (0.04nM to 5nM) of siRNA compounds. Control siRNAs (SCRM) and two independent Tcf7l1-specific (#1, #2) siRNAs were used. Reporter activity was stimulated by treating with Wnt3a-conditioned media or control conditioned media for 24hrs. Values represent means +/- standard deviations of biological triplicates.

(**B**) (top) Western blot showing degree of Tcf7l1 protein knockdown caused by siRNA used for reporter assay (A) and (bottom) coomassie stained gel showing even loading of protein lysates samples.

(**C**) Western blot analysis (top, middle) of whole e8.5 mouse embryos determined to have Tcf7l1+/+ and Tcf7l1+/- genotypes based on PCR genotyping reactions (bottom).

(**D**) Recovery of offspring with the indicated genotypes from mating Tcf7l1+/- and Tcf7l1+/ΔN mice. Note the normal viability of Tcf7l1-/ΔN mice.

(**E**) Images of whole e15.5 embryos of the indicated genotype. Note the lack of edema exhibited by Tcf7l1-/ΔN mice.

(**F**) Images of whole e18.5 embryos of the indicated genotype. Note the lack of hemorrhage in the Tcf7l1-/ΔN mice.

(**G,H**) BAT-Gal transgenic mice harboring the Tcf/Lef-β-catenin reporter transgene were X-gal stained to identify Tcf/Lef-β-catenin activity. (G) In the limb buds of e10.5 embryos, the intense domain of activity at the posterior region (arrows) is absent in Tcf7l1ΔN/ΔN embryos and returns in Tcf7l1-/ΔN embryos. (H) In 8um thin cryosections of the eyelids from e14.5 embryos, the domain of BAT-Gal activity at the mucocutaneous junction (dotted line) is reduced in Tcf7l1ΔN/ΔN and restored to normal in Tcf7l1-/ΔN embryos.

A

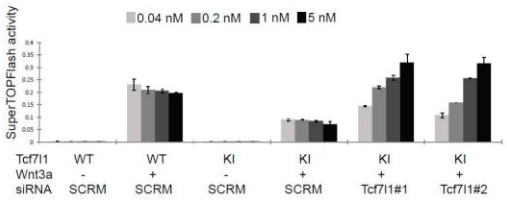

B

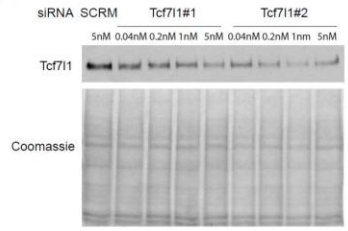

C

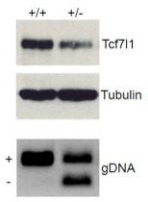

D

Stage	Total number of mice	Number of mice of each genotype			
		Tcf7l1+/+	Tcf7l1+/-	Tcf7l1+/ΔN	Tcf7l1-/ΔN
E10.5	70	16	17	16	21
E15.5	135	30	31	46	28
E18.5	14	2	5	3	4
P20	190	46	51	51	42

E

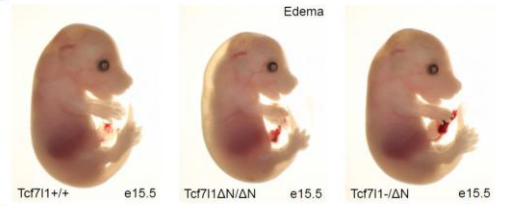

F

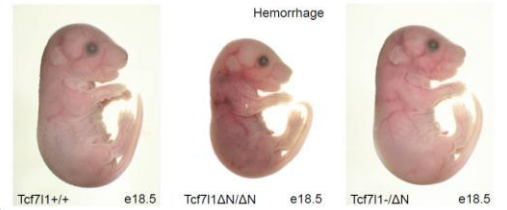

G

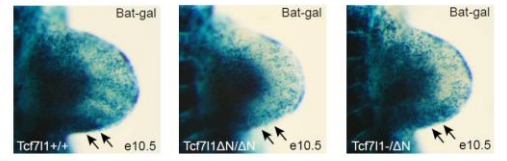

H

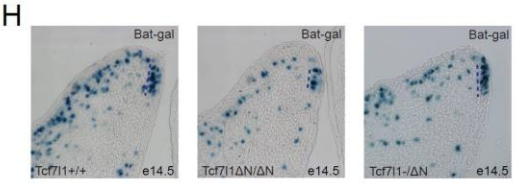

Figure 17. Reducing Tcf7l1 levels replaces the requirement for β-catenin interaction in mice.

(**A-D’’**) Tcf7l1-/ΔN mice appear normal at birth (A) and through adult stages (B) (see also Figure S2D-F). Phenotypes observed in Tcf7l1ΔN/ΔN embryos, including oligodactyly (C-C’’) and opened eyelids at birth (D-D’’), were not observed in Tcf7l1-/ΔN embryos. (See also Figure S2E,F).

(**E-G’’’**) Tcf/Lef-β-catenin activation of BAT-Gal reporter is restored in the Tcf7l1-/ΔN eyelid. Immunofluorescence for Tcf7l1 (green), Lef1 (red), and β-galactosidase (blue) displayed for e14.5 eyelids from BAT-Gal transgenic Tcf7l1+/+ (E-E’’’), Tcf7l1ΔN/ΔN (F-F’’’), and Tcf7l1-/ΔN (G-G’’’) embryos. Arrows point to Lef1 positive nuclei with low levels of Tcf7l1. Arrowheads point to Tcf7l1 and Lef1 double positive nuclei, which were observed in Tcf7l1+/+ (E-E’’’) and Tcf7l1-/ΔN (G-G’’’) but not Tcf7l1ΔN/ΔN (F-F’’’). The dotted line denotes the BAT-Gal-positive region. Asterisks in (F) mark Tcf7l1 positive cells in the nearby cornea.

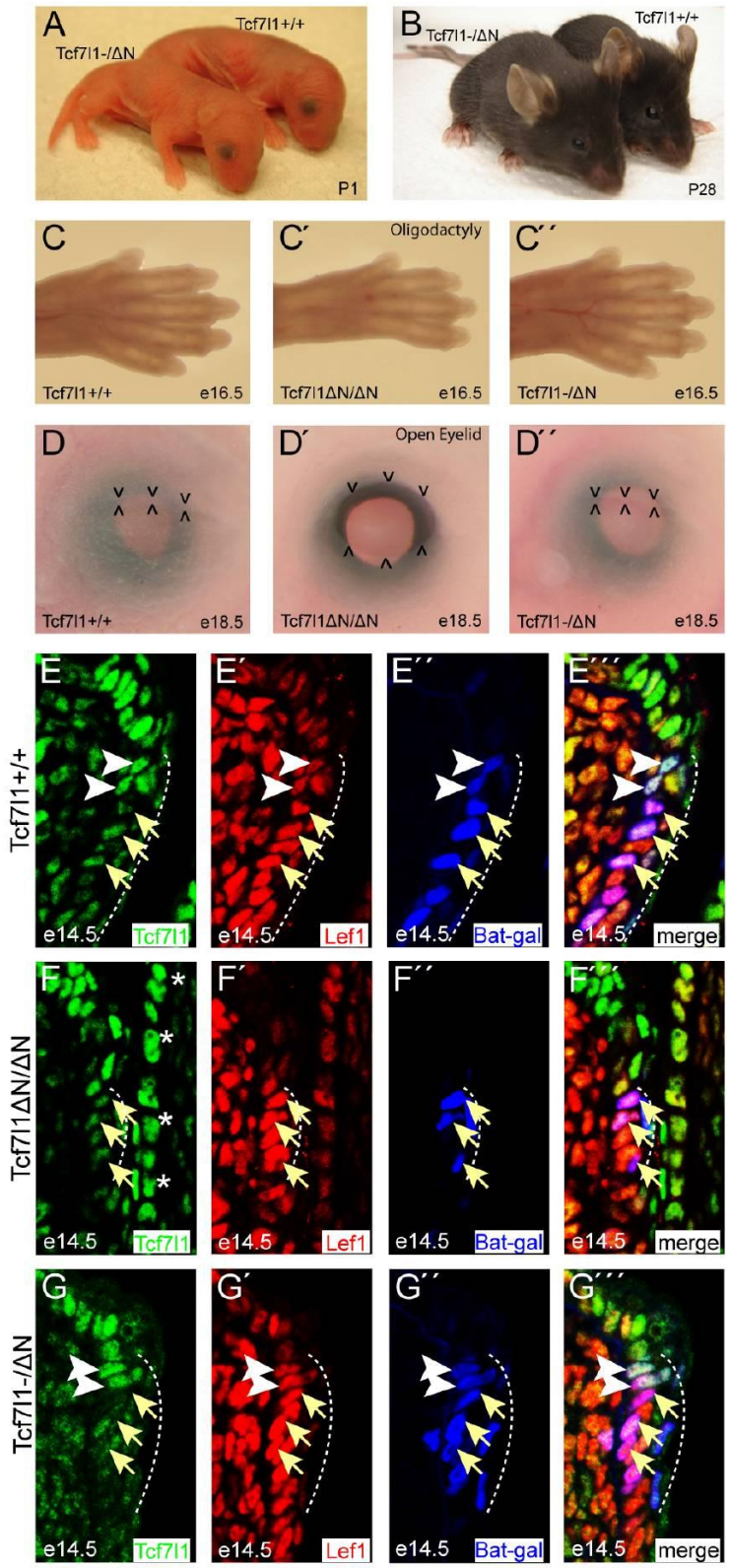
A
Tcf7l1+/+
Tcf7l1-/ΔN
P1
B
Tcf7l1-/ΔN
Tcf7l1+/+
P28
C
Tcf7l1+/+
e16.5
C´
Oligodactyly
Tcf7l1ΔN/ΔN
e16.5
C´´
Tcf7l1-/ΔN
e16.5
D
Tcf7l1+/+
e18.5
D´
Open Eyelid
Tcf7l1ΔN/ΔN
e18.5
D´´
Tcf7l1-/ΔN
e18.5
Tcf7l1+/+
E
E´
E´´
E´´´
e14.5
Tcf7l1
Lef1
Bat-gal
merge
Tcf7l1ΔN/ΔN
F
F´
F´´
F´´´
Tcf7l1-/ΔN
G
G´
G´´
G´´´

Tcf7l1-/ΔN mice advanced to adulthood and appeared indistinguishable from Tcf7l1+/+ littermates throughout their ostensibly normal lifetimes (Figure 17B). Thus, removing one copy of Tcf7l1ΔN genetically rescued the defects caused by ablating the Tcf7l1-β-catenin interaction. These results demonstrate that inactivation of Tcf7l1 by β-catenin is the necessary effect downstream of Tcf7l1-β-catenin interaction for mouse embryogenesis and postnatal viability.

To determine the effects of reducing Tcf7l1 at the target gene level in mice, tissues that were previously shown to be affected in Tcf7l1ΔN/ΔN embryos were examined in Tcf7l1-/ΔN embryos harboring the BAT-Gal reporter. Compared with Tcf7l1+/+ embryonic day 14.5 (e14.5) eyelids (Figures 17E-E’’’), Tcf7l1ΔN/ΔN displayed a restricted domain of BAT-Gal activity and decreased expression of Lef1, a Wnt/β-catenin target, in the mucocutaneous junction of the eyelid (Figures 17F-17F’’’;(142)). The domain of Lef1 expression and BAT-Gal activity was increased in Tcf7l1-/ΔN relative to Tcf7l1ΔN/ΔN, and BAT-Gal activity was detected only in cells expressing Lef1 (Figures 17F-17G’’’, 16G, and 16H). Given the inability of Tcf7l1ΔN to respond to β-catenin, the rescue of BAT-Gal activity in Tcf7l1-/ΔN embryos shows that activation is mediated by Lef1, and attenuation of this activation depends on the level of Tcf7l1 repressor.

Figure 18. Inhibition of chromatin occupancy is upstream of Tcf7l1 protein degradation.

(**A**) Quantitative chromatin immunoprecipitation using anti-Tcf7l1 antibody. Chromatin was isolated from ESCs treated for 12 hours with 3μM CH and/or 5μM MG-132. qPCR measurement of Tcf7l1 bound DNA is shown for regions near AXIN2, CDX1, and MYCN genes. Values represent the mean plus standard deviation of percent of precipitated DNA relative to input for duplicate technical measurements of five biological replicates.**p<0.01; ***p<0.001; NS p>0.05.

(**B**) (top) Western blot analysis of Tcf7l1 protein from lysates of Tcf7l1-/- ESCs stably expressing either wild-type Tcf7l1 (WT) or the mutant Tcf7l1 HMG * (HMG*) protein. Cells were treated with 30μg/ml cyclohexamide to block new translation, and the stability of the two proteins was compared, relative to tubulin internal control, over a 12 hour periods. (bottom) Quantitation of Western blot and normalization of Tcf7l1 protein levels was calculated for WT (blue) and HMG* (red) proteins. Each data point represents the mean of biological triplicates.

(**C**) Western blot analysis comparing the CH-mediated reduction WT and HMG* Tcf7l1 proteins using same ESCs as (B).

(**D**) Co-IP experiments using anti-Tcf7l1 (top) or anti-β-catenin (middle). Protein was immunoprecipitated from lysates of cells treated +/- 3 μM CHIR99021 and +/- 5 μM MG-132 (bottom).

(**E**) Quantitative chromatin immunoprecipitation using anti-β-catenin antibody. Chromatin was isolated from ESCs treated for 12 hours with 3μM CH and/or 5μM MG-132. qPCR measurement of β-catenin bound DNA is shown for regions near AXIN2 and CDX1 genes. Values represent the mean plus standard deviation of percent of precipitated DNA relative to input for duplicate technical measurements of three biological replicates.

(This figure was contributed by Brian Shy, Merrill lab)

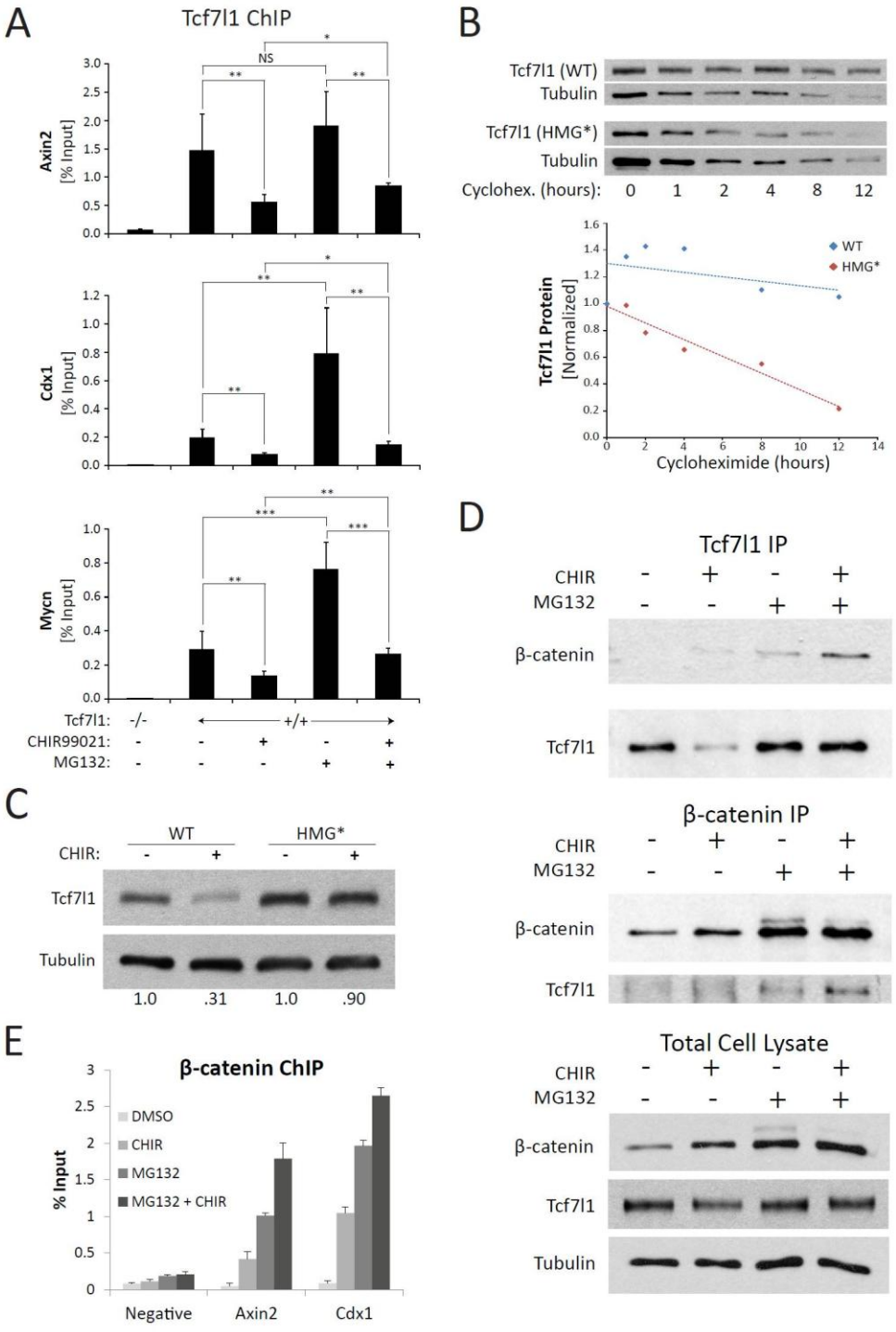
A
Tcf7l1 ChIP
Axin2 [% Input]
Cdx1 [% Input]
Mycn [% Input]
NS
Tcf7l1: -/- +/+
CHIR99021:
MG132:
B
Tcf7l1 (WT)
Tubulin
Tcf7l1 (HMG*)
Tubulin
Cyclohex. (hours): 0 1 2 4 8 12
Tcf7l1 Protein [Normalized]
WT
HMG*
Cycloheximide (hours)
C
WT
HMG*
CHIR:
Tcf7l1
Tubulin
1.0 .31 1.0 .90
D
Tcf7l1 IP
CHIR
MG132
β-catenin
Tcf7l1
β-catenin IP
β-catenin
Tcf7l1
Total Cell Lysate
β-catenin
Tcf7l1
Tubulin
E
β-catenin ChIP
% Input
DMSO
CHIR
MG132
MG132 + CHIR
Negative
Axin2
Cdx1

3.3 Reduction of chromatin occupancy provides the critical upstream point of Tcf7l1 regulation

To elucidate how the reduction of chromatin occupancy is causally linked to protein degradation, we conducted quantitative chromatin immunoprecipitation (ChIP) experiments to measure Tcf7l1 chromatin occupancy following the combined CHIR + MG-132 treatment. As expected from the changes in Tcf7l1 protein levels (Figure 14B), CHIR reduced Tcf7l1 occupancy on target genes (Axin2, Cdx1, and Mycn), and MG-132 increased occupancy (Figure 18A). Importantly, CHIR treatment reduced chromatin occupancy even when destabilization of Tcf7l1 was blocked by MG-132 (Figure 18A), indicating the reduction in DNA binding was upstream of degradation.

To examine the role of chromatin occupancy in regulating Tcf7l1 stability, we used the Tcf7l1 HMG* mutation, which affects the DNA-binding HMG domain and disrupts DNA binding (72). The HMG* mutation was sufficient to reduce Tcf7l1 protein stability in the absence of CHIR (Figure 18B). Moreover, stability of the mutant Tcf7l1 HMG* protein was not substantially decreased by CHIR (Figure 18C), indicating that destabilization of Tcf7l1 requires a change in chromatin occupancy. In support of the model focused on reduction of chromatin occupancy, coimmunoprecipitation (coIP) experiments showed that Tcf7l1-β-catenin interaction was stimulated by CHIR + MG-132 (Figure 18D), and β-catenin chromatin occupancy increased (Figure 18E) while Tcf7l1 occupancy decreased (Figure 18A). Together, these data are most consistent with the notion that the

primary effect of the Tcf7l1-β-catenin interaction is to inhibit chromatin occupancy. The secondary effect of Tcf7l1 degradation provides an additional mechanism by lowering Tcf7l1 levels, which further reduces the amount of Tcf7l1 available to bind to chromatin. Thus, the combination of reduced DNA binding and Tcf7l1 degradation leads to an additive reduction of Tcf7l1 repression in response to Wnt/β-catenin activity.

4. Discussion

The molecular effects of Wnt/β-catenin and GSK3 inhibition on Tcf7l1 described here indicate that Tcf7l1 primarily functions outside of the classic model of canonical Wnt/β-catenin signaling. In ESCs, β-catenin was sufficient to reduce Tcf7l1 levels without exogenous pathway stimulation. These results are consistent with a mechanism of inactivation wherein β-catenin binding inhibits Tcf7l1-repression by reducing chromatin occupancy, consequently stimulating its degradation.

Pro-self-renewal effects in β-cateninΔC mutant ESCs are controversial (122,146,147). Doble's group generated GSK3α/β double knockout mouse ESCs that experienced complete blockage of neurectodermal differentiation (122). Overexpress stabilized β-catenin in WT mouse ESCs is able to phenocopy the phenotype of GSK3α/β double knockout mouse ESCs. In addition, overexpression of β-cateninΔC, which lacks the carboxy terminal domain necessary for Tcf/Lef-β-catenin transactivation activity, results in a similar phenotype to GSK3α/β double knockout mouse ESCs. In addition, it was shown that stabilized β-catenin forms a complex with Oct4 and enhances Oct4 activity, suggesting that β-catenin maintains pluripotency by enhancing Oct4 activity instead of through interaction with Tcf/Lefs.

Both Hartmann and Smith's groups independently generated β-catenin conditional knockouts in ESCs and found that ESCs self-renewal is maintained in the absence of β-catenin (146,147). Hartmann's group discovered through

embryoid body differentiation assays that β-catenin-deficient ESCs possess defects in mesendoderm formation and neuronal differentiation (146). Reintroduction of β-cateninΔC rescued endoderm and neuronal differential defects, leading to the conclusion that β-catenin's cell-adhesion functions may be critical during these processes.

Smith's group also showed elimination of β-catenin removes the ability of GSK3 inhibition to promote ESCs self-renewal (147). Reintroduction of β-cateninΔC restored effects of GSK3 inhibition on ESCs self-renewal. In addition, they suggest that β-catenin directly reduce Tcf7l1 repression function. Thus, GSK3 inhibition may promote self-renewal through removal of Tcf7l1 repression on the pluripotency network.

Wnt reduces Tcf7l1 protein mechanism provides a simple explanation for the controversial pro-self-renewal effects of the β-cateninΔC mutant in ESCs (122,146,147): the critical effect of inactivating Tcf7l1 is stimulated by the β-cateninΔC form, thus making β-catenin's carboxy-terminal transactivation domain dispensable in ESCs.

The results from mouse genetic experiments indicate that inactivation of Tcf7l1 is the predominant mechanism whereby Wnt/β-catenin signaling interacts with this mammalian Tcf/Lef protein. The viability of Tcf7l1-/ΔN mice genetically demonstrates that inactivation of Tcf7l1 is the only effect of Tcf7l1-β-catenin binding that is required for normal mouse development and life. That said, additional activities downstream of Tcf7l1-β-catenin interaction likely exist. Indeed,

reporter gene assays support rare Tcf7l1-β-catenin transactivator activity in some cell types (e.g., 293T, COS7, and human keratinocytes; (72,142,149)); however, the biological significance of this effect remains to be determined.

The effects of β-catenin on Tcf7l1 are most parsimoniously explained by a mechanism of β-catenin directly inhibiting Tcf7l1 binding to chromatin. Experiments examining the effects of β-catenin on the Tcf/Lef interaction with naked DNA showed little or no effect on binding *in vitro*, whereas β-catenin interaction significantly affected binding to chromatin by Lef1 (150). Interestingly, mutational analysis of Lef1 indicated that an amino terminal region provides intramolecular inhibition of chromatin binding. β-catenin binding blocks the intramolecular inhibition, thereby stimulating Lef1 binding to chromatin (150). Although the effect of β-catenin on Lef1 is different from that predicted for Tcf7l1, these previous findings demonstrate both positive and negative regulation of chromatin binding via the β-catenin interaction region of Tcf/Lef proteins. Further research is necessary to elucidate the biophysical and biochemical nature of β-catenin's effects on the chromatin binding properties of Tcf7l1.

Chapter IV

Discussion

Activation of Wnt/β-catenin target genes classically occurs through bipartite transactivator complexes formed by β-catenin binding to a member of the Tcf/Lef family of DNA binding proteins. β-catenin is believed to function as a switch, turning Tcf/Lefs from transcriptional repressors to transcriptional activators. All Tcf7l1 homologs encode a conserved β-catenin binding domain, suggesting that β-catenin might also switch Tcf7l1 from a repressor to an activator. Here, I show that instead of switching Tcf7l1 into a transactivator, β-catenin binding to Tcf7l1 leads to Tcf7l1 degradation. Furthermore, mouse genetic experiments showed that this Tcf7l1-β-catenin interaction is required for mouse viability, which is rescued when the level of Tcf7l1 is genetically reduced. Mouse ESCs experiments showed that β-catenin inhibits Tcf7l1 repression of Wnt target gene transcription by removing Tcf7l1 from chromatin for proteasome-mediated degradation. Thus, Wnt/β-catenin signaling regulates Tcf7l1 through a fundamentally different mechanism as compared to other Tcf/Lefs.

Wnt-mediated reduction of Tcf7l1 protein is a novel mechanism in mouse development, but it shares some salient features with regulation of Tcf/Lef orthologs in *C. elegans*. In *C. elegans*, Pop-1, like mouse Tcf7l1, must be reduced to activate Wnt signaling; however, Pop-1 is required to function as an activator at low concentrations, at which its high affinity for β-catenin orthologs overrides its low affinity for co-repressors (88). Furthermore, Wnt-mediated reduction of Tcf7l1 and Pop-1 both require nuclear export machinery (93,151). However, some differences do exist between Tcf7l1 and Pop-1 regulation. While Pop-1 functions

as an activator upon binding to a β-catenin ortholog, the ostensibly normal phenotype of Tcf7l1-/ΔN mice indicates that there is no requirement for Tcf7l1-β-catenin activator activity in mice. As there are four Tcf/Lefs in mice compared to only one Tcf/Lef, Pop-1, in *C. elegans*, the requirement of Pop-1's activator function is likely substituted by other Tcf/Lefs in mice. Also, while NLK phosphorylation of Pop-1 promotes its nuclear export, our data shows that the Tcf7l1 phosphorylation by HIPK2 and NLK at conserved residues is not necessary for its degradation (93,151). In addition, the amino terminal β-catenin binding domain is required for Tcf7l1 degradation in mouse, while Pop-1 regulation depends instead on a carboxy-terminal domain (91,151). Still, similarities between canonical Wnt regulation of Tcf7l1 and Pop-1 suggest that this mechanism may be more broadly conserved than previously appreciated.

It is worth mentioning that some KI defects such as open eyelids at birth and open neural tubes are also phenotypes ascribed to defects in the Wnt/planar cell polarity pathway. For instance, Dvl1/2 double mutant embryos display open neural tubes (152), while Fzd3 and Fzd6 double mutant embryo have defects in neural tube closure, eyelid closure and the planar orientation of hair bundles on auditory and vestibular sensory cells (153). Eyelid and neural tube closure both involve a process in which two flanking epithelial sheets converge medially. The fact that KI mice have similar defects in eyelid and neural tube closure as those observed in Dvl1/2 and Fzd3/6 mutant mice suggests that both Wnt/β-catenin and Wnt/planar cell polarity signaling are required at this stage to regulate either

different or overlapping downstream effectors. More experiments are required to understand how defects in these two different Wnt pathways produce similar phenotypes. It is possible that canonical and noncanonical Wnt signaling pathways are not as divided as previously thought.

Aberrant Wnt/β-catenin signaling has been implicated in many cancers (14). Tcf/Lef-β-catenin complexes are downstream factors in Wnt/β-catenin signaling which may serve as potential targets for cancer therapy. Several groups have screened for potential small molecule inhibitors of Tcf/Lef-β-catenin complexes. One identified molecule, diterpenoid derivative 15-oxospiramilactone (NC043), was found to inhibit Wnt3a-induced TOPFlash activity in HEK293T cells (154). NC043 also decreases Tcf7l2-β-catenin interaction and inhibits growth of colon cancer cell lines, SW480 and Caco-2. Furthermore, NC043 also inhibits xenograft tumorigenesis after injection of SW480 cells into nude mice. In addition, a chemical library screening of Drosophila cells using dTF12 Wnt-responsive luciferase reporter identified three small molecule inhibitors, iCRT3, iCRT5 and iCRT14 (155). Each of these three compounds can inhibit Tcf7l2-β-catenin interaction in HEK293 cells**.** In addition, all compounds block Wnt-induced cell invasion of MCF7 human breast adenocarcinoma cell lines. Furthermore, iCRT3 has been shown to reduce the growth of human colon cancer cells derived by patient biopsy, while iCRT14 inhibits xenograft tumorigenesis of HCT116 and HT29 colon cancer cell lines. Additionally, an *in vitro* screening assay was designed to search for natural compounds to disrupt Tcf7l2-β-catenin interaction.

Three compounds identified, PKF115-584, CGP049090, and PKF118- 310, could each inhibit β-catenin-induced axis duplication in *Xenopus* embryos and reduce proliferation of HCT116 and HT29 colon cancer cell lines (156). All three compounds could also inhibit growth of HepG2 hepatocellular carcinoma cells in mouse xenograft models.

Whereas several small molecules have been confirmed to block Tcf7l2-β-catenin interaction, they have not been tested on the Tcf7l1-β-catenin interaction even though Tcf7l1 may be the more relevant target for several cell types. Tcf7l1 is expressed in a variety of stem cells affected by Wnt-stabilized β-catenin, including ESCs (107,147), neural stem cells (157,158), hematopoietic stem cells (159), and hair follicle stem cells (72,98,101). In addition, high levels of Tcf7l1 mRNA have been detected in poorly differentiated mammary tumors, most notably in triple negative mammary gland tumors (103). Comparison of Tcf7l1 and β-catenin protein levels and localization in breast cancer biopsy samples indicate that stabilized β-catenin reduced Tcf7l1 protein in triple negative cancers (151). The discovery that Wnt/β-catenin utilizes a novel mechanism in Tcf7l1 regulation provides an understanding of how Wnt/β-catenin signaling functions at the molecular level in Tcf7l1-expressing stem cells and tumor cells. Additional experiments are needed to confirm if small molecule inhibitors of Tcf7l2-β-catenin interaction may also disrupt Tcf7l1-β-catenin interaction and how Wnt target gene expression is subsequently affected.

Materials and methods

Generation and genotyping of Tcf7l1ΔN/ΔN mice

Two independent Tcf7l1+/ΔN ESCs clones from Yi et al (107) were injected into C57BL/6 blastocysts to produce male chimeras selected for mating with wildtype C57BL/6 females. Tcf7l1+/ΔN heterozygotes were backcrossed ten times to C57BL/6 mice background prior to analysis of viability, penetrance of phenotypes, and expressivity of phenotypes. Tcf7l1+/- and Tcf7l1+/ΔN mice were maintained on a C57BL/6 background throughout the study. Primers used for genotyping are: 'forward', 5'-agtcgtccctggtcaacgaat-3', 'reverse', 5'-acagagtagctat ctggagctcgg-3'.

Embryo whole mount *in situ* hybridization

Embryos were dissected in 1x PBS, fixed in 4% paraformaldehyde in PBS at 4 °C overnight. Next day, embryos were washed in cold PBST (PBS + 0.1% Tween 20) for three times, dehydrated in a series of graded methanol/PBST (5 minutes each in 25%, 50%, 75% and twice in 100% methanol) and stored at -20 °C in 100% methanol. Embryos can be stored in -20 °C in 100% methanol for months. When whole mount *in situ* hybridization was performed, fixed embryos were rehydrated in a series of graded methanol/PBST (5 minutes each in 75%, 50%, and 25% methanol/PBST), bleached in methanol/30% H_2O_2 (4:1) for 1 hour,

and washed in PBST for three times. Embryos were then treated with proteinase K (8-10 minutes E10.0, 10-12 minutes E10.5, 12-14 minutes E11.5), washed with 2mg/ml glycine in PBST, and post-fixed in 4% paraformaldehyde/0.2% glutaraldehyde. Next, embryos were treated with prehybidization solution for five hours at 70 °C and hybridized with digoxigenin-labeled cRNA probes at 70 °C overnight. Each hybridized cRNA probes were detected using anti-digoxigenin AP antibody (Roche). After using NBT/BCIP (Roche) to develop signal, embryos were dehydrate in a series of graded methanol/PBST (5 minutes each in 25%, 50%, 75% and twice in 100% methanol) to develop the purple colored precipitate. Embryos were then rehydrated in a series of graded methanol/PBST (5 minutes each in 75%, 50%, and 25% methanol/PBST) and cleared in 50% glycerol/PBST for imaging. Genotypes of embryos were determined by digesting embryos in proteinase K and using lysates for PCR reactions. Probes used in this thesis were specific for *Tcf7l1* (Merrill Lab), *Brachyury* (D. Wilkinson), *Shh* (A. P. McMahon), *Patched1* (M. P. Scott), *Fgf8* and *Gremlin1* (G. Martin), *Msx1 and 2* (R. Harland and P. Sharpe) and *Tbx2* (V. Papaioannou).

Eyelid and limb immunofluorescence staining

All immunofluorescent staining was performed on 8-μm frozen sections of tissue embedded in OCT. Frozen sections were fixed in 4% paraformaldehyde. For immunofluorescent detection of proteins in mouse eyelid and limb using mouse primary antibodies, the Mouse on Mouse kit (MOM kit; Vector Laboratories)

was used according the manufacturers' protocol. Immunofluorescent detection of proteins was performed with the following antibodies: guinea pig anti-Tcf7l1(72), rabbit anti-Lef1 (Cell Signaling), rabbit anti-Tcf7 (Cell Signaling), rabbit anti-Tcf7l2 (Cell Signaling), mouse anti-β-galactosidase (Developmental Studies Hybridoma Bank), rabbit anti-Ki67 (Abcam), fluorescent phalloidin (Invitrogen), rabbit anti-phospho-ERK (Cell Signaling), rabbit anti-phospho-JNK (Cell Signaling) and rabbit anti-phospho-c-Jun (Cell Signaling). Cy5, FITC and Texas Red-conjugated secondary antibodies (Jackson Labs) were used at 1:100 dilution. All fluorescent images were taken with a Zeiss LSM 5 Pascal system.

Embryonic stem cell culture

Feeder-free mouse ESCs were maintained using standard ESCs culture conditions with LIF as described previously (160). ESCs were propagated on gelatinized (15 minutes at room temperature) 10 cm tissue culture dishes (Falcon) in Knockout-DMEM (Gibco) supplemented with 15% fetal bovine serum (Atlanta Biologicals), 10 mM HEPES (Thermo Scientific), 100 U/ml penicillin (Gibco), 100 mg/ml streptomycin (Gibco), 2 mM L-glutamine (Gibco), 0.1 mM nonessential amino acids (Gibco), 0.1 mM β-mercaptoethanol (Gibco), and 1000 U/ml LIF (Chemicon). ESCs media were replaced daily. Every two days, ESCs were treated with trypsin (0.25% trypsin-EDTA; Gibco) for 5 minutes in 37 °C, suspended in single cells and passaged onto new gelatinized plates. For Wnt signaling activation, ESCs were culture with either 50ng/ml rmWnt3A (R&D

System) or Wnt3a conditioned media from transgenic L-cells. Conditioned media from non-transgenic L-cells were used for control experiments.

Lef1 promoter luciferase assays

ESCs were trypsinize and resuspended in ESCs media without antibiotics. Human Lef1 promoter luciferase constructs were transfected at the time of plating on 24-well plates coated with 0.1% gelatin. For each experiment, 100,000 cells per well were combined with Lipofectamine 2000 transfection complexes following the manufacturer's protocol (Invitrogen). After 6 hours, ESCs were culture with Wnt3a conditioned media from transgenic L-cells. Conditioned media from non-transgenic L-cells were used for control experiments. After 30 hours, ESCs were washed with PBS twice and lysed in 1x passive lysis buffer for 30 minutes at room temperature following the manufacturer's protocol (Promega). Luciferase activity was measured using a dual luciferase reporter assay system (Promega) with a Clarity luminometer (Bio-Tek). Each transfection experiment was done in duplicate and repeated twice. The relative luciferase activity was determined by the ratio of the reporter plasmid to the control *Renilla* luciferase activity (pRL-CMV).

Chromatin immunoprecipitation (ChIP)

Approximately 2 x 10^7 ESCs were used for each ChIP experiment as described previously (107). ESCs were chemically crosslinked by adding

one-tenth of total volume of fresh formaldehyde solution (11% formaldehyde, 0.1M NaCl, 1mM EDTA, 0.5mM EGTA, 50mM HEPES at pH 8) and incubated at room temperature for 10 minutes. One-twentieth of total volume of 2.5M glycine (0.125M final concentration) was added to quench formaldehyde and incubated at room temperature for 10 minutes. ESCs were rinsed twice with cold 1x PBS, harvested using a silicon scraper and frozen in liquid nitrogen. ESCs were then stored at -80 ^{0}C.

ESCs were suspended in lysis buffer 1 with protease inhibitors (50mM HEPES at pH 7.5, 140mM NaCl, 1mM EDTA, 10% glycerol, 0.5% NP-40 and 0.25% Triton X-100), incubated on ice for 20 minutes and centrifuged at 4 ^{0}C for 10 minutes. The cell pellet was resuspended in lysis buffer 2 with protease inhibitors (200mM NaCl, 1mM EDTA, 0.5mM EGTA and 10mM Tris at pH 7.5), incubated on ice for 10 minutes and centrifuged at 4 ^{0}C for 10 minutes. Finally, the cell pellet was suspended in lysis buffer 3 with protease inhibitors (1mM EDTA, 0.5mM EGTA, 10mM Tris at pH 7.5, 100mM NaCl and 0.1% Na-deoxycholate) and sonicated to shear crosslinked DNA. Sonication was done using a Branson sonicator for 20 cycles of 30 seconds pulses each (60 seconds pause between pulses) at 60% amplitude. After sonication, Triton X-100 was added to the lysates to a final concentration of 1%, and cellular debris was removed by centrifugation.

Gel analysis shows that the resulting chromatin extract containing an average size of 500 bp DNA fragments. Chromatin extract was immunoprecipitated at 4 ^{0}C overnight using magnetic beads (Protein G

Dynabeads, Invitrogen) that had been pre-incubated with 10 µg of the Tcf7l1 antibody. Beads were then washed three times with wash buffer (50mM HEPES at pH 7.6, 1mM EDTA, 0.7% Na-deoxycholate, 1% NP-40 and 0.5M LiCl) and washed once with Tris-buffered saline (TBS; 50mM Tris and 150mM NaCl at pH 7.6). Elute DNA-protein complexes from the beads by heating at 65 ^{0}C for 20 minutes with brief vortexing every 2 minutes. DNA-protein crosslinks were reversed by incubation at 65 ^{0}C overnight. Eluted protein-DNA complexes were then treated with RNase A (0.2 µg/µl) at 37 ^{0}C for 1 hour and proteinase K (0.2 µg/µl) at 55 ^{0}C for 1 hour. DNA was extracted by phenol-chloroform, precipitated by ethanol, and dissolved in Tris-EDTA.

Western blot analysis

ESCs lysates were made using SDS sample buffer (80mM Tris, pH 6.8, 2% sodium dodecyl sulfate [SDS], 10% glycerol, 0.6M DTT, 0.02% bromphenol blue). Protein samples were separated by using SDS polyacrylamide gel electrophoresis and then transferred to nitrocellulose membranes (Bio-Rad). The membranes were blocked with PBST (PBS with 0.05% Tween 20)-5% milk for 1 hour at room temperature and incubated with primary antibody in PBST-5% milk overnight at 4 °C.

Primary antibodies used were Tcf7l1 (1:3,000; (73)), Tcf7 (1:1,000; Cell Signaling), Lef1 (1:1,000; Cell Signaling), Tcf7l2 (1:3000; Cell Signaling), β-catenin (1:2,000; Sigma), active β-catenin (1:1,000; Millipore) and tubulin

(1:3,000; Developmental Studies Hybridoma Bank). Secondary antibodies used were horseradish peroxidase-conjugated anti-guinea pig, -mouse, and -rabbit antibodies at 1:3,000 dilution (The Jackson Laboratory). Signals were detected using ECL Western blotting detection reagents (Amersham Biosciences).

Quantitative Immunofluorescence

ESCs were cultured in 15 mm diameter microscope cover glass (Fisher Scientific, 12-545-83) coated with 15 ug/ml human plasma fibronectin (Millipore, FC010) and transfected with Lipofectamine 2000 (Invitrogen) following the manufacturer's protocol. Cells were fixed for 8-10 minutes at room temperature with freshly prepared 4% paraformaldehyde dissolved in 1x PBS, and processed for immunofluorescent staining. All fluorescent images were taken with a Zeiss LSM 700 confocal microscope system. Different sample images of the same antigen were acquired under constant acquisition settings. Grayscale images of individual fluorescence channels were imported into ImageJ software (http://rsbweb.nih.gov/ij/) for measurement of Tcf7l1 immunofluorescence. Nuclear areas were individually selected using freehand selection tool. The mean gray value for each fluorescence channel was determined for each nucleus using the ROI manager function of ImageJ. Tcf7l1 immunofluorescence intensity was measured in non-transfected cells for each treatment to ensure the Tcf7l1 immunofluorescence staining intensity was comparable between different

experiments. 200 cells were examined for each condition in each experiment. Each experiment was performed at least twice through independent transfections.

siRNA Downregulation of Tcf7l1

Mouse Tcf7l1 siRNA (TCF7l1MSS238262: 5'-GGAAGAAAGUGGCACAACC UGUCAA-3', TCF7l1MSS277861:5'-CAAGGACACAAGGUCGCCAUCUCCA) were used to specifically downregulate Tcf7l1 mRNA expression levels designed by Stealth siRNA duplexes (Invitrogen). ESCs were trypsinize and resuspended in media without antibiotics. For each experiment, 100,000 cells per well were combined with Lipofectamine 2000 transfection complexes of control siRNA (5'-GGAAGACUAGAGGCGGUCAUGAGUU-3') or Tcf7l1 siRNA (0.04, 0.2, 1 and 5nM) following the manufacturer's protocol (Invitrogen) and plated on gelatin in a 24-well dish.

β-galactosidase Staining of Mouse Tissue

Embryos were dissected in 1x PBS and pre-fixed for 20 minutes in 4% paraformaldehyde in PBS at 4 °C. The embryos were washed five time in 1x PBS and then stained in X-Gal stain solution (100 mM Na Phosphate pH 7.3, 1.3 mM MgCl2, 3 mM $K_3Fe(CN)_6$, 3 mM $K_4Fe(CN)_6$, 1 mg/ml X-Gal, 0.1% Na deoxycholate, and 0.2% NP40). Staining was performed in the dark at 37 °C for 2-3 hours. After staining, the embryos were post-fixed in 4% paraformaldehyde at 4 °C overnight.

Frozen 8 µm-think sections of tissue were fixed with 0.5% glutaraldehyde for two minutes. After washing 7-8 times in 1x PBS, slides were then transferred into X-Gal stain solution without detergent. Staining was performed in the dark at 37 °C for 30 minutes and, after mounting in 80% glycerol, images were taken with a Zeiss Axiovert 200M inverted microscope.

References

1. van Amerongen, R. (2012) Alternative Wnt pathways and receptors. *Cold Spring Harbor perspectives in biology* **4**
2. Habas, R., Dawid, I. B., and He, X. (2003) Coactivation of Rac and Rho by Wnt/Frizzled signaling is required for vertebrate gastrulation. *Genes & development* **17**, 295-309
3. Marlow, F., Topczewski, J., Sepich, D., and Solnica-Krezel, L. (2002) Zebrafish Rho kinase 2 acts downstream of Wnt11 to mediate cell polarity and effective convergence and extension movements. *Current biology : CB* **12**, 876-884
4. Freisinger, C. M., Fisher, R. A., and Slusarski, D. C. (2010) Regulator of g protein signaling 3 modulates wnt5b calcium dynamics and somite patterning. *PLoS genetics* **6**, e1001020
5. Slusarski, D. C., Yang-Snyder, J., Busa, W. B., and Moon, R. T. (1997) Modulation of embryonic intracellular Ca2+ signaling by Wnt-5A. *Developmental biology* **182**, 114-120
6. Yoshida, Y., Kim, S., Chiba, K., Kawai, S., Tachikawa, H., and Takahashi, N. (2004) Calcineurin inhibitors block dorsal-side signaling that affect late-stage development of the heart, kidney, liver, gut and somitic tissue during Xenopus embryogenesis. *Development, growth & differentiation* **46**, 139-152
7. Slusarski, D. C., Corces, V. G., and Moon, R. T. (1997) Interaction of Wnt and a Frizzled homologue triggers G-protein-linked phosphatidylinositol signalling. *Nature* **390**, 410-413
8. Kuhl, M., Sheldahl, L. C., Malbon, C. C., and Moon, R. T. (2000) Ca(2+)/calmodulin-dependent protein kinase II is stimulated by Wnt and Frizzled homologs and promotes ventral cell fates in Xenopus. *The Journal of biological chemistry* **275**, 12701-12711
9. Sheldahl, L. C., Park, M., Malbon, C. C., and Moon, R. T. (1999) Protein kinase C is differentially stimulated by Wnt and Frizzled homologs in a G-protein-dependent manner. *Current biology : CB* **9**, 695-698
10. Saneyoshi, T., Kume, S., Amasaki, Y., and Mikoshiba, K. (2002) The Wnt/calcium pathway activates NF-AT and promotes ventral cell fate in Xenopus embryos. *Nature* **417**, 295-299

11. Tam, P. P., and Loebel, D. A. (2007) Gene function in mouse embryogenesis: get set for gastrulation. *Nature reviews. Genetics* **8**, 368-381
12. Arnold, S. J., and Robertson, E. J. (2009) Making a commitment: cell lineage allocation and axis patterning in the early mouse embryo. *Nature reviews. Molecular cell biology* **10**, 91-103
13. Church, V. L., and Francis-West, P. (2002) Wnt signalling during limb development. *The International journal of developmental biology* **46**, 927-936
14. Anastas, J. N., and Moon, R. T. (2013) WNT signalling pathways as therapeutic targets in cancer. *Nature reviews. Cancer* **13**, 11-26
15. Liu, P., Wakamiya, M., Shea, M. J., Albrecht, U., Behringer, R. R., and Bradley, A. (1999) Requirement for Wnt3 in vertebrate axis formation. *Nature genetics* **22**, 361-365
16. Kelly, O. G., Pinson, K. I., and Skarnes, W. C. (2004) The Wnt co-receptors Lrp5 and Lrp6 are essential for gastrulation in mice. *Development (Cambridge, England)* **131**, 2803-2815
17. Huelsken, J., Vogel, R., Brinkmann, V., Erdmann, B., Birchmeier, C., and Birchmeier, W. (2000) Requirement for beta-catenin in anterior-posterior axis formation in mice. *The Journal of cell biology* **148**, 567-578
18. Brennan, J., Lu, C. C., Norris, D. P., Rodriguez, T. A., Beddington, R. S., and Robertson, E. J. (2001) Nodal signalling in the epiblast patterns the early mouse embryo. *Nature* **411**, 965-969
19. Ding, J., Yang, L., Yan, Y. T., Chen, A., Desai, N., Wynshaw-Boris, A., and Shen, M. M. (1998) Cripto is required for correct orientation of the anterior-posterior axis in the mouse embryo. *Nature* **395**, 702-707
20. Mishina, Y., Suzuki, A., Ueno, N., and Behringer, R. R. (1995) Bmpr encodes a type I bone morphogenetic protein receptor that is essential for gastrulation during mouse embryogenesis. *Genes & development* **9**, 3027-3037
21. Perea-Gomez, A., Vella, F. D., Shawlot, W., Oulad-Abdelghani, M., Chazaud, C., Meno, C., Pfister, V., Chen, L., Robertson, E., Hamada, H., Behringer, R. R., and Ang, S. L. (2002) Nodal antagonists in the anterior visceral endoderm prevent the formation of multiple primitive streaks. *Developmental cell* **3**, 745-756
22. Tickle, C. (2006) Making digit patterns in the vertebrate limb. *Nature reviews. Molecular cell biology* **7**, 45-53

23. Saunders, J. W., Jr. (1998) The proximo-distal sequence of origin of the parts of the chick wing and the role of the ectoderm. 1948. *The Journal of experimental zoology* **282**, 628-668
24. Lewandoski, M., Sun, X., and Martin, G. R. (2000) Fgf8 signalling from the AER is essential for normal limb development. *Nature genetics* **26**, 460-463
25. Mariani, F. V., Ahn, C. P., and Martin, G. R. (2008) Genetic evidence that FGFs have an instructive role in limb proximal-distal patterning. *Nature* **453**, 401-405
26. Sun, X., Mariani, F. V., and Martin, G. R. (2002) Functions of FGF signalling from the apical ectodermal ridge in limb development. *Nature* **418**, 501-508
27. Tickle, C., Summerbell, D., and Wolpert, L. (1975) Positional signalling and specification of digits in chick limb morphogenesis. *Nature* **254**, 199-202
28. Crossley, P. H., Minowada, G., MacArthur, C. A., and Martin, G. R. (1996) Roles for FGF8 in the induction, initiation, and maintenance of chick limb development. *Cell* **84**, 127-136
29. Khokha, M. K., Hsu, D., Brunet, L. J., Dionne, M. S., and Harland, R. M. (2003) Gremlin is the BMP antagonist required for maintenance of Shh and Fgf signals during limb patterning. *Nature genetics* **34**, 303-307
30. Niswander, L., Jeffrey, S., Martin, G. R., and Tickle, C. (1994) A positive feedback loop coordinates growth and patterning in the vertebrate limb. *Nature* **371**, 609-612
31. Barrow, J. R., Thomas, K. R., Boussadia-Zahui, O., Moore, R., Kemler, R., Capecchi, M. R., and McMahon, A. P. (2003) Ectodermal Wnt3/beta-catenin signaling is required for the establishment and maintenance of the apical ectodermal ridge. *Genes & development* **17**, 394-409
32. Yamaguchi, T. P., Bradley, A., McMahon, A. P., and Jones, S. (1999) A Wnt5a pathway underlies outgrowth of multiple structures in the vertebrate embryo. *Development (Cambridge, England)* **126**, 1211-1223
33. Parr, B. A., and McMahon, A. P. (1995) Dorsalizing signal Wnt-7a required for normal polarity of D-V and A-P axes of mouse limb. *Nature* **374**, 350-353
34. Hill, T. P., Taketo, M. M., Birchmeier, W., and Hartmann, C. (2006) Multiple roles of mesenchymal beta-catenin during murine limb patterning. *Development (Cambridge, England)* **133**, 1219-1229
35. MacDonald, B. T., Tamai, K., and He, X. (2009) Wnt/beta-catenin signaling: components, mechanisms, and diseases. *Developmental cell* **17**, 9-26

36. Aberle, H., Bauer, A., Stappert, J., Kispert, A., and Kemler, R. (1997) beta-catenin is a target for the ubiquitin-proteasome pathway. *The EMBO journal* **16**, 3797-3804

37. Liu, C., Li, Y., Semenov, M., Han, C., Baeg, G. H., Tan, Y., Zhang, Z., Lin, X., and He, X. (2002) Control of beta-catenin phosphorylation/degradation by a dual-kinase mechanism. *Cell* **108**, 837-847

38. Behrens, J., Jerchow, B. A., Wurtele, M., Grimm, J., Asbrand, C., Wirtz, R., Kuhl, M., Wedlich, D., and Birchmeier, W. (1998) Functional interaction of an axin homolog, conductin, with beta-catenin, APC, and GSK3beta. *Science (New York, N.Y.)* **280**, 596-599

39. Ikeda, S., Kishida, S., Yamamoto, H., Murai, H., Koyama, S., and Kikuchi, A. (1998) Axin, a negative regulator of the Wnt signaling pathway, forms a complex with GSK-3beta and beta-catenin and promotes GSK-3beta-dependent phosphorylation of beta-catenin. *The EMBO journal* **17**, 1371-1384

40. Kitagawa, M., Hatakeyama, S., Shirane, M., Matsumoto, M., Ishida, N., Hattori, K., Nakamichi, I., Kikuchi, A., Nakayama, K., and Nakayama, K. (1999) An F-box protein, FWD1, mediates ubiquitin-dependent proteolysis of beta-catenin. *The EMBO journal* **18**, 2401-2410

41. Molenaar, M., van de Wetering, M., Oosterwegel, M., Peterson-Maduro, J., Godsave, S., Korinek, V., Roose, J., Destree, O., and Clevers, H. (1996) XTcf-3 transcription factor mediates beta-catenin-induced axis formation in Xenopus embryos. *Cell* **86**, 391-399

42. van de Wetering, M., Cavallo, R., Dooijes, D., van Beest, M., van Es, J., Loureiro, J., Ypma, A., Hursh, D., Jones, T., Bejsovec, A., Peifer, M., Mortin, M., and Clevers, H. (1997) Armadillo coactivates transcription driven by the product of the Drosophila segment polarity gene dTCF. *Cell* **88**, 789-799

43. Vleminckx, K., Kemler, R., and Hecht, A. (1999) The C-terminal transactivation domain of beta-catenin is necessary and sufficient for signaling by the LEF-1/beta-catenin complex in Xenopus laevis. *Mechanisms of development* **81**, 65-74

44. Cavallo, R. A., Cox, R. T., Moline, M. M., Roose, J., Polevoy, G. A., Clevers, H., Peifer, M., and Bejsovec, A. (1998) Drosophila Tcf and Groucho interact to repress Wingless signalling activity. *Nature* **395**, 604-608

45. Roose, J., Molenaar, M., Peterson, J., Hurenkamp, J., Brantjes, H., Moerer, P., van de Wetering, M., Destree, O., and Clevers, H. (1998) The Xenopus Wnt effector XTcf-3 interacts with Groucho-related transcriptional repressors. *Nature* **395**, 608-612

46. Brannon, M., Brown, J. D., Bates, R., Kimelman, D., and Moon, R. T. (1999) XCtBP is a XTcf-3 co-repressor with roles throughout Xenopus development. *Development (Cambridge, England)* **126**, 3159-3170

47. Daniels, D. L., and Weis, W. I. (2005) Beta-catenin directly displaces Groucho/TLE repressors from Tcf/Lef in Wnt-mediated transcription activation. *Nature structural & molecular biology* **12**, 364-371

48. Hecht, A., Vleminckx, K., Stemmler, M. P., van Roy, F., and Kemler, R. (2000) The p300/CBP acetyltransferases function as transcriptional coactivators of beta-catenin in vertebrates. *The EMBO journal* **19**, 1839-1850

49. Sun, Y., Kolligs, F. T., Hottiger, M. O., Mosavin, R., Fearon, E. R., and Nabel, G. J. (2000) Regulation of beta -catenin transformation by the p300 transcriptional coactivator. *Proceedings of the National Academy of Sciences of the United States of America* **97**, 12613-12618

50. Takemaru, K. I., and Moon, R. T. (2000) The transcriptional coactivator CBP interacts with beta-catenin to activate gene expression. *The Journal of cell biology* **149**, 249-254

51. Barker, N., Hurlstone, A., Musisi, H., Miles, A., Bienz, M., and Clevers, H. (2001) The chromatin remodelling factor Brg-1 interacts with beta-catenin to promote target gene activation. *The EMBO journal* **20**, 4935-4943

52. Kramps, T., Peter, O., Brunner, E., Nellen, D., Froesch, B., Chatterjee, S., Murone, M., Zullig, S., and Basler, K. (2002) Wnt/wingless signaling requires BCL9/legless-mediated recruitment of pygopus to the nuclear beta-catenin-TCF complex. *Cell* **109**, 47-60

53. Mao, J., Wang, J., Liu, B., Pan, W., Farr, G. H., 3rd, Flynn, C., Yuan, H., Takada, S., Kimelman, D., Li, L., and Wu, D. (2001) Low-density lipoprotein receptor-related protein-5 binds to Axin and regulates the canonical Wnt signaling pathway. *Molecular cell* **7**, 801-809

54. Davidson, G., Wu, W., Shen, J., Bilic, J., Fenger, U., Stannek, P., Glinka, A., and Niehrs, C. (2005) Casein kinase 1 gamma couples Wnt receptor activation to cytoplasmic signal transduction. *Nature* **438**, 867-872

55. Zeng, X., Tamai, K., Doble, B., Li, S., Huang, H., Habas, R., Okamura, H., Woodgett, J., and He, X. (2005) A dual-kinase mechanism for Wnt co-receptor phosphorylation and activation. *Nature* **438**, 873-877

56. Tolwinski, N. S., Wehrli, M., Rives, A., Erdeniz, N., DiNardo, S., and Wieschaus, E. (2003) Wg/Wnt signal can be transmitted through arrow/LRP5,6 and Axin independently of Zw3/Gsk3beta activity. *Developmental cell* **4**, 407-418

57. Huang, S. M., Mishina, Y. M., Liu, S., Cheung, A., Stegmeier, F., Michaud, G. A., Charlat, O., Wiellette, E., Zhang, Y., Wiessner, S., Hild, M., Shi, X., Wilson, C. J., Mickanin, C., Myer, V., Fazal, A., Tomlinson, R., Serluca, F., Shao, W., Cheng, H., Shultz, M., Rau, C., Schirle, M., Schlegl, J., Ghidelli, S., Fawell, S., Lu, C., Curtis, D., Kirschner, M. W., Lengauer, C., Finan, P. M., Tallarico, J. A., Bouwmeester, T., Porter, J. A., Bauer, A., and Cong, F. (2009) Tankyrase inhibition stabilizes axin and antagonizes Wnt signalling. *Nature* **461**, 614-620

58. Luo, W., Peterson, A., Garcia, B. A., Coombs, G., Kofahl, B., Heinrich, R., Shabanowitz, J., Hunt, D. F., Yost, H. J., and Virshup, D. M. (2007) Protein phosphatase 1 regulates assembly and function of the beta-catenin degradation complex. *The EMBO journal* **26**, 1511-1521

59. Strovel, E. T., Wu, D., and Sussman, D. J. (2000) Protein phosphatase 2Calpha dephosphorylates axin and activates LEF-1-dependent transcription. *The Journal of biological chemistry* **275**, 2399-2403

60. Cselenyi, C. S., Jernigan, K. K., Tahinci, E., Thorne, C. A., Lee, L. A., and Lee, E. (2008) LRP6 transduces a canonical Wnt signal independently of Axin degradation by inhibiting GSK3's phosphorylation of beta-catenin. *Proceedings of the National Academy of Sciences of the United States of America* **105**, 8032-8037

61. Piao, S., Lee, S. H., Kim, H., Yum, S., Stamos, J. L., Xu, Y., Lee, S. J., Lee, J., Oh, S., Han, J. K., Park, B. J., Weis, W. I., and Ha, N. C. (2008) Direct inhibition of GSK3beta by the phosphorylated cytoplasmic domain of LRP6 in Wnt/beta-catenin signaling. *PloS one* **3**, e4046

62. Wu, G., Huang, H., Garcia Abreu, J., and He, X. (2009) Inhibition of GSK3 phosphorylation of beta-catenin via phosphorylated PPPSPXS motifs of Wnt coreceptor LRP6. *PloS one* **4**, e4926

63. Li, V. S., Ng, S. S., Boersema, P. J., Low, T. Y., Karthaus, W. R., Gerlach, J. P., Mohammed, S., Heck, A. J., Maurice, M. M., Mahmoudi, T., and Clevers, H. (2012) Wnt signaling through inhibition of beta-catenin degradation in an intact Axin1 complex. *Cell* **149**, 1245-1256

64. Behrens, J., von Kries, J. P., Kuhl, M., Bruhn, L., Wedlich, D., Grosschedl, R., and Birchmeier, W. (1996) Functional interaction of beta-catenin with the transcription factor LEF-1. *Nature* **382**, 638-642

65. Brannon, M., Gomperts, M., Sumoy, L., Moon, R. T., and Kimelman, D. (1997) A beta-catenin/XTcf-3 complex binds to the siamois promoter to regulate dorsal axis specification in Xenopus. *Genes & development* **11**, 2359-2370

66. Prieve, M. G., Guttridge, K. L., Munguia, J., and Waterman, M. L. (1998) Differential importin-alpha recognition and nuclear transport by nuclear localization signals within the high-mobility-group DNA binding domains of lymphoid enhancer factor 1 and T-cell factor 1. *Molecular and cellular biology* **18**, 4819-4832

67. van de Wetering, M., and Clevers, H. (1992) Sequence-specific interaction of the HMG box proteins TCF-1 and SRY occurs within the minor groove of a Watson-Crick double helix. *The EMBO journal* **11**, 3039-3044

68. van Beest, M., Dooijes, D., van De Wetering, M., Kjaerulff, S., Bonvin, A., Nielsen, O., and Clevers, H. (2000) Sequence-specific high mobility group box factors recognize 10-12-base pair minor groove motifs. *The Journal of biological chemistry* **275**, 27266-27273

69. Atcha, F. A., Syed, A., Wu, B., Hoverter, N. P., Yokoyama, N. N., Ting, J. H., Munguia, J. E., Mangalam, H. J., Marsh, J. L., and Waterman, M. L. (2007) A unique DNA binding domain converts T-cell factors into strong Wnt effectors. *Molecular and cellular biology* **27**, 8352-8363

70. Brantjes, H., Roose, J., van De Wetering, M., and Clevers, H. (2001) All Tcf HMG box transcription factors interact with Groucho-related co-repressors. *Nucleic acids research* **29**, 1410-1419

71. Atcha, F. A., Munguia, J. E., Li, T. W., Hovanes, K., and Waterman, M. L. (2003) A new beta-catenin-dependent activation domain in T cell factor. *The Journal of biological chemistry* **278**, 16169-16175

72. Merrill, B. J., Gat, U., DasGupta, R., and Fuchs, E. (2001) Tcf3 and Lef1 regulate lineage differentiation of multipotent stem cells in skin. *Genes & development* **15**, 1688-1705

73. Pereira, L., Yi, F., and Merrill, B. J. (2006) Repression of Nanog gene transcription by Tcf3 limits embryonic stem cell self-renewal. *Molecular and cellular biology* **26**, 7479-7491

74. van Genderen, C., Okamura, R. M., Farinas, I., Quo, R. G., Parslow, T. G., Bruhn, L., and Grosschedl, R. (1994) Development of several organs that require inductive

epithelial-mesenchymal interactions is impaired in LEF-1-deficient mice. *Genes & development* **8**, 2691-2703

75. Verbeek, S., Izon, D., Hofhuis, F., Robanus-Maandag, E., te Riele, H., van de Wetering, M., Oosterwegel, M., Wilson, A., MacDonald, H. R., and Clevers, H. (1995) An HMG-box-containing T-cell factor required for thymocyte differentiation. *Nature* **374**, 70-74
76. Schilham, M. W., Wilson, A., Moerer, P., Benaissa-Trouw, B. J., Cumano, A., and Clevers, H. C. (1998) Critical involvement of Tcf-1 in expansion of thymocytes. *Journal of immunology (Baltimore, Md. : 1950)* **161**, 3984-3991
77. Korinek, V., Barker, N., Moerer, P., van Donselaar, E., Huls, G., Peters, P. J., and Clevers, H. (1998) Depletion of epithelial stem-cell compartments in the small intestine of mice lacking Tcf-4. *Nature genetics* **19**, 379-383
78. Houston, D. W., Kofron, M., Resnik, E., Langland, R., Destree, O., Wylie, C., and Heasman, J. (2002) Repression of organizer genes in dorsal and ventral Xenopus cells mediated by maternal XTcf3. *Development (Cambridge, England)* **129**, 4015-4025
79. Kim, C. H., Oda, T., Itoh, M., Jiang, D., Artinger, K. B., Chandrasekharappa, S. C., Driever, W., and Chitnis, A. B. (2000) Repressor activity of Headless/Tcf3 is essential for vertebrate head formation. *Nature* **407**, 913-916
80. Merrill, B. J., Pasolli, H. A., Polak, L., Rendl, M., Garcia-Garcia, M. J., Anderson, K. V., and Fuchs, E. (2004) Tcf3: a transcriptional regulator of axis induction in the early embryo. *Development (Cambridge, England)* **131**, 263-274
81. Ishikawa, T. O., Tamai, Y., Li, Q., Oshima, M., and Taketo, M. M. (2003) Requirement for tumor suppressor Apc in the morphogenesis of anterior and ventral mouse embryo. *Developmental biology* **253**, 230-246
82. Zeng, L., Fagotto, F., Zhang, T., Hsu, W., Vasicek, T. J., Perry, W. L., 3rd, Lee, J. J., Tilghman, S. M., Gumbiner, B. M., and Costantini, F. (1997) The mouse Fused locus encodes Axin, an inhibitor of the Wnt signaling pathway that regulates embryonic axis formation. *Cell* **90**, 181-192
83. Popperl, H., Schmidt, C., Wilson, V., Hume, C. R., Dodd, J., Krumlauf, R., and Beddington, R. S. (1997) Misexpression of Cwnt8C in the mouse induces an ectopic embryonic axis and causes a truncation of the anterior neuroectoderm. *Development (Cambridge, England)* **124**, 2997-3005

84. Galceran, J., Farinas, I., Depew, M. J., Clevers, H., and Grosschedl, R. (1999) Wnt3a-/--like phenotype and limb deficiency in Lef1(-/-)Tcf1(-/-) mice. *Genes & development* **13**, 709-717

85. Yoshikawa, Y., Fujimori, T., McMahon, A. P., and Takada, S. (1997) Evidence that absence of Wnt-3a signaling promotes neuralization instead of paraxial mesoderm development in the mouse. *Developmental biology* **183**, 234-242

86. Monkley, S. J., Delaney, S. J., Pennisi, D. J., Christiansen, J. H., and Wainwright, B. J. (1996) Targeted disruption of the Wnt2 gene results in placentation defects. *Development (Cambridge, England)* **122**, 3343-3353

87. Nguyen, H., Merrill, B. J., Polak, L., Nikolova, M., Rendl, M., Shaver, T. M., Pasolli, H. A., and Fuchs, E. (2009) Tcf3 and Tcf4 are essential for long-term homeostasis of skin epithelia. *Nature genetics* **41**, 1068-1075

88. Phillips, B. T., and Kimble, J. (2009) A new look at TCF and beta-catenin through the lens of a divergent C. elegans Wnt pathway. *Developmental cell* **17**, 27-34

89. Shetty, P., Lo, M. C., Robertson, S. M., and Lin, R. (2005) C. elegans TCF protein, POP-1, converts from repressor to activator as a result of Wnt-induced lowering of nuclear levels. *Developmental biology* **285**, 584-592

90. Mizumoto, K., and Sawa, H. (2007) Two betas or not two betas: regulation of asymmetric division by beta-catenin. *Trends in cell biology* **17**, 465-473

91. Yang, X. D., Huang, S., Lo, M. C., Mizumoto, K., Sawa, H., Xu, W., Robertson, S., and Lin, R. (2011) Distinct and mutually inhibitory binding by two divergent beta-catenins coordinates TCF levels and activity in C. elegans. *Development (Cambridge, England)* **138**, 4255-4265

92. Rocheleau, C. E., Yasuda, J., Shin, T. H., Lin, R., Sawa, H., Okano, H., Priess, J. R., Davis, R. J., and Mello, C. C. (1999) WRM-1 activates the LIT-1 protein kinase to transduce anterior/posterior polarity signals in C. elegans. *Cell* **97**, 717-726

93. Lo, M. C., Gay, F., Odom, R., Shi, Y., and Lin, R. (2004) Phosphorylation by the beta-catenin/MAPK complex promotes 14-3-3-mediated nuclear export of TCF/POP-1 in signal-responsive cells in C. elegans. *Cell* **117**, 95-106

94. Kidd, A. R., 3rd, Miskowski, J. A., Siegfried, K. R., Sawa, H., and Kimble, J. (2005) A beta-catenin identified by functional rather than sequence criteria and its role in Wnt/MAPK signaling. *Cell* **121**, 761-772

95. Moon, R. T., Bowerman, B., Boutros, M., and Perrimon, N. (2002) The promise and perils of Wnt signaling through beta-catenin. *Science (New York, N.Y.)* **296**, 1644-1646

96. Yi, F., and Merrill, B. J. (2007) Stem cells and TCF proteins: a role for beta-catenin--independent functions. *Stem cell reviews* **3**, 39-48

97. Zhou, P., Byrne, C., Jacobs, J., and Fuchs, E. (1995) Lymphoid enhancer factor 1 directs hair follicle patterning and epithelial cell fate. *Genes & development* **9**, 700-713

98. Nguyen, H., Rendl, M., and Fuchs, E. (2006) Tcf3 governs stem cell features and represses cell fate determination in skin. *Cell* **127**, 171-183

99. Kemler, R., Hierholzer, A., Kanzler, B., Kuppig, S., Hansen, K., Taketo, M. M., de Vries, W. N., Knowles, B. B., and Solter, D. (2004) Stabilization of beta-catenin in the mouse zygote leads to premature epithelial-mesenchymal transition in the epiblast. *Development (Cambridge, England)* **131**, 5817-5824

100. Dorsky, R. I., Itoh, M., Moon, R. T., and Chitnis, A. (2003) Two tcf3 genes cooperate to pattern the zebrafish brain. *Development (Cambridge, England)* **130**, 1937-1947

101. DasGupta, R., and Fuchs, E. (1999) Multiple roles for activated LEF/TCF transcription complexes during hair follicle development and differentiation. *Development (Cambridge, England)* **126**, 4557-4568

102. Ivanova, N. B., Dimos, J. T., Schaniel, C., Hackney, J. A., Moore, K. A., and Lemischka, I. R. (2002) A stem cell molecular signature. *Science (New York, N.Y.)* **298**, 601-604

103. Ben-Porath, I., Thomson, M. W., Carey, V. J., Ge, R., Bell, G. W., Regev, A., and Weinberg, R. A. (2008) An embryonic stem cell-like gene expression signature in poorly differentiated aggressive human tumors. *Nature genetics* **40**, 499-507

104. Arnold, S. J., Stappert, J., Bauer, A., Kispert, A., Herrmann, B. G., and Kemler, R. (2000) Brachyury is a target gene of the Wnt/beta-catenin signaling pathway. *Mechanisms of development* **91**, 249-258

105. Galceran, J., Hsu, S. C., and Grosschedl, R. (2001) Rescue of a Wnt mutation by an activated form of LEF-1: regulation of maintenance but not initiation of Brachyury expression. *Proceedings of the National Academy of Sciences of the United States of America* **98**, 8668-8673

106. Graham, T. A., Weaver, C., Mao, F., Kimelman, D., and Xu, W. (2000) Crystal structure of a beta-catenin/Tcf complex. *Cell* **103**, 885-896

107. Yi, F., Pereira, L., Hoffman, J. A., Shy, B. R., Yuen, C. M., Liu, D. R., and Merrill, B. J. (2011) Opposing effects of Tcf3 and Tcf1 control Wnt stimulation of embryonic stem cell self-renewal. *Nature cell biology* **13**, 762-770

108. Maretto, S., Cordenonsi, M., Dupont, S., Braghetta, P., Broccoli, V., Hassan, A. B., Volpin, D., Bressan, G. M., and Piccolo, S. (2003) Mapping Wnt/beta-catenin signaling during mouse development and in colorectal tumors. *Proceedings of the National Academy of Sciences of the United States of America* **100**, 3299-3304

109. Laufer, E., Nelson, C. E., Johnson, R. L., Morgan, B. A., and Tabin, C. (1994) Sonic hedgehog and Fgf-4 act through a signaling cascade and feedback loop to integrate growth and patterning of the developing limb bud. *Cell* **79**, 993-1003

110. Riddle, R. D., Johnson, R. L., Laufer, E., and Tabin, C. (1993) Sonic hedgehog mediates the polarizing activity of the ZPA. *Cell* **75**, 1401-1416

111. Kengaku, M., Capdevila, J., Rodriguez-Esteban, C., De La Pena, J., Johnson, R. L., Izpisua Belmonte, J. C., and Tabin, C. J. (1998) Distinct WNT pathways regulating AER formation and dorsoventral polarity in the chick limb bud. *Science (New York, N.Y.)* **280**, 1274-1277

112. Zuniga, A., and Zeller, R. (1999) Gli3 (Xt) and formin (ld) participate in the positioning of the polarising region and control of posterior limb-bud identity. *Development (Cambridge, England)* **126**, 13-21

113. Findlater, G. S., McDougall, R. D., and Kaufman, M. H. (1993) Eyelid development, fusion and subsequent reopening in the mouse. *Journal of anatomy* **183 (Pt 1)**, 121-129

114. Tao, H., Shimizu, M., Kusumoto, R., Ono, K., Noji, S., and Ohuchi, H. (2005) A dual role of FGF10 in proliferation and coordinated migration of epithelial leading edge cells during mouse eyelid development. *Development (Cambridge, England)* **132**, 3217-3230

115. Vassalli, A., Matzuk, M. M., Gardner, H. A., Lee, K. F., and Jaenisch, R. (1994) Activin/inhibin beta B subunit gene disruption leads to defects in eyelid development and female reproduction. *Genes & development* **8**, 414-427

116. Zenz, R., Scheuch, H., Martin, P., Frank, C., Eferl, R., Kenner, L., Sibilia, M., and Wagner, E. F. (2003) c-Jun regulates eyelid closure and skin tumor development through EGFR signaling. *Developmental cell* **4**, 879-889

117. Zhang, L., Wang, W., Hayashi, Y., Jester, J. V., Birk, D. E., Gao, M., Liu, C. Y., Kao, W. W., Karin, M., and Xia, Y. (2003) A role for MEK kinase 1 in TGF-beta/activin-induced epithelium movement and embryonic eyelid closure. *The EMBO journal* **22**, 4443-4454

118. Knop, E., Korb, D. R., Blackie, C. A., and Knop, N. (2010) The lid margin is an underestimated structure for preservation of ocular surface health and development of dry eye disease. *Developments in ophthalmology* **45**, 108-122

119. Riau, A. K., Barathi, V. A., and Beuerman, R. W. (2008) Mucocutaneous junction of eyelid and lip: a study of the transition zone using epithelial cell markers. *Current eye research* **33**, 912-922

120. Liu, S., Li, J., Tan, D. T., and Beuerman, R. W. (2007) The eyelid margin: a transitional zone for 2 epithelial phenotypes. *Archives of ophthalmology* **125**, 523-532

121. Wirtschafter, J. D., McLoon, L. K., Ketcham, J. M., Weinstock, R. J., and Cheung, J. C. (1997) Palpebral conjunctival transient amplifying cells originate at the mucocutaneous junction and their progeny migrate toward the fornix. *Transactions of the American Ophthalmological Society* **95**, 417-429; discussion 429-432

122. Kelly, K. F., Ng, D. Y., Jayakumaran, G., Wood, G. A., Koide, H., and Doble, B. W. (2011) beta-catenin enhances Oct-4 activity and reinforces pluripotency through a TCF-independent mechanism. *Cell stem cell* **8**, 214-227

123. Hecht, A., and Stemmler, M. P. (2003) Identification of a promoter-specific transcriptional activation domain at the C terminus of the Wnt effector protein T-cell factor 4. *The Journal of biological chemistry* **278**, 3776-3785

124. Jho, E. H., Zhang, T., Domon, C., Joo, C. K., Freund, J. N., and Costantini, F. (2002) Wnt/beta-catenin/Tcf signaling induces the transcription of Axin2, a negative regulator of the signaling pathway. *Molecular and cellular biology* **22**, 1172-1183

125. Rendl, M., Lewis, L., and Fuchs, E. (2005) Molecular dissection of mesenchymal-epithelial interactions in the hair follicle. *PLoS biology* **3**, e331

126. Graham, T. A., Ferkey, D. M., Mao, F., Kimelman, D., and Xu, W. (2001) Tcf4 can specifically recognize beta-catenin using alternative conformations. *Nature structural biology* **8**, 1048-1052

127. Zhou, C. J., Borello, U., Rubenstein, J. L., and Pleasure, S. J. (2006) Neuronal production and precursor proliferation defects in the neocortex of mice with loss of function in the canonical Wnt signaling pathway. *Neuroscience* **142**, 1119-1131

128. Cygan, J. A., Johnson, R. L., and McMahon, A. P. (1997) Novel regulatory interactions revealed by studies of murine limb pattern in Wnt-7a and En-1 mutants. *Development (Cambridge, England)* **124**, 5021-5032

129. Hovanes, K., Li, T. W., Munguia, J. E., Truong, T., Milovanovic, T., Lawrence Marsh, J., Holcombe, R. F., and Waterman, M. L. (2001) Beta-catenin-sensitive isoforms of lymphoid enhancer factor-1 are selectively expressed in colon cancer. *Nature genetics* **28**, 53-57

130. Filali, M., Cheng, N., Abbott, D., Leontiev, V., and Engelhardt, J. F. (2002) Wnt-3A/beta-catenin signaling induces transcription from the LEF-1 promoter. *The Journal of biological chemistry* **277**, 33398-33410

131. Roose, J., Huls, G., van Beest, M., Moerer, P., van der Horn, K., Goldschmeding, R., Logtenberg, T., and Clevers, H. (1999) Synergy between tumor suppressor APC and the beta-catenin-Tcf4 target Tcf1. *Science (New York, N.Y.)* **285**, 1923-1926

132. Waterman, M. L. (2004) Lymphoid enhancer factor/T cell factor expression in colorectal cancer. *Cancer metastasis reviews* **23**, 41-52

133. Tamai, K., Semenov, M., Kato, Y., Spokony, R., Liu, C., Katsuyama, Y., Hess, F., Saint-Jeannet, J. P., and He, X. (2000) LDL-receptor-related proteins in Wnt signal transduction. *Nature* **407**, 530-535

134. Pinson, K. I., Brennan, J., Monkley, S., Avery, B. J., and Skarnes, W. C. (2000) An LDL-receptor-related protein mediates Wnt signalling in mice. *Nature* **407**, 535-538

135. Gray, J. D., Nakouzi, G., Slowinska-Castaldo, B., Dazard, J. E., Rao, J. S., Nadeau, J. H., and Ross, M. E. (2010) Functional interactions between the LRP6 WNT co-receptor and folate supplementation. *Human molecular genetics* **19**, 4560-4572

136. Clevers, H., and Nusse, R. (2012) Wnt/beta-catenin signaling and disease. *Cell* **149**, 1192-1205

137. Nusse, R. (2012) Wnt signaling. *Cold Spring Harbor perspectives in biology* **4**

138. Stamos, J. L., and Weis, W. I. (2013) The beta-catenin destruction complex. *Cold Spring Harbor perspectives in biology* **5**, a007898

139. Hart, M., Concordet, J. P., Lassot, I., Albert, I., del los Santos, R., Durand, H., Perret, C., Rubinfeld, B., Margottin, F., Benarous, R., and Polakis, P. (1999) The F-box protein beta-TrCP associates with phosphorylated beta-catenin and regulates its activity in the cell. *Current biology : CB* **9**, 207-210

140. Yost, C., Torres, M., Miller, J. R., Huang, E., Kimelman, D., and Moon, R. T. (1996) The axis-inducing activity, stability, and subcellular distribution of beta-catenin is regulated in Xenopus embryos by glycogen synthase kinase 3. *Genes & development* **10**, 1443-1454

141. Cadigan, K. M., and Waterman, M. L. (2012) TCF/LEFs and Wnt signaling in the nucleus. *Cold Spring Harbor perspectives in biology* **4**

142. Wu, C. I., Hoffman, J. A., Shy, B. R., Ford, E. M., Fuchs, E., Nguyen, H., and Merrill, B. J. (2012) Function of Wnt/beta-catenin in counteracting Tcf3 repression through the Tcf3-beta-catenin interaction. *Development (Cambridge, England)* **139**, 2118-2129

143. Staal, F. J., Burgering, B. M., van de Wetering, M., and Clevers, H. C. (1999) Tcf-1-mediated transcription in T lymphocytes: differential role for glycogen synthase kinase-3 in fibroblasts and T cells. *International immunology* **11**, 317-323

144. Hovanes, K., Li, T. W., and Waterman, M. L. (2000) The human LEF-1 gene contains a promoter preferentially active in lymphocytes and encodes multiple isoforms derived from alternative splicing. *Nucleic acids research* **28**, 1994-2003

145. Wang, Y., Medvid, R., Melton, C., Jaenisch, R., and Blelloch, R. (2007) DGCR8 is essential for microRNA biogenesis and silencing of embryonic stem cell self-renewal. *Nature genetics* **39**, 380-385

146. Lyashenko, N., Winter, M., Migliorini, D., Biechele, T., Moon, R. T., and Hartmann, C. (2011) Differential requirement for the dual functions of beta-catenin in embryonic stem cell self-renewal and germ layer formation. *Nature cell biology* **13**, 753-761

147. Wray, J., Kalkan, T., Gomez-Lopez, S., Eckardt, D., Cook, A., Kemler, R., and Smith, A. (2011) Inhibition of glycogen synthase kinase-3 alleviates Tcf3 repression of the pluripotency network and increases embryonic stem cell resistance to differentiation. *Nature cell biology* **13**, 838-845

148. Hoffman, J. A., Wu, C. I., and Merrill, B. J. (2013) Tcf7l1 prepares epiblast cells in the gastrulating mouse embryo for lineage specification. *Development (Cambridge, England)* **140**, 1665-1675

149. Slyper, M., Shahar, A., Bar-Ziv, A., Granit, R. Z., Hamburger, T., Maly, B., Peretz, T., and Ben-Porath, I. (2012) Control of breast cancer growth and initiation by the stem cell-associated transcription factor TCF3. *Cancer research* **72**, 5613-5624

150. Tutter, A. V., Fryer, C. J., and Jones, K. A. (2001) Chromatin-specific regulation of LEF-1-beta-catenin transcription activation and inhibition in vitro. *Genes & development* **15**, 3342-3354

151. Shy, B. R., Wu, C. I., Khramtsova, G. F., Zhang, J. Y., Olopade, O. I., Goss, K. H., and Merrill, B. J. (2013) Regulation of Tcf7l1 DNA binding and protein stability as principal mechanisms of Wnt/beta-catenin signaling. *Cell reports* **4**, 1-9

152. Wang, J., Hamblet, N. S., Mark, S., Dickinson, M. E., Brinkman, B. C., Segil, N., Fraser, S. E., Chen, P., Wallingford, J. B., and Wynshaw-Boris, A. (2006) Dishevelled genes mediate a conserved mammalian PCP pathway to regulate convergent extension during neurulation. *Development (Cambridge, England)* **133**, 1767-1778

153. Wang, Y., Guo, N., and Nathans, J. (2006) The role of Frizzled3 and Frizzled6 in neural tube closure and in the planar polarity of inner-ear sensory hair cells. *The Journal of neuroscience : the official journal of the Society for Neuroscience* **26**, 2147-2156

154. Wang, W., Liu, H., Wang, S., Hao, X., and Li, L. (2011) A diterpenoid derivative 15-oxospiramilactone inhibits Wnt/beta-catenin signaling and colon cancer cell tumorigenesis. *Cell research* **21**, 730-740

155. Gonsalves, F. C., Klein, K., Carson, B. B., Katz, S., Ekas, L. A., Evans, S., Nagourney, R., Cardozo, T., Brown, A. M., and DasGupta, R. (2011) An RNAi-based chemical genetic screen identifies three small-molecule inhibitors of the Wnt/wingless signaling pathway. *Proceedings of the National Academy of Sciences of the United States of America* **108**, 5954-5963

156. Lepourcelet, M., Chen, Y. N., France, D. S., Wang, H., Crews, P., Petersen, F., Bruseo, C., Wood, A. W., and Shivdasani, R. A. (2004) Small-molecule antagonists of the oncogenic Tcf/beta-catenin protein complex. *Cancer cell* **5**, 91-102

157. Kuwabara, T., Hsieh, J., Muotri, A., Yeo, G., Warashina, M., Lie, D. C., Moore, L., Nakashima, K., Asashima, M., and Gage, F. H. (2009) Wnt-mediated activation of NeuroD1 and retro-elements during adult neurogenesis. *Nature neuroscience* **12**, 1097-1105

158. Lie, D. C., Colamarino, S. A., Song, H. J., Desire, L., Mira, H., Consiglio, A., Lein, E. S., Jessberger, S., Lansford, H., Dearie, A. R., and Gage, F. H. (2005) Wnt signalling regulates adult hippocampal neurogenesis. *Nature* **437**, 1370-1375

159. Reya, T., Duncan, A. W., Ailles, L., Domen, J., Scherer, D. C., Willert, K., Hintz, L., Nusse, R., and Weissman, I. L. (2003) A role for Wnt signalling in self-renewal of haematopoietic stem cells. *Nature* **423**, 409-414

160. Yi, F., Pereira, L., and Merrill, B. J. (2008) Tcf3 Functions as a Steady State Limiter of Transcriptional Programs of Mouse Embryonic Stem Cell Self Renewal. *Stem Cells*

APPENDICES

Copyright and Permissions

The Company of Biologists Subscription Journals: *Development*, *Journal of Cell Science* and *The Journal of Experimental Biology*

Author Rights

(these rights are retained when publishing an Open Access article)

Authors remain the owners of the copyright to the article and retain the following non-exclusive rights (for further details, please refer to the license agreement that accompanies article proofs):

(1) authors may reproduce the article, in whole or in part, in any printed book (including a thesis) of which they are author, provided the original article is properly and fully attributed;

(2) authors and any academic institution where they are employed may reproduce the article, in whole or in part, for the purpose of teaching students;

(3) authors may post a copy of the article on their website, provided that it has already been published by the journal and is linked to the journal's website.

(4) authors may use data contained in the article in other works they create.

Development 139, 2118-2129 (2012) doi:10.1242/dev.076067

Function of Wnt/β-catenin in counteracting Tcf3 repression through the Tcf3–β-catenin interaction

Chun-I Wu[1], Jackson A. Hoffman[1], Brian R. Shy[1], Erin M. Ford[2], Elaine Fuchs[3], Hoang Nguyen[2] and Bradley J. Merrill[1,*]

SUMMARY

The canonical Wnt/β-catenin signaling pathway classically functions through the activation of target genes by Tcf/Lef–β-catenin complexes. In contrast to β-catenin-dependent functions described for Tcf1, Tcf4 and Lef1, the known embryonic functions for Tcf3 in mice, frogs and fish are consistent with β-catenin-independent repressor activity. In this study, we genetically define Tcf3–β-catenin functions in mice by generating a *Tcf3*ΔN knock-in mutation that specifically ablates Tcf3–β-catenin. Mouse embryos homozygous for the knock-in mutation (*Tcf3*$^{\Delta N/\Delta N}$) progress through gastrulation without apparent defects, thus genetically proving that Tcf3 function during gastrulation is independent of β-catenin interaction. *Tcf3*$^{\Delta N/\Delta N}$ mice were not viable, and several post-gastrulation defects revealed the first in vivo functions of Tcf3–β-catenin interaction affecting limb development, vascular integrity, neural tube closure and eyelid closure. Interestingly, the etiology of defects indicated an indirect role for Tcf3–β-catenin in the activation of target genes. Tcf3 directly represses transcription of *Lef1*, which is stimulated by Wnt/β-catenin activity. These genetic data indicate that Tcf3–β-catenin is not necessary to activate target genes directly. Instead, our findings support the existence of a regulatory circuit whereby Wnt/β-catenin counteracts Tcf3 repression of *Lef1*, which subsequently activates target gene expression via Lef1–β-catenin complexes. We propose that the Tcf/Lef circuit model provides a mechanism downstream of β-catenin stability for controlling the strength of Wnt signaling activity during embryonic development.

KEY WORDS: Tcf3, Wnt signaling, beta-catenin, Embryonic stem cell, Mouse embryogenesis

INTRODUCTION

The canonical Wnt signaling pathway is required for morphogenesis of many organs, and its activity is necessary in adults through the regulation of stem cell properties. Overactivation of Wnt/β-catenin signaling causes cancer (Moon et al., 2002), which demonstrates a need to regulate the pathway through adulthood. Activity of the pathway is controlled through the regulation of β-catenin protein stability (MacDonald et al., 2009). In the absence of a Wnt ligand, β-catenin is targeted for ubiquitin- and proteasome-mediated degradation by phosphorylation at serine and threonine residues near the N-terminus (Aberle et al., 1997; Liu et al., 2002). Phosphorylation of β-catenin occurs within a polyprotein complex that includes adenomatous polyposis coli (APC), Axin, and the kinases casein kinase 1 and glycogen synthase kinase 3 (GSK3) (Behrens et al., 1998; Ikeda et al., 1998; Liu et al., 2002). Wnt ligands bind to Frizzled-Lrp5/6 receptor complexes and initiate a downstream cascade that inhibits GSK3 phosphorylation of β-catenin. This effect stabilizes β-catenin and stimulates its interaction with DNA-binding transcriptional regulators, of which Tcf/Lef proteins are the best characterized (Molenaar et al., 1996; van de Wetering et al., 1997). When bound to Tcf/Lef proteins, β-catenin can function as a transcriptional co-activator by recruiting several nuclear factors to chromatin, such as BCL9, Pygopus, Brg-1 and CBP (Barker et al., 2001; Hecht et al., 2000; Kramps et al., 2002; Sun et al., 2000; Takemaru and Moon, 2000).

[1]Department of Biochemistry and Molecular Genetics, University of Illinois at Chicago, Chicago, IL 60607, USA. [2]Center for Stem Cell and Regenerative Medicine, Department of Molecular and Cellular Biology, Baylor College of Medicine, Houston, TX 77030, USA. [3]Laboratory of Mammalian Cell Biology and Development, The Rockefeller University, New York, NY 10065, USA.

*Author for correspondence (merrillb@uic.edu)

Accepted 28 March 2012

Mammals have four Tcf/Lef factors: Tcf1 (Tcf7), Tcf3 (Tcf7L1), Tcf4 (Tcf712) and Lef1. They possess nearly identical DNA-binding domains that allow them to bind the same consensus sequence ($^{A}/_{T}{}^{A}/_{T}$CAAAG) and regulate the transcription of target genes (Atcha et al., 2007; van Beest et al., 2000; van de Wetering and Clevers, 1992). All Tcf/Lefs also possess conserved β-catenin interaction domains near the N-terminus, which are necessary for Tcf/Lef proteins to stimulate target gene transcription in response to Wnt-stabilized β-catenin (Behrens et al., 1996; Brannon et al., 1997; Molenaar et al., 1996; van de Wetering et al., 1997). Full-length Tcf/Lef proteins also have β-catenin-independent activities as transcriptional repressors. Although all Tcf/Lef proteins have been reported to interact with co-repressor proteins such as Groucho (Brantjes et al., 2001), the extent to which the embryonic function of Tcf/Lefs depends on β-catenin-independent activities appears to be different for each Tcf/Lef protein (Yi and Merrill, 2007). Lef1 sits at one end of the spectrum, as knockout and transgenic mouse models predominantly show Wnt/β-catenin-dependent functions for Lef1 (van Genderen et al., 1994; Zhou et al., 1995).

At the other end of the spectrum, Tcf3 appears to function primarily as a transcriptional repressor. Transgenic mice showed that full-length wild-type Tcf3 and β-catenin interaction-defective ΔNTcf3 cause essentially identical phenotypes when ectopically expressed in the epidermis (Merrill et al., 2001). Importantly, transgenic mice engineered to overexpress repressor-defective mutant forms of Tcf3 did not exhibit an abnormal phenotype (Merrill et al., 2001). Subsequently, through the use of inducible Tcf3 expression in the skin, the Tcf3 overexpression phenotype was shown to be caused by a reversion of adult cells to an embryonic-like state, and analysis of downstream transcriptional effects showed that Tcf3 did not require Wnt/β-catenin (Nguyen et al., 2006). Genetic ablation of *Tcf3* affected gastrulation to produce

Licensing Policy

Cell Reports allows authors to retain copyright in their articles. We ask authors to sign a publishing agreement offering a choice of two Creative Commons licenses and ensuring that any attributions in reproductions of the work acknowledge the journal as the primary reference publication.

Creative Commons Attribution 3.0 Unported License

The first option is the Creative Commons Attribution 3.0 Unported License, which allows users to alter and build upon the article and then distribute the resulting work, even commercially. As with all Creative Commons licenses, the work must be attributed to the original author and publisher. This license encourages maximum use and redistribution but gives the author the least control about how the work might appear. The full details of the license are available at http://creativecommons.org/licenses/by/3.0/legalcode

Creative Commons Attribution-Noncommercial-No Derivative Works 3.0 Unported license

The second option is the Creative Commons Attribution-Noncommercial-No Derivative Works 3.0 Unported License, which allows users to copy and distribute the article, provided the work is attributed back to the original author and publisher. The article cannot be changed in any way or used commercially. This license gives the author the most control about how the work might be published. The full details of the license are available at http://creativecommons.org/licenses/by-nc-nd/3.0/legalcode.

Cell Reports
Report

Cell PRESS
Open ACCESS

Regulation of Tcf7l1 DNA Binding and Protein Stability as Principal Mechanisms of Wnt/β-Catenin Signaling

Brian R. Shy,[1,4] Chun-I. Wu,[1,4] Galina F. Khramtsova,[2] Jenny Y. Zhang,[1] Olufunmilayo I. Olopade,[2] Kathleen H. Goss,[3] and Bradley J. Merrill[1,*]
[1]Department of Biochemistry and Molecular Genetics, University of Illinois at Chicago, Chicago, IL 60607, USA
[2]Department of Medicine, University of Chicago, Chicago, IL 60637, USA
[3]Department of Surgery, University of Chicago, Chicago, IL 60637, USA
[4]These authors contributed equally to this work as co-first authors
*Correspondence: merrillb@uic.edu
http://dx.doi.org/10.1016/j.celrep.2013.06.001

SUMMARY

Wnt/β-catenin signal transduction requires direct binding of β-catenin to Tcf/Lef proteins, an event that is classically associated with stimulating transcription by recruiting coactivators. This molecular cascade plays critical roles throughout embryonic development and normal postnatal life by affecting stem cell characteristics and tumor formation. Here, we show that this pathway utilizes a fundamentally different mechanism to regulate Tcf7l1 (formerly named Tcf3) activity. β-catenin inactivates Tcf7l1 without a switch to a coactivator complex by removing it from DNA, which leads to Tcf7l1 protein degradation. Mouse genetic experiments demonstrate that Tcf7l1 inactivation is the only required effect of the Tcf7l1-β-catenin interaction. Given the expression of Tcf7l1 in pluripotent embryonic and adult stem cells, as well as in poorly differentiated breast cancer, these findings provide mechanistic insights into the regulation of pluripotency and the role of Wnt/β-catenin in breast cancer.

INTRODUCTION

Canonical Wnt/β-catenin signaling impacts a wide range of biological activities, including stem cell self-renewal, organ morphogenesis, and tumor formation (Clevers and Nusse, 2012; Nusse, 2012). Regulation of the pathway centers on the stability of β-catenin, which is targeted for proteasome-mediated degradation by a complex containing adenomatous polyposis coli (APC), Axin structural proteins, and glycogen synthase kinase 3 (GSK3) (Stamos and Weis, 2013). Phosphorylation of β-catenin by GSK3 stimulates degradation dependent upon APC, Axin, and the β-TrCP E3 ligase (Aberle et al., 1997; Hart et al., 1999; Yost et al., 1996). Wnt signaling inhibits degradation of β-catenin by blocking its ubiquitination (Li et al., 2012). Pharmacological GSK3 inhibitors similarly inhibit β-catenin degradation by blocking β-catenin phosphorylation.

An important downstream mechanism of the Wnt/β-catenin pathway occurs as β-catenin binds to the amino terminal of Tcf/Lef proteins, thereby displacing corepressor proteins bound to the Tcf/Lef (Cavallo et al., 1998; Daniels and Weis, 2005; Roose et al., 1998). Tcf-β-catenin binding subsequently recruits transactivator proteins to the genomic sites that were previously occupied by corepressors (Brannon et al., 1997; Molenaar et al., 1996; van de Wetering et al., 1997). This accepted model of canonical Wnt/β-catenin signaling is consistent with observed effects of Tcf/Lef proteins in many contexts (Cadigan and Waterman, 2012); however, it is not consistent with recent observations for mammalian Tcf7l1 (formerly Tcf3). In cells where Lef1 and Tcf7 (formerly Tcf1) act as β-catenin-dependent transactivators, only transcriptional repressor activity for Tcf7l1 was detected (Merrill et al., 2001; Wu et al., 2012a). Here, we show that β-catenin binding to Tcf7l1 does not form a transactivation complex, but instead initiates a fundamentally distinct mechanism. β-catenin binding inactivates Tcf7l1 by reducing its chromatin occupancy and secondarily stimulates its protein degradation. Mouse genetic experiments demonstrate that this inactivation is the only necessary function of the Tcf7l1-β-catenin interaction. These molecular and genetic findings provide insights into the role of Wnt/β-catenin signaling in cells where Tcf7l1 expression is prominent, including embryonic stem cells (ESCs) and poorly differentiated breast cancer.

RESULTS

β-Catenin Reduces Tcf7l1 Protein Levels by Stimulating Protein Degradation

Molecular support for a conversion into transactivators by β-catenin includes the ability of a β-catenin-Tcf7 fusion protein to activate target genes without Wnt pathway stimulation (Staal et al., 1999). If Tcf7l1 were switched to a transactivator by β-catenin, one would expect a β-catenin-Tcf7l1 fusion protein to similarly activate target genes. In ESCs, the β-catenin-Tcf7l1 fusion was

Vita

Name: Chun-I Wu

Education: B.S., Life Science, National Yang-Ming University, Taiwan, 2000

M.S., Microbiology and Immunology, National Yang-Ming University, Taiwan, 2002

Ph.D., Biochemistry and Molecular Genetics, University of Illinois at Chicago, Chicago, Illinois, 2014

Publications: Shy BR*, Wu CI*, Khramtsova GF, Zhang JY, Olopade OI, Goss KH, Merrill BJ. *Regulation of Tcf7l1 DNA Binding and Protein Stability as Principal Mechanisms of Wnt/β-Catenin Signaling*. Cell Reports. 2013 Jul 11;4(1):1-9. *These authors contributed equally to this work as co-first authors.

Hoffman JA, Wu CI, Merrill BJ. *Tcf7l1 prepares epiblast cells in the gastrulating mouse embryo for lineage specification.* Development. 2013 Apr;140(8):1665-75.

Wu CI, Hoffman JA, Shy BR, Ford EM, Fuchs E, Nguyen H, Merrill BJ. *Function of Wnt/β-catenin in counteracting Tcf7l1 repression through the Tcf7l1-β-catenin interaction.* Development. 2012 Jun;139(12):2118-29.

Hung CS, Lin YL, Wu CI, Huang CJ, Ting LP. *Suppression of hepatitis B viral gene expression by phosphoinositide 5-phosphatase SKIP.* Cell Microbiology. 2009 Jan;11(1):37-50.

Honors: Student Travel Award, International Society for Stem Cell Research, Boston, MA, 2013

Student Travel Award, Society for Developmental Biology Meeting, Albuquerque, NM, 2010